

May 28, 2021

Tipton County Seismic and Liquefaction Hazard Maps  
(HUD Grant Year Four Products)

Chris H. Cramer, Roy B. Van Arsdale, Valarie Harrison, David Arellano, Hamed Tohidi, and  
Roshan Bhattarai

Abstract

A five-year seismic and liquefaction hazard mapping project for five western Tennessee counties began in 2017 under a Disaster Resilience Competition grant from the U.S. Department of Housing and Urban Development to the State of Tennessee. The project supports natural hazard (flood and earthquake) mitigation efforts in these five counties. The seismic hazard maps for Tipton County in western Tennessee were completed in 2021. Additional geological and geotechnical information has been gathered in Tipton Co. to improve the base northern Mississippi Embayment hazard maps of Dhar and Cramer (2018). Information gathered includes additional geological and geotechnical subsurface exploration logs, and water table level data collection and measurements. Improvements were made in the 3D geological model, water table model, and the geotechnical liquefaction probability curves. The  $V_s$  correlation with lithology model for Lauderdale County was used for Tipton County. Resulting improved soil response amplification distributions on a 0.5 km grid were combined with the 2014 U.S. Geological Survey seismic hazard model (Petersen et al., 2014) sources and attenuation models to add the effect of local geology for Tipton Co. Resulting products are an improved 3D-geology, geotechnical, seismic hazard, and liquefaction hazard models and maps for Tipton Co. Seismic hazard maps at PGA and 1.0 s show a 10-50% decrease in hazard at short periods and a 10-100% increase at long periods compared with USGS NSHMP maps.

Introduction

As part of the 2015 Disaster Resilience Competition, the State of Tennessee received funds from the Department of Housing and Urban Development (HUD) for several grants for flood hazard mitigation efforts. The University of Memphis received one of the grants for flood and seismic hazard mapping efforts in five western Tennessee counties (Figure 1) covering a five-year period starting in 2017. The fourth-year seismic hazard mapping effort is for Tipton County seismic and liquefaction hazard maps (this report).

The goal for the seismic hazard mapping project is to develop seismic and liquefaction hazard maps for use in flood hazard mitigation efforts in other portions of the HUD grant effort via the University of Memphis. The hazard maps will also be useful for other earthquake hazard mitigation efforts in the five western Tennessee counties.

## HUD Project Counties

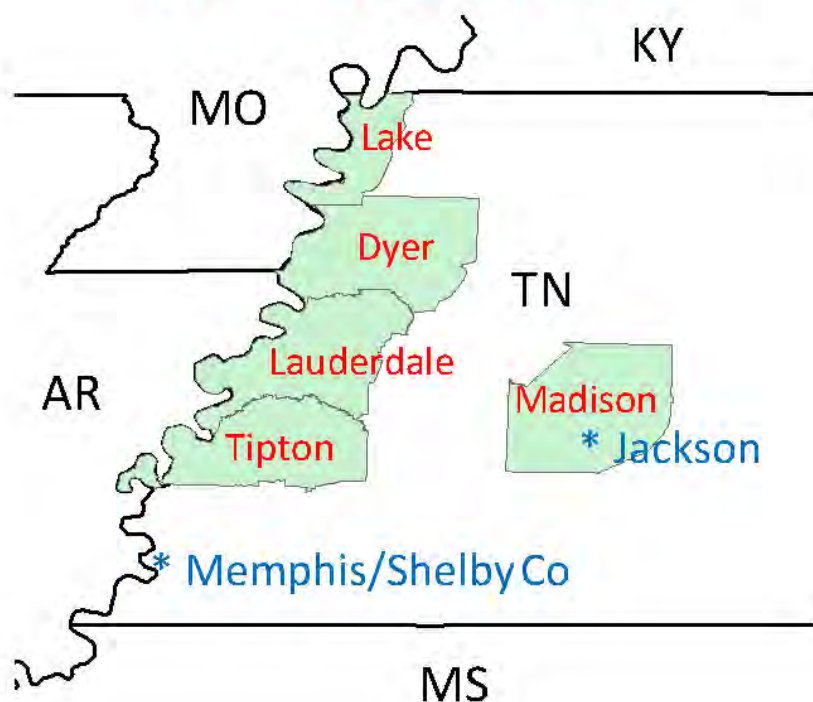


Figure 1: Five western Tennessee counties of the HUD grant supported seismic hazard study. AR – Arkansas, KY – Kentucky, MO – Missouri, MS – Mississippi, and TN – Tennessee.

The major elements to the seismic and liquefaction hazard mapping in this project are (1) geological 3D model development, (2) geotechnical (soil response to ground motions) model development, and (3) hazard maps generation. The 3D geological model of sediments above bedrock involves the gathering and interpretation of boring logs, entering geological information into a geographic information system (GIS), and developing maps of the depth to the tops of key geological sediment layers. The accompanying geotechnical model involves the gathering of geotechnical information (sediment properties and water table levels) from boring logs, and modeling liquefaction potential of the shallow sediments. Seismological models for hazard analysis are carried over from Lauderdale County (Cramer et al., 2020b). The final step is to integrate the geological, geotechnical, and seismological data into a county wide hazard model and maps that included the effects of local geology (sediments).

## Geological Model

### Introduction

Tipton County in western Tennessee was mapped as part of a five-county earthquake hazard mapping program (Figure 2A) (Cramer et al., 2018b; Weathers and Van Arsdale, 2019). Located southeast of the New Madrid seismic zone, Tipton County is vulnerable to both earthquake ground shaking and liquefaction in the event of future large earthquakes (Chiu et al., 1992; Cramer, 2006; Csontos and Van Arsdale, 2008; Cramer and Boyd, 2014; Cramer et al., 2018a and b).

The topography of Tipton County consists of lowland (<80 m) floodplains of the Mississippi and Hatchie rivers and loess covered terraces of these rivers, intermediate elevations (80-107 m) covered by loess, and upland elevations (>107 m) covered by loess that overlies 3.6 Ma ancestral Mississippi River floodplain sand and gravel (Figure 3). Beneath the near-surface geology are Eocene (~34 Ma) sediments that overlie older Paleogene, Late Cretaceous, and Paleozoic strata (Hardeman, 1966; Weathers and Van Arsdale, 2019). Structurally, the county overlies Cambrian age Reelfoot rift faults (Figure 4) (Csontos et al., 2008; Van Arsdale and Cupples, 2013; Martin and Van Arsdale, 2017), which have Quaternary reactivation in adjacent Lauderdale and Shelby counties (Cox et al., 2001; 2006; 2013). Quaternary structures have also been mapped in Tipton County (Figure 4) (Vanderlip et al., 2020). The surface and subsurface geology of a region influences how the landscape will react during a large earthquake. In this section we present geologic maps of Tipton County that provide important information for companion seismologic and liquefaction hazard modeling studies.

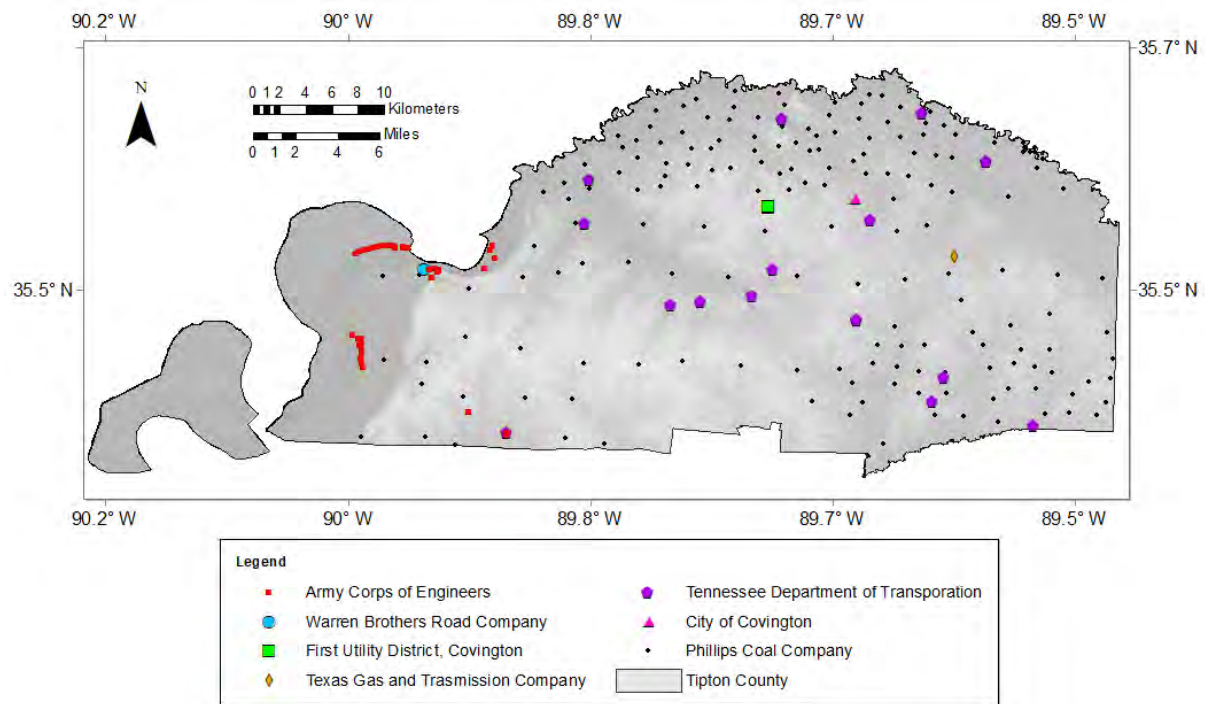
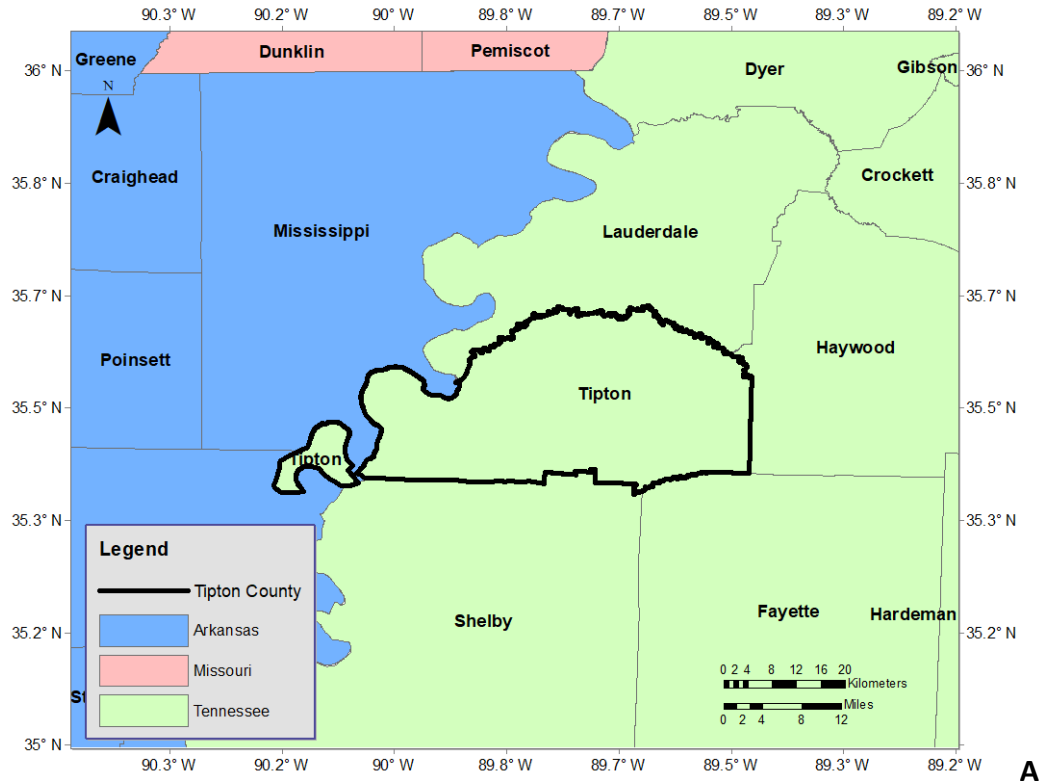
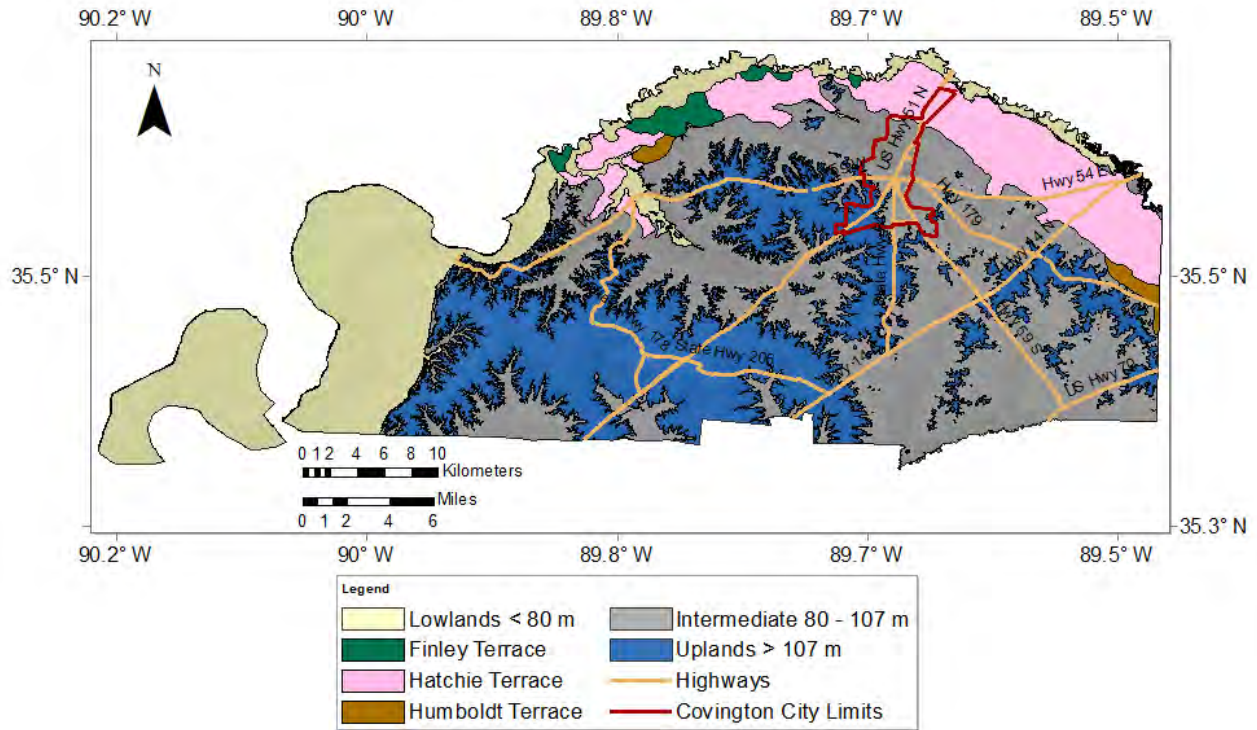
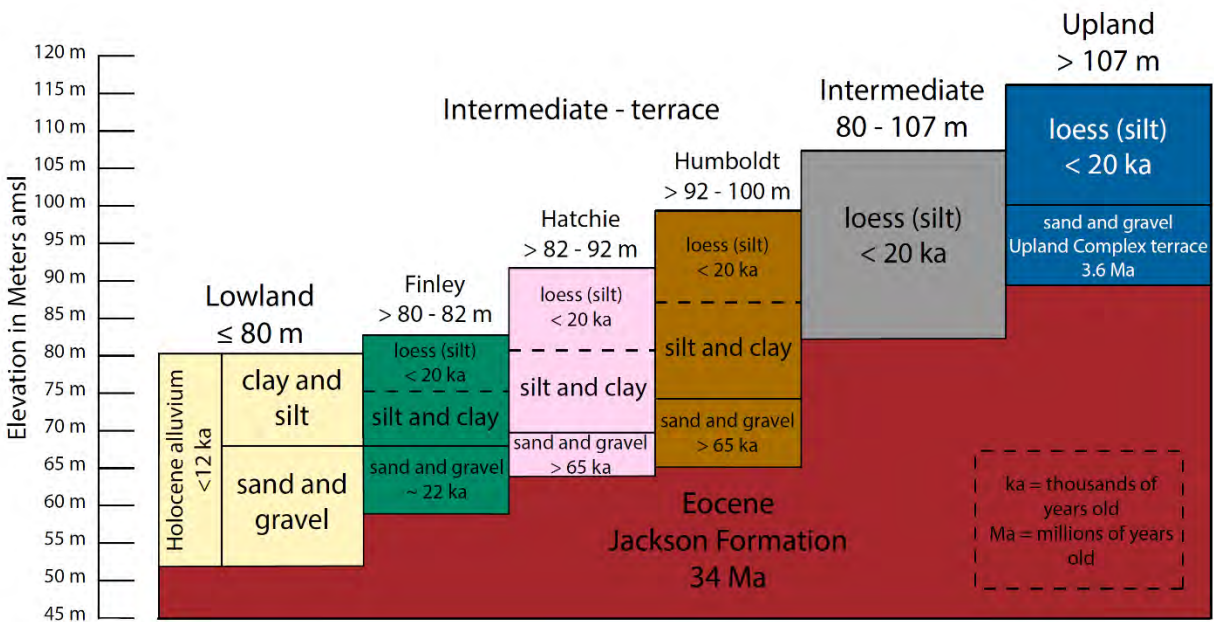


Figure 2: A) Tipton County in western Tennessee. B) Dots show geologic drill holes used in near-surface mapping of Tipton County.

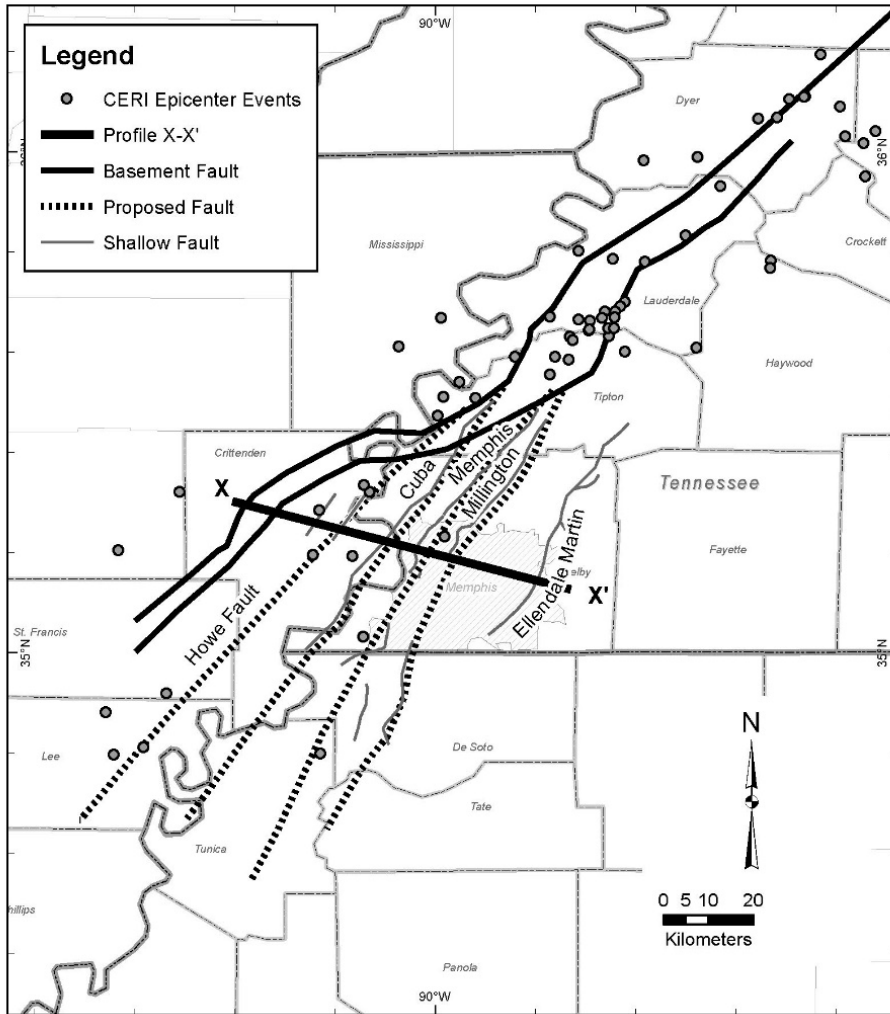


**A**

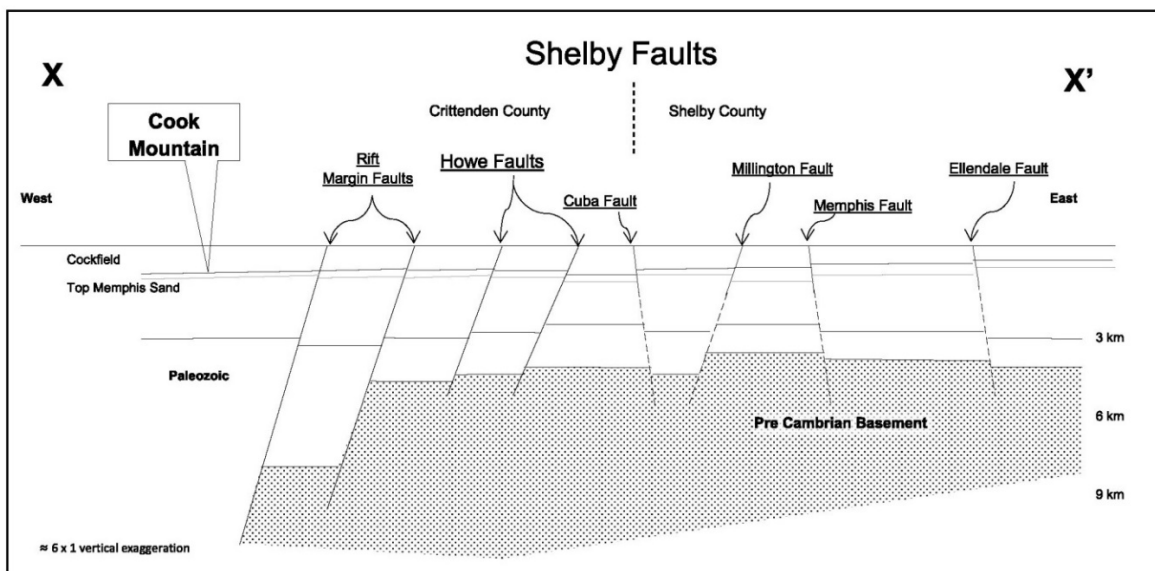


**B**

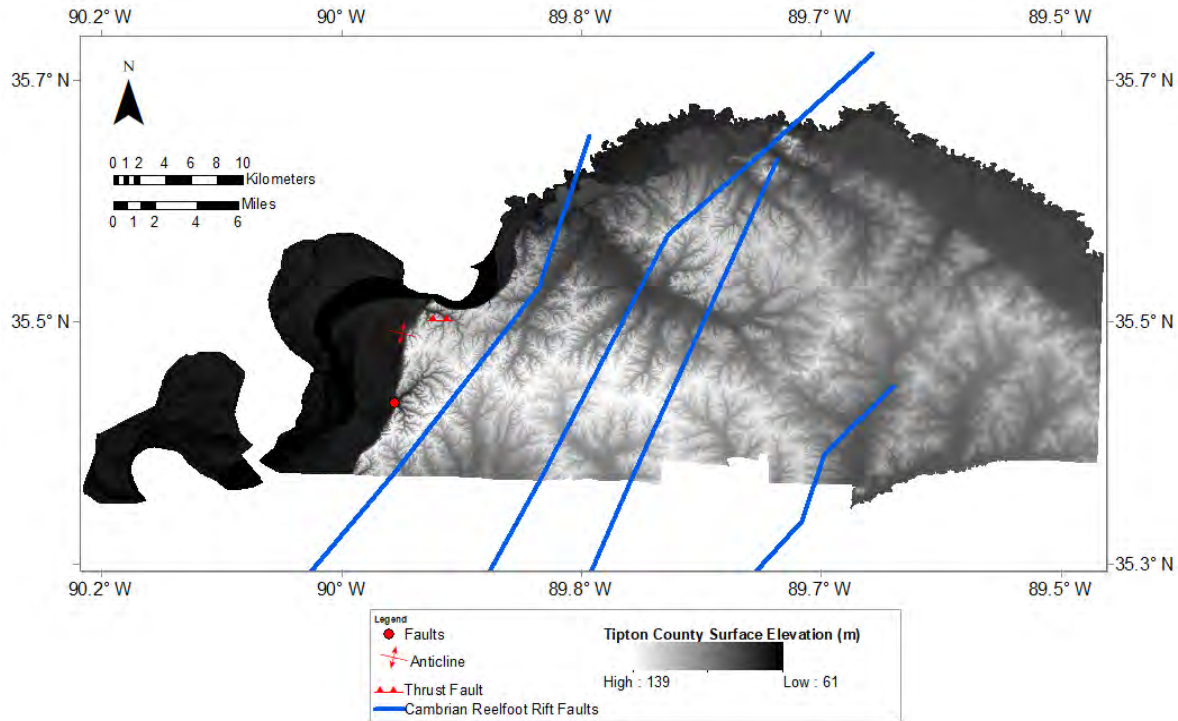
Figure 3: A) Generalized geologic map of Tipton County. B) General geologic cross section illustrating the near-surface geology beneath the Lowland, Intermediate, and Upland surfaces in Tipton County.



A



B



C

Figure 4: A) Faults mapped in the subsurface of Shelby and southern Tipton counties (from Martin and Van Arsdale, 2017). B) Cross section X-X' in Shelby County (from Howe, 1985). C) Tipton County Reelfoot Rift faults from Martin and Van Arsdale (2017) and Parrish and Van Arsdale (2004) used in Figures 5C, and 6B-8B. Quaternary anticline and faults in red from Vanderlip et al. (2001).

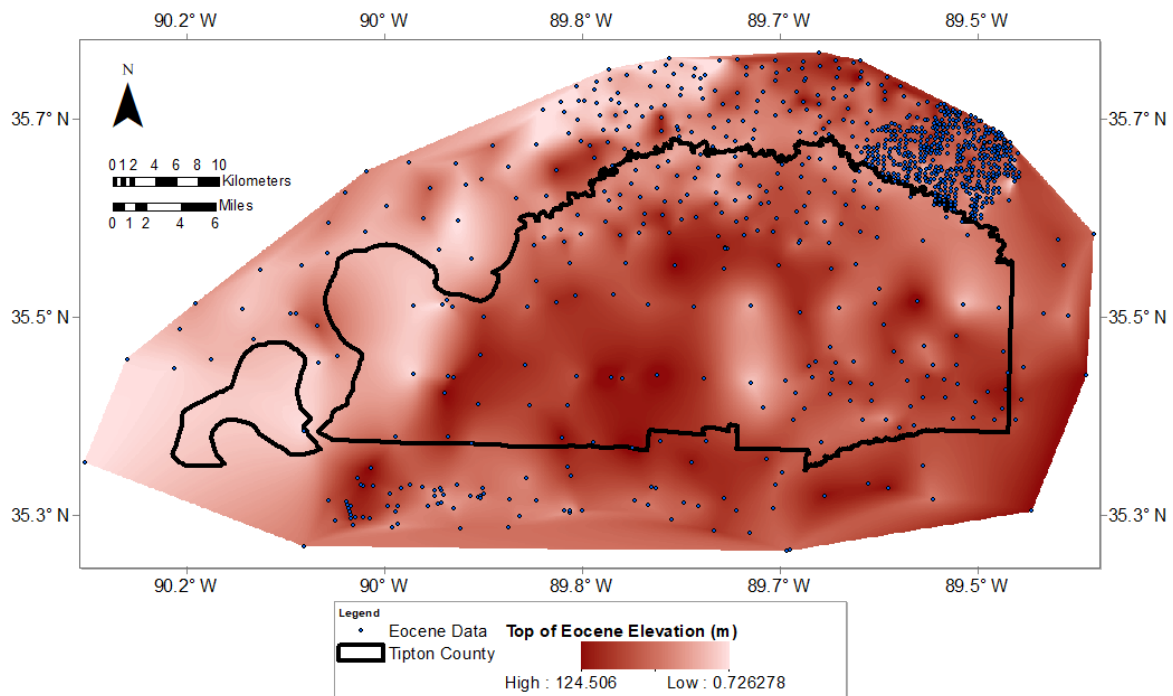
## Methods

Subsurface lithologic boring logs were acquired from North American Coal Company, US Army Corps of Engineers, Tennessee Department of Transportation, petroleum exploration wells, Tennessee Department of Environmental Control (Luke Ewing and William Mann), and the Center of Applied Earth Science and Engineering Research at the University of Memphis. The lithologic boring logs were geologically interpreted and recorded in Excel Spread sheets. A Lidar based 10-meter digital elevation model (DEM) of Tipton county was the base map upon which surface and near-surface geology was mapped from 250 bore holes (Figure 2B). River terraces along the Hatchie River in Figure 3 were derived from previously published maps (Saucier, 1994). Deep bedrock mapping was conducted down to the top of the Paleozoic strata, which is at an average depth of 850 m below Tipton County.

The top of the Eocene was mapped using 938 borings and the top of the Memphis Sand was mapped using 138 borings. The contact between the fine-grained Eocene sediment and the overlying alluvium is identified by the basal conglomeratic facies of the alluvium. The underlying top of the Cretaceous and top of the Paleozoic were mapped primarily from DOW Chemical seismic reflection lines (Parrish and Van Arsdale, 2004) and a few oil-exploration wells.

Structure contour maps were made of the elevation of the tops of the Eocene, Memphis Sand, Cretaceous, and Paleozoic beneath Tipton County and within a boundary zone (Figures 5A and B, 6A - 8A). These maps were made using the Natural Neighbor contouring algorithm. Bedrock faults have been mapped beneath Tipton County (Parrish and Van Arsdale, 2004; Martin and Van Arsdale, 2017). These previously mapped faults (Figure 4) were used in our mapping to produce faulted structure contour maps of the tops of the Eocene, Memphis Sand, Cretaceous, and Paleozoic using the Spline with Barriers contouring algorithm (Figs. 5C, 6B-8B).

Isopach (unit thickness) maps were made of the Lowland river floodplain alluvium and the silt/clay uppermost portion of the floodplain alluvium (Figure 9).



A

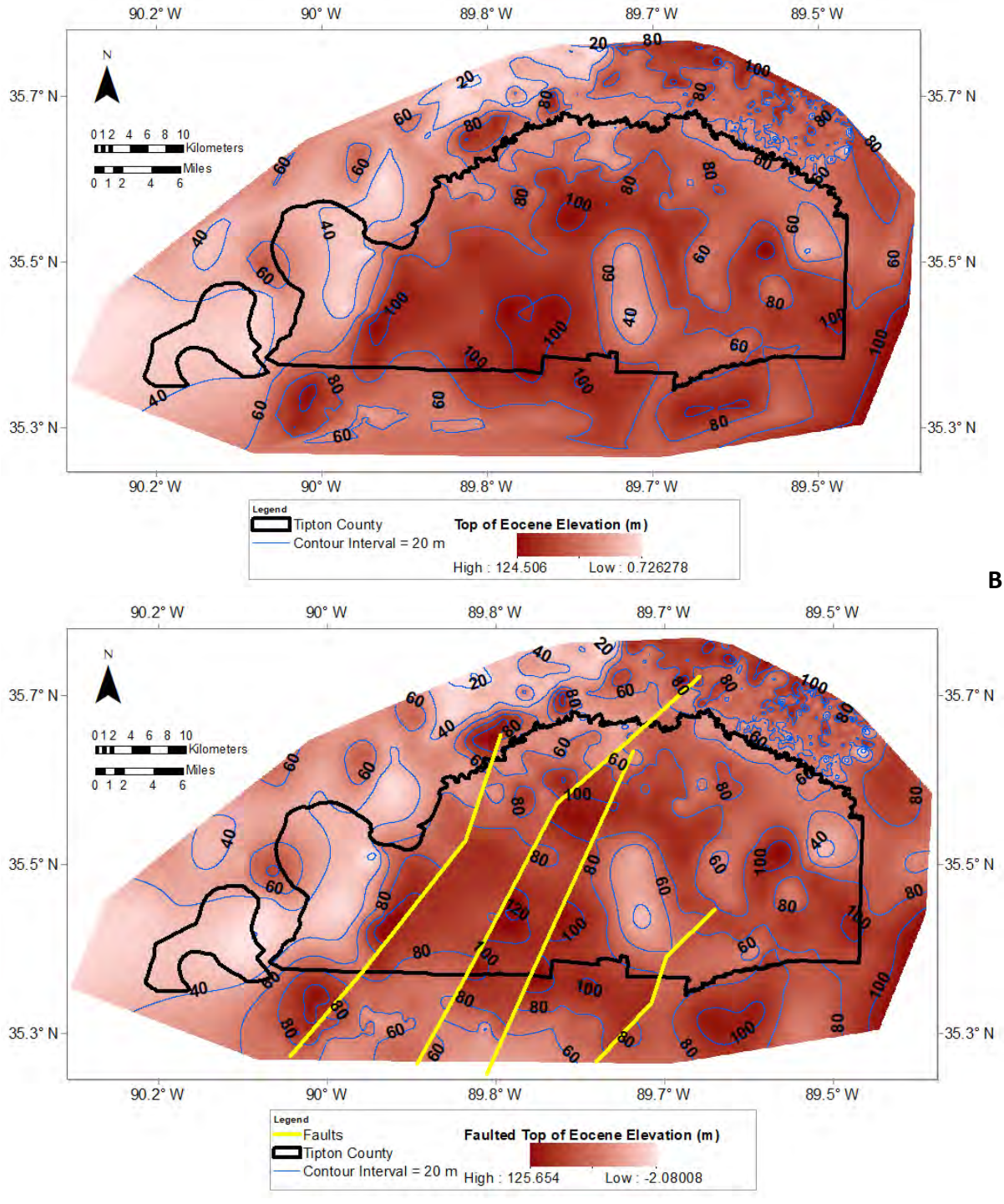
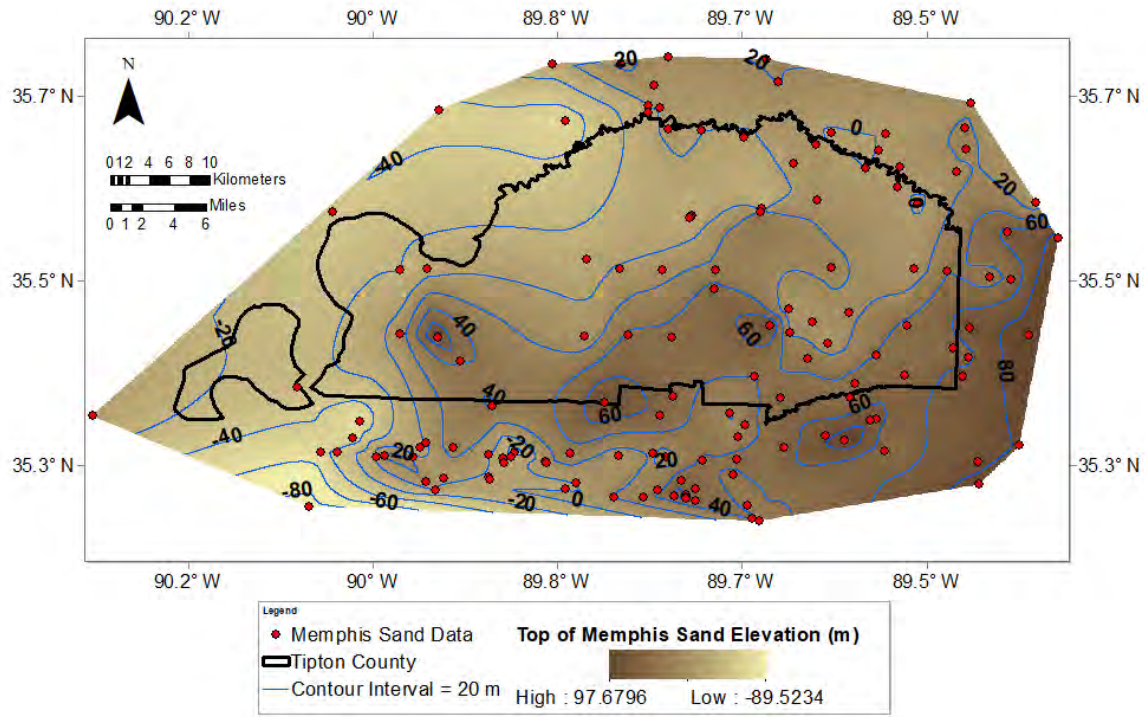
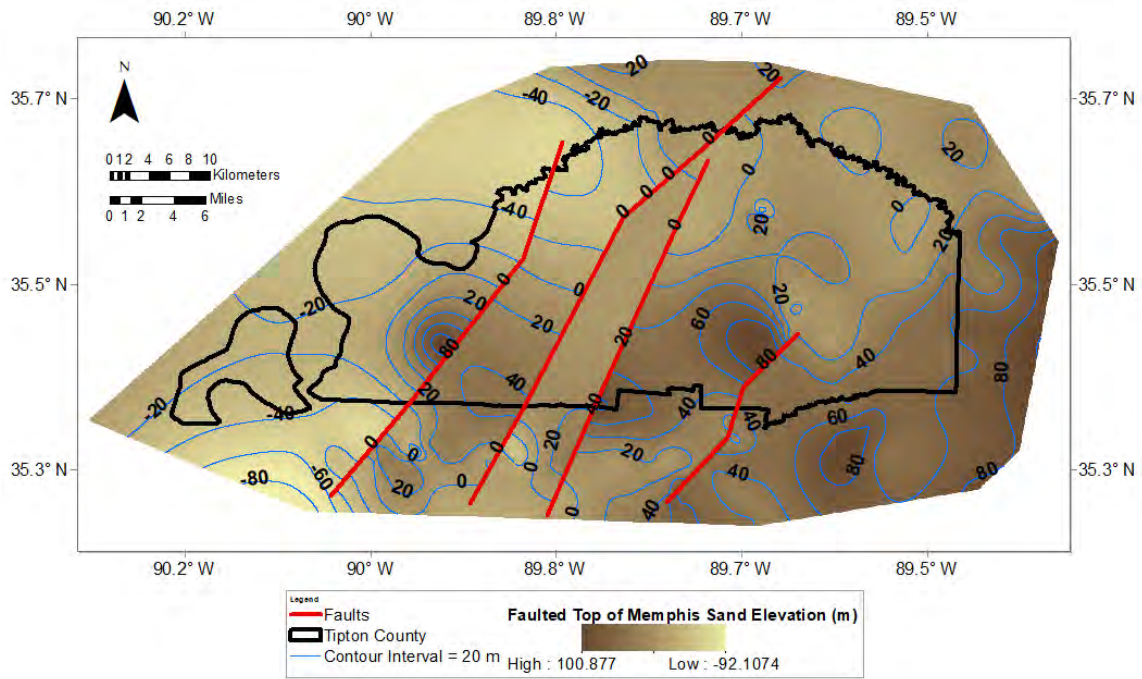


Figure 5: A) Drill holes (black dots) used to map top of Eocene strata in Tipton County. B) Structure contour map of the un-faulted top of Eocene strata. (C) Structure contour map of the faulted top of Eocene strata.

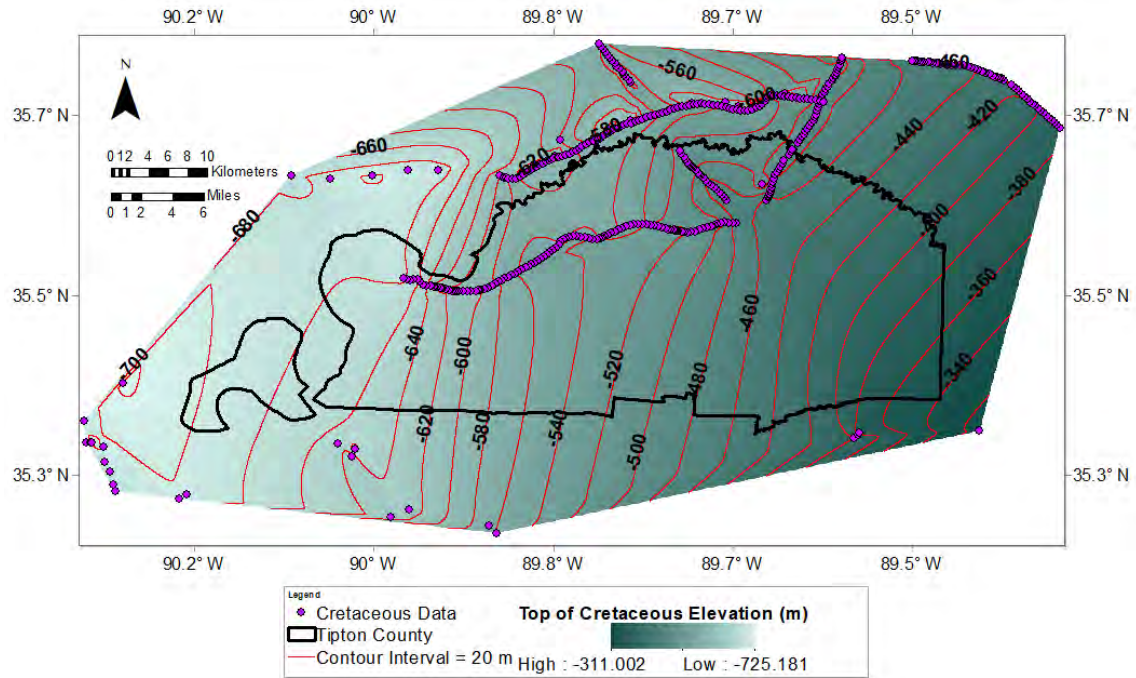


A

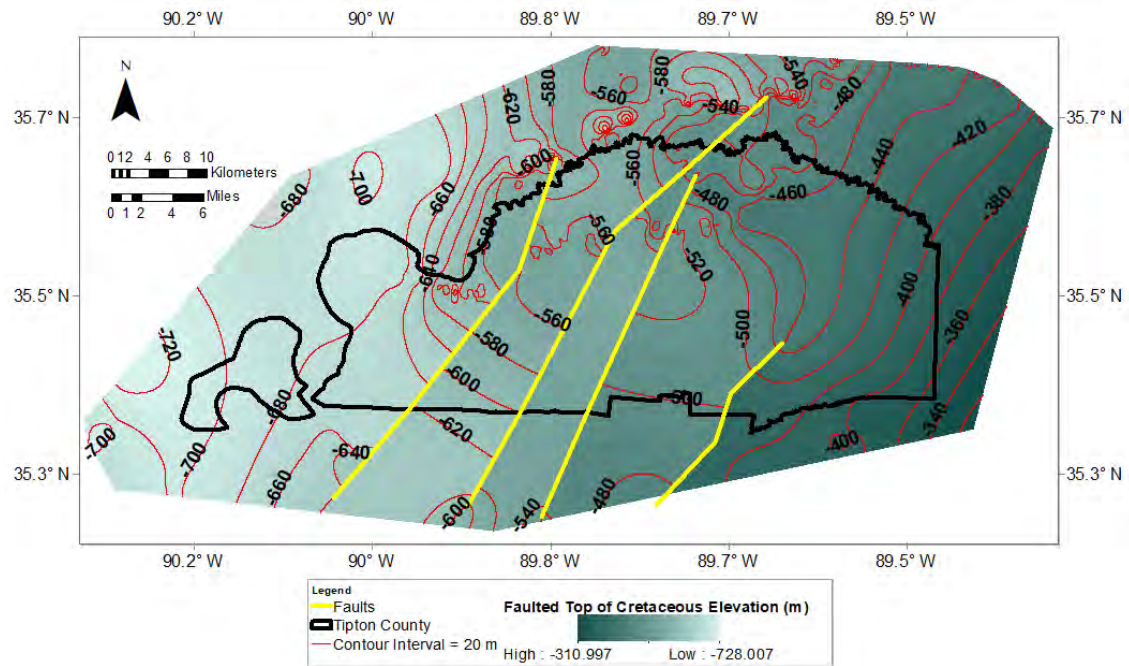


B

Figure 6: Un-faulted (A) and faulted (B) structure contour maps of the top of the Memphis Sand strata in Tipton County with red dots illustrating drill holes used to make the maps.

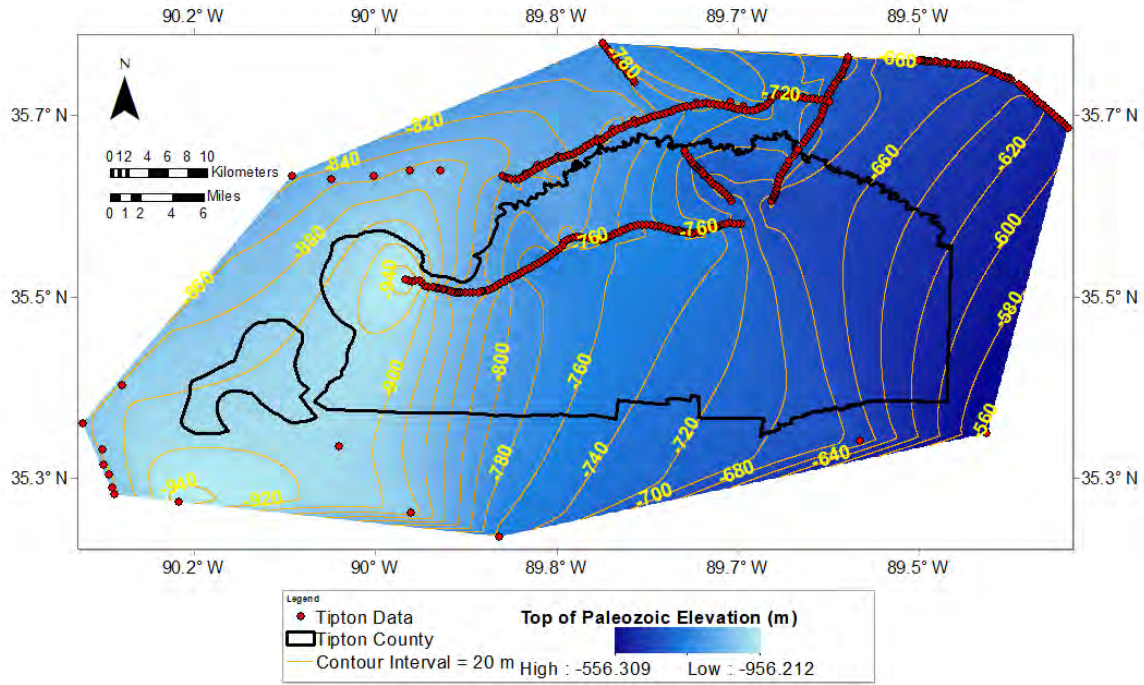


A

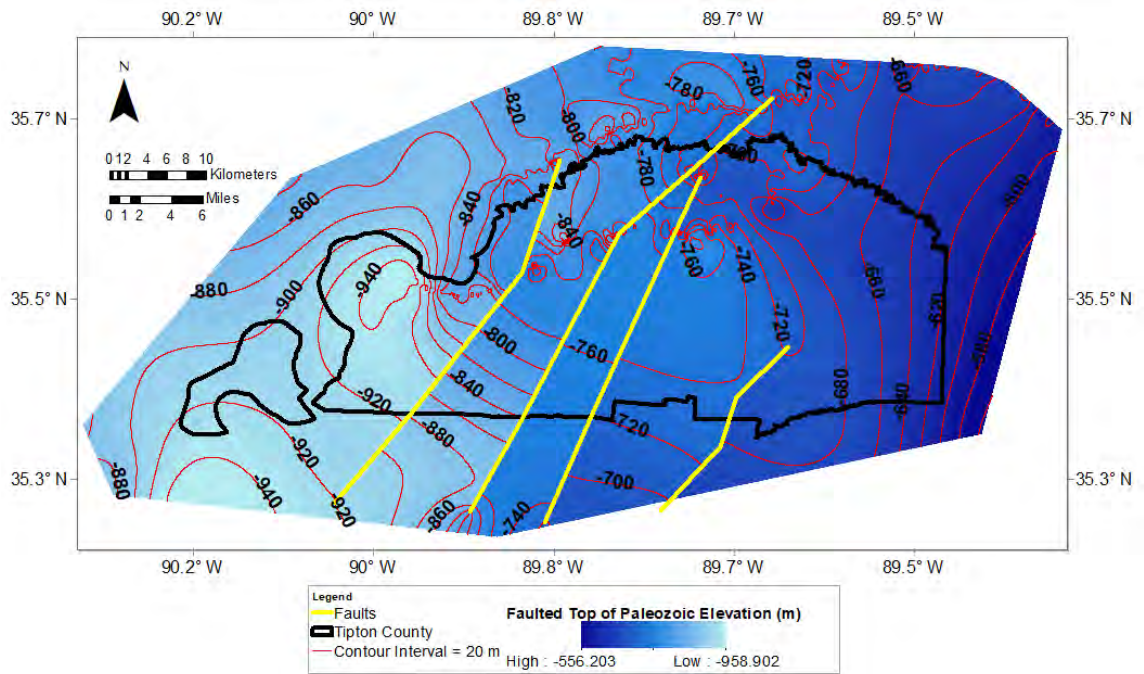


B

Figure 7: Un-faulted (A) and faulted (B) structure contour maps of the top of the Cretaceous strata in Tipton County with dots illustrating seismic reflection shot points and drill holes used to make the maps.

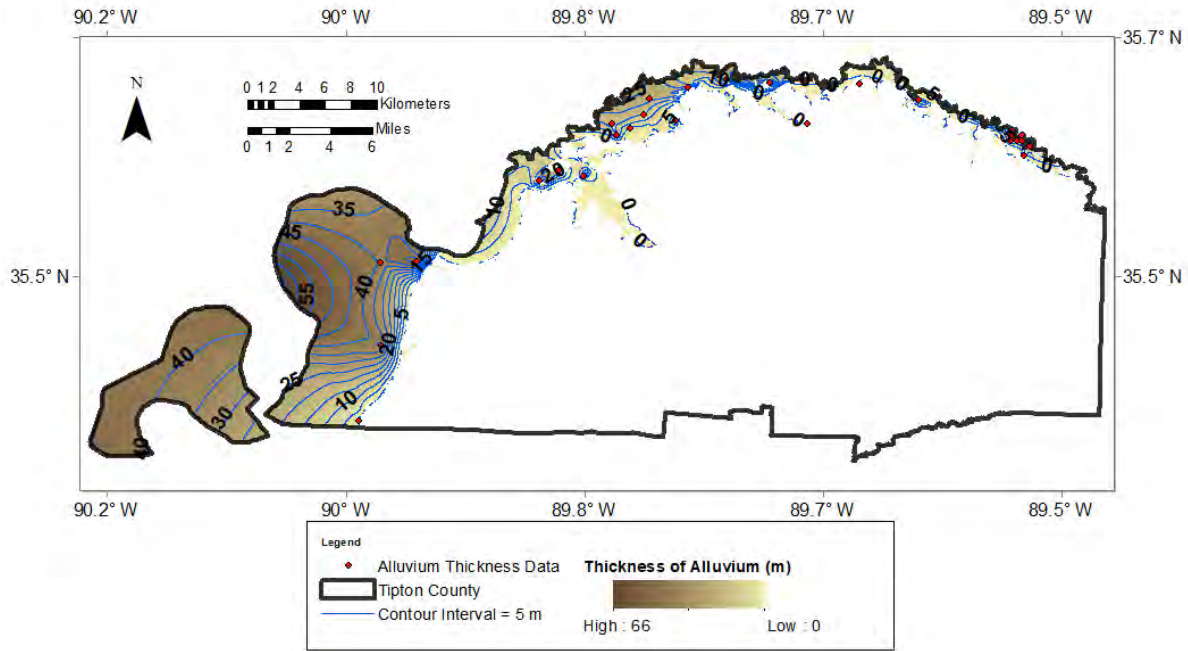


**A**

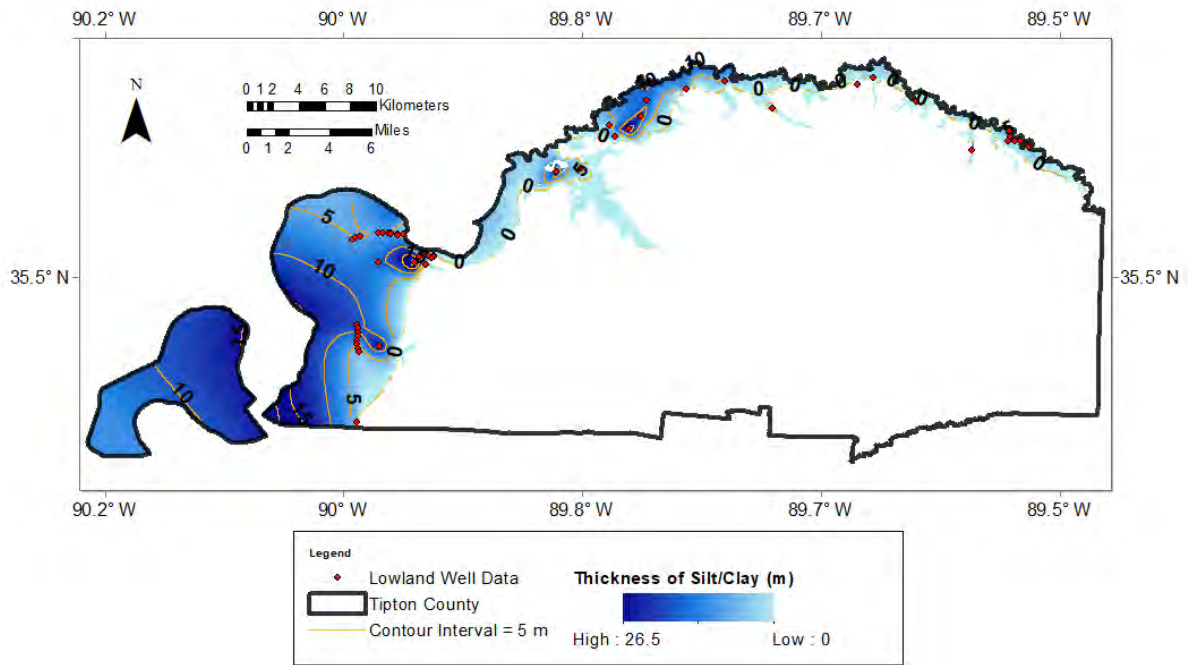


**B**

Figure 8: Un-faulted (A) and faulted (B) structure contour maps of the top of the Paleozoic strata in Tipton County with dots illustrating seismic reflection shot points and drill holes used to make the map.



A



B

Figure 9: A) Isopach of the Holocene alluvium in Tipton County. B) Isopach of the uppermost silt and clay portion of the Holocene alluvium in Tipton County.

## Results

### Near-Surface Geologic Map

The near-surface geology of Tipton County was geologically differentiated into three mapping units (Lowlands, Intermediate, Uplands) that differ in their elevation and near-surface geology (Figure. 3). The Figure 3 cross section does not represent a particular place on the map but is a general depiction of the near-surface geology. Unit surface elevations and unit thicknesses in Figure 3B are averages from values measured throughout the county.

The Lowlands are at an elevation of  $\leq 80$  m and consists of Holocene ( $< 12$  ka) river floodplain alluvium (Saucier, 1994; Rittenour et al., 2007). In general, the alluvium consists of surface silt and clay overbank sediment that overlies laterally accreted sand and gravel sediment. Between elevations of 80 m and 107 m are the Intermediate units. Intermediate units are differentiated into Hatchie River terraces and areas where loess (wind-blown silt) overlies Eocene strata. The terraces have been mapped from topographically highest to lowest as the Humboldt, Hatchie, and Finley terraces (Saucier, 1987). All Intermediate units are covered with Peoria loess that is less than 20 ka. The Hatchie and Humboldt terraces have older loess units beneath the Peoria loess in adjacent Lauderdale County (Saucier, 1987). We think the older loess identified in Lauderdale County also underlies the Peoria loess in the Hatchie and Humboldt terraces in Tipton County. Beneath the loess, the terrace strata consist of silt and clay overbank sediment and underlying laterally accreted sand and gravel sediment that is  $\sim 22$  ka (Finley) and  $> 65$  ka (Hatchie and Humboldt). The Upland unit is at an elevation  $> 107$  m and is a loess-covered high-level terrace of the ancestral ( $\sim 3.6$  Ma) Mississippi/Ohio river system (Figure 3) (Van Arsdale et al., 2007; Odum et al., 2020). This high-level terrace alluvium, called the Upland Complex, consists of sand and gravel that is regionally a major source of aggregate (Van Arsdale et al., 2012; Lumsden et al., 2016).

### Structure Contour Maps

The top of the Eocene strata is presented as an un-faulted surface and as a faulted surface (Figure 5). There is a lot of subsurface relief on the top of the Eocene because the Eocene has been eroded by the Mississippi and Hatchie rivers and because it has undergone minor structural deformation. When inserting the bedrock faults into this data set and contouring it with the Spline with Barriers contouring algorithm, fault displacement is apparent (Figure 5C).

The less well constrained tops of the Memphis Sand, Cretaceous strata, and Paleozoic strata were contoured without faults (Figures 6A - 8A). These surfaces slope westerly. When inserting the faults, the tops of the Memphis Sand, Cretaceous, and Paleozoic reveal fault displacements (Figures 6B - 8B).

## Isopach Maps

The Quaternary floodplain alluvium, in general, consists of two layers. A surface silt and clay layer that averages 8.5 m thick and an underlying sand and gravel layer that averages 15.5 m thick. The isopach map of the thickness of the entire Quaternary floodplain alluvium reveals variation in thickness due to rivers of different sizes and scour depths (Figure 9A). Thickness of the uppermost silt and clay layer is also variable (Figure 9B).

## Geologic Summary

The near-surface geology of Tipton County reveals the incision of the ancestral Mississippi/Ohio river system through time. Approximately 3.6 Ma the ancestral Mississippi/Ohio river system (Upland Complex) flowed across a vast floodplain surface that extended beyond Tipton County (Van Arsdale et al., 2007; Cupples and Van Arsdale, 2014; Cox et al., 2014; Lumsden et al., 2016). Incision through the Upland Complex throughout the lower Mississippi/Ohio river system began in the early Pleistocene with growth of continental ice sheets and resultant lower sea levels (Saucier, 1994; Van Arsdale et al., 2007). During the Pleistocene, up to four loess layers were deposited in western Tennessee (Markewich et al., 1998). In adjacent Lauderdale County, Rodbell (1996) identified Peoria loess (< 20 ka) covering the Upland and Intermediate surfaces with underlying Roxanna silt (loess) that is > 65 ka on top of the floodplain alluvium of the Humboldt and Hatchie terraces. Based on the Lauderdale County geologic history we believe the ancestral Mississippi/Ohio river system and its tributaries entrenched > 65 ka in Tipton County because the Humboldt terrace alluvium is overlain by the > 65 ka loess (Figure 3). Subsequently, the Mississippi/Ohio river system and its tributaries further entrenched to form the Hatchie (also > 65 ka) and then Finley (~ 22 ka) terrace levels. The final entrenchment of the Mississippi and Hatchie rivers in Tipton County occurred within the last 22 ka resulting in most of the Lowlands being underlain by floodplain alluvium that is < 12 ka.

Faults within the eastern margin of the Reelfoot Rift underlie Tipton County (Csontos et al., 2008; Van Arsdale and Cupples, 2013; Martin and Van Arsdale, 2017; Vanderlip et al., 2020). The Bluff Lineament fault in adjacent Shelby County (Cox et al., 2013), the Porters Gap fault in Lauderdale County (Cox et al., 2001; 2006), and faults in Tipton County (Vanderlip et al., 2020) have Quaternary displacement. The Ellendale-Martin fault in southeastern Tipton County is an inverted fault with down-to-the-east displacement on the top of the Paleozoic and down-to-the-west displacement on the top of the Memphis Sand and Eocene (Figure 4). This fault may be responsible for the low on the top of the Eocene strata immediately west of the fault (Figure 5C). If so, then the Ellendale-Martin fault has been active since the Eocene. It is also apparent that there is a major window (breach) through the aquiclude above the Memphis Sand where the Cook Mountain, Cockfield, and Jackson formations (Hardeman, 1966) are missing (Figure 10). This window permits direct connection between surface water of the shallow alluvial aquifer and Memphis Sand aquifer water, which is a threat to ground water quality at the window location and down groundwater gradient.

Surface and subsurface geologic mapping of Tipton County has provided insight into the three-dimensional geology (Figure 11) and the Quaternary geologic history of the county. Of importance to the county's earthquake hazards are the seismic velocity structure of the underlying geologic strata, the recurrence intervals of Reelfoot rift faults (Tuttle et al., 2002; Cox et al., 2001; 2006; 2013) and the liquefaction potential of the Holocene floodplain sediments of the Mississippi and Hatchie rivers.

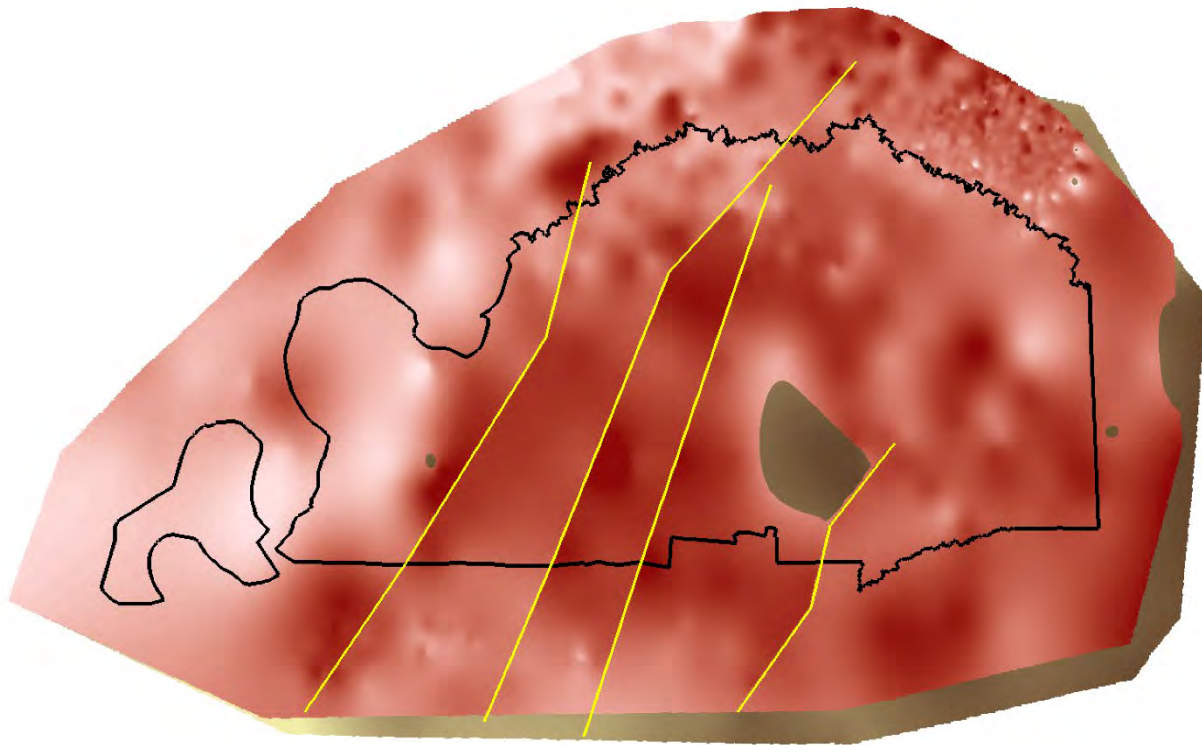
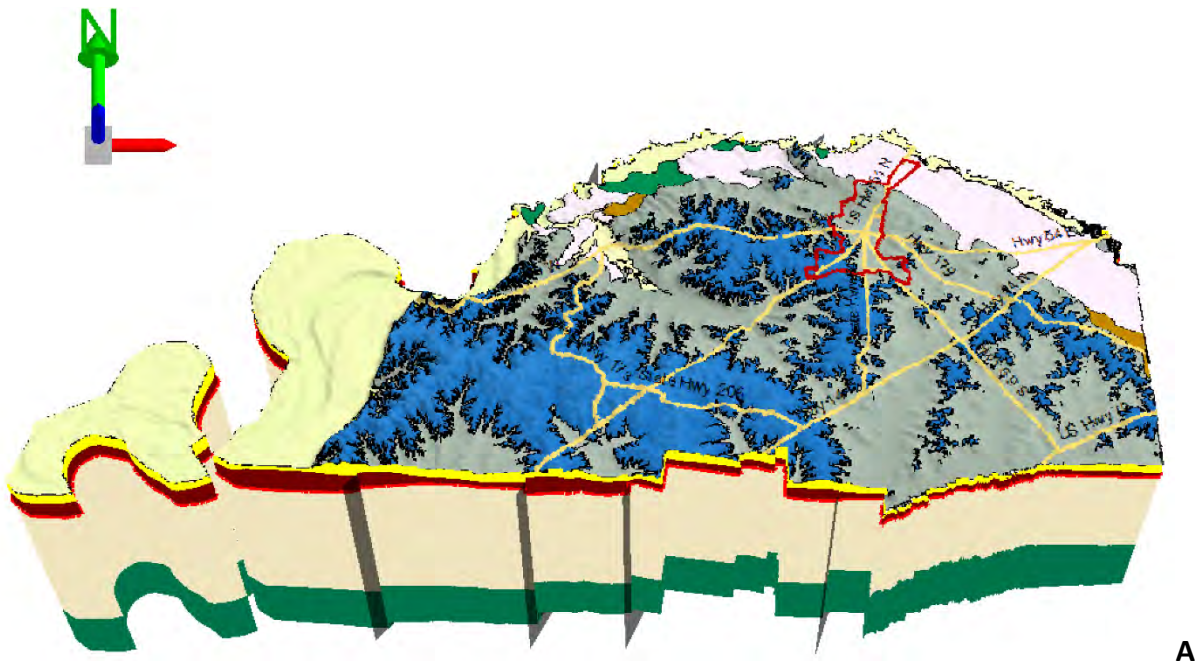
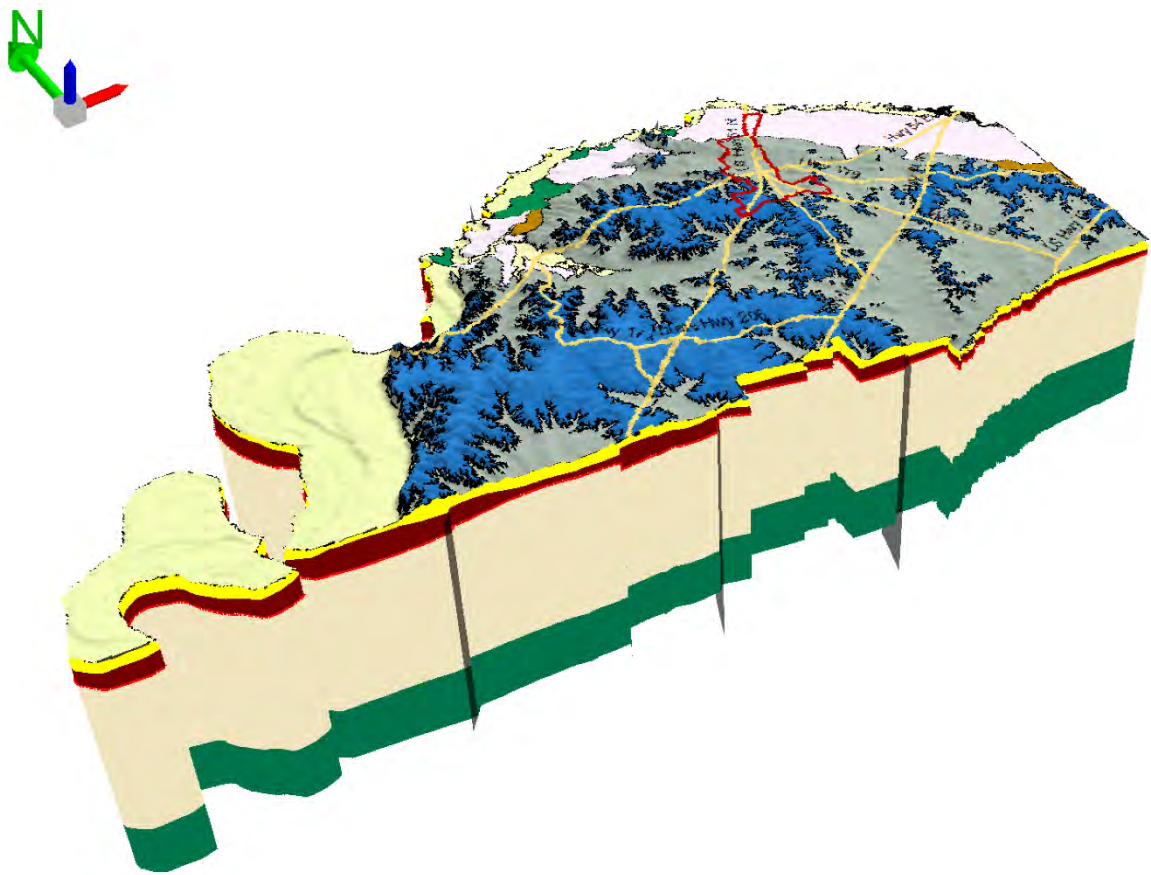


Figure 10: Faulted top of Eocene unconformity consisting locally of Cook Mountain, Cockfield, and Jackson formations (red) and Memphis Sand (brown). Brown Memphis Sand margin is due to larger map area of underlying Memphis Sand map.



A



B

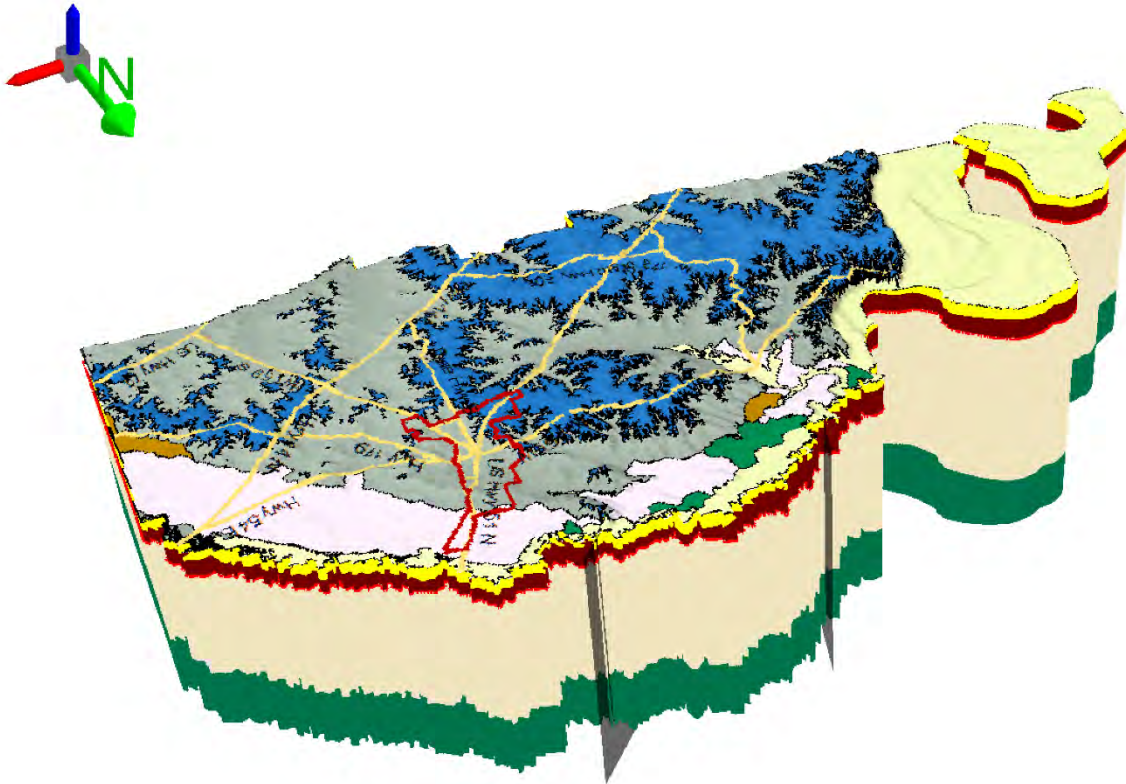


Figure 11: Three-dimensional perspective diagrams of Tipton County subsurface geology A) looking north, B) looking northeast, and C) looking southwest. Vertical exaggeration is 15X. The base of the models lay on Paleozoic strata, green is Cretaceous strata, tan is Paleogene strata, red line is top of Eocene Memphis Sand (base of Memphis Sand not mapped), brown is Eocene strata, yellow is Pliocene and Quaternary sediment. Gray vertical lines/panels are faults. Colors of surface geologic units defined in Figure 3A. This model used a Projected Coordinate System for Transverse Mercator - WGS 1984 UTM Zone 16N. See Appendix for 3D video.

## Geotechnical Model

### Introduction

A summary of geotechnical analyses conducted to develop Liquefaction Probability Curves (LPCs) of Tipton County is provided in this section. General information of the subsurface data collection approach is presented initially followed by the description of methodologies used to generate LPCs.

### Data Collection

The collected subsurface data for geotechnical analysis of Tipton county, include Standard Penetration Test (SPT) boring logs and Ground Water Level (GWL) data. The procedure of obtaining each set of data is summarized and provided in the next sections.

## SPT Data

A total of 113 SPT soil borings within Tipton County were received from three organizations: U.S Army Corps of Engineers (USACE), Tennessee Department of Transportation, and Construction Material Laboratory, Inc. The total number of soil boring logs that were obtained from each organization is provided in Table 1.

Table 1: Summary of the total number of borings.

<b>Organization</b>	<b>Number of Boring Logs</b>
USACE	53
TDOT	31
Construction Material Lab, Inc.	29
Total	113

For the boring logs of the USACE and soil borings of bridge projects that were received from Construction Material Laboratory, Inc. the coordinate locations were provided by the organizations but like Dyer (Cramer et al., 2020a) and Lauderdale (Cramer et al., 2020b) counties, the TDOT boring logs did not provide a coordinate location of where the boring was obtained. We were only provided with a project location map (without scale) or a general project location description. Using Google Earth and Google Map, we estimated the location of the projects and used the project location for all soil borings of a project to find the geologic unit of the borings and to interpolate the GWL of each boring using the GWL contour map described later in this report.

The borings indicated in Table 1 were evaluated for use in developing LPCs using the same criteria that were utilized to select SPT soil boring logs of Lake, Dyer, and Lauderdale counties (Cramer et al., 2019, 2020a, 2020b). The selection criteria are summarized as:

- Borings must be at least 20 m (66 ft) deep.
- Borings must include N-values and USCS classifications to a depth of 20 m (66 ft).
- The boring locations must have latitude and longitude coordinates. An exception to this is the TDOT boring locations previously mentioned.

As shown in Table 1 only a total of 113 soil boring logs were obtained for Tipton County. Therefore, to include more soil boring logs data to the geotechnical database for developing LPCs of Tipton County, an extra selection criterion was added to the above criteria. Based on the new selection criterion, boring logs with most N-values included to a depth of 15 m (50 ft) instead of 20 m (66 ft) were also accepted and we completed the new selected boring logs to a depth of 20 m (66ft) based on the following strategies:

- Missing N-values for any depth at a given boring location was estimated by using the same N-value for a given N-value above or below the depth of the missing N-value if the overlying and underlying soil had the same soil classification.
- If the soil layers above and below the layer of missing N-value did not have the same classification or did not have N-value in each boring, the N-value was extracted from

closest boring for the same classification and the same depth as classification and depth of the missing N-value.

A total of 66 out of the 113 boring logs obtained within Tipton County were selected for use in developing LPCs: 16 from USACE, 33 from 9 TDOT projects, and 17 from Construction Material Laboratory, Inc.

Figure 12 shows the locations of the 66 selected soil boring logs within Tipton County.

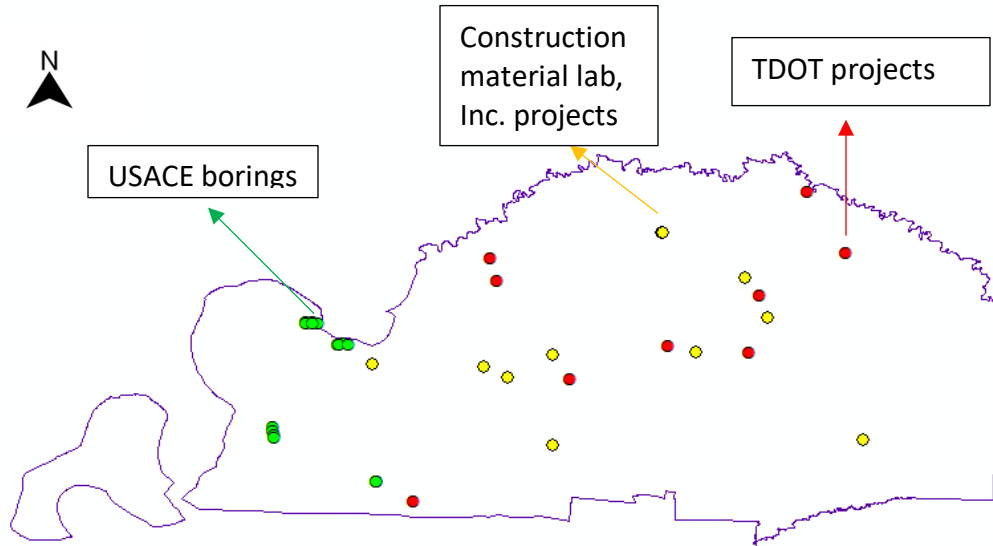


Figure 12: Locations of selected soil borings for use in developing LPCs.

#### Geology Classification of selected SPT boring logs

Figure 13 shows the surface geology map of Tipton County. Tipton county consists of three primary geologic units: Lowland, Intermediate, and Upland. Intermediate includes loess overlying Finley, Hatchie, and Humboldt terraces and loess overlying Eocene strata.

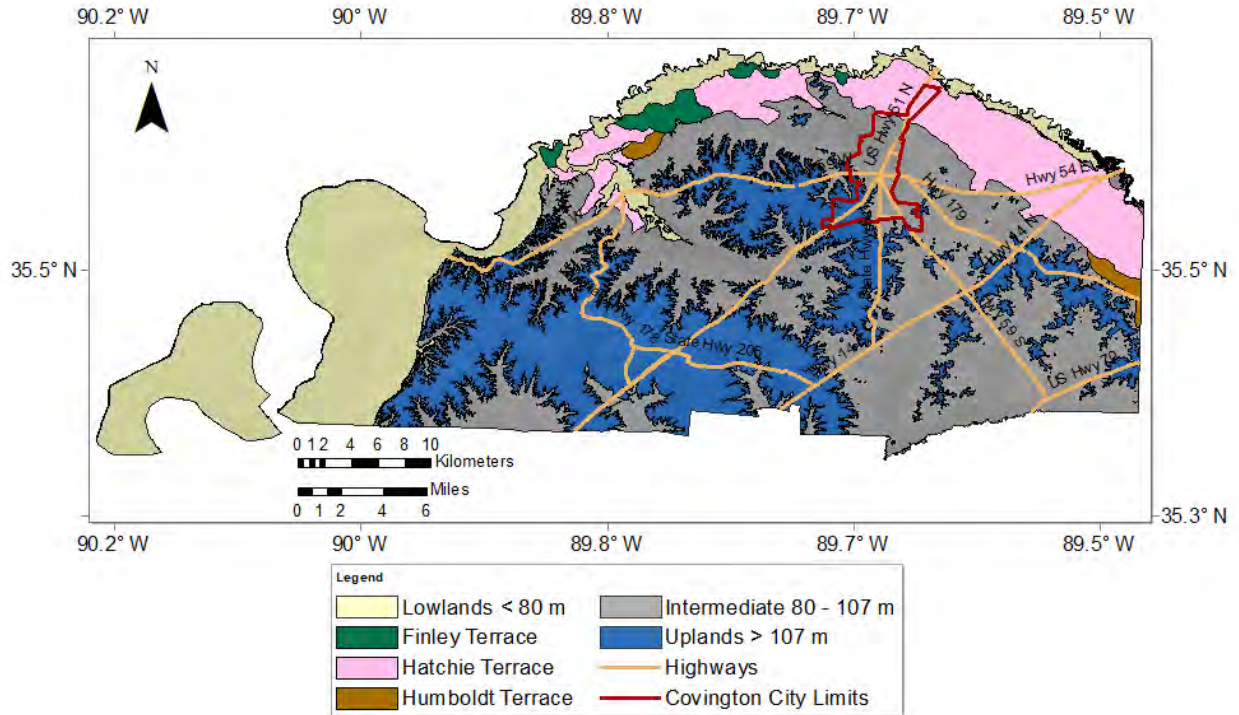


Figure 13: Surface geology map of Lauderdale County.

Like Dyer and Lauderdale counties, due to the variety of surficial geologic units, the selected SPT soil boring logs must be separated by geologic units to develop specific LPCs for each geologic unit.

Figure 14 illustrates the distribution of the geologic units and the boring locations in relation to geologic units. Table 2 provides the total number of selected boring logs within each geologic unit.

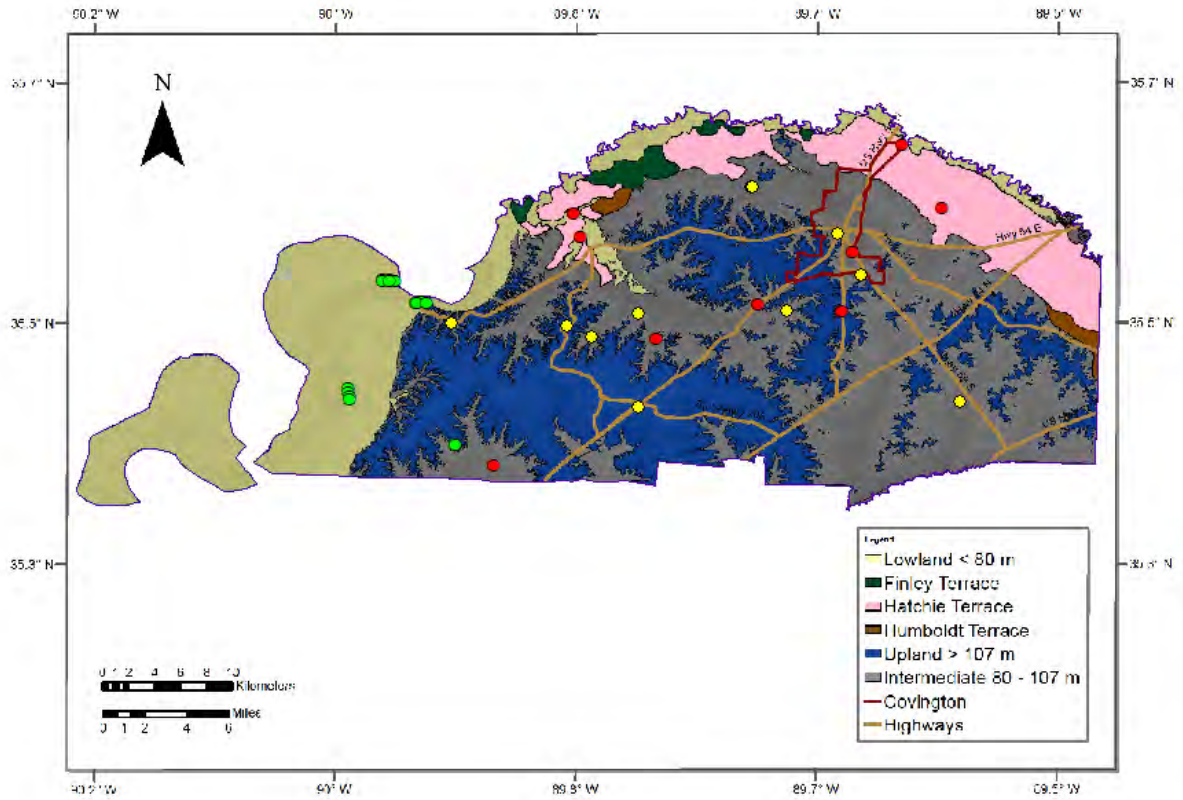


Figure 14: Soil boring locations on the surface geology map.

Table 2: Summary of the number of borings in each geology.

Geology	Organization	USACE	TDOT	Construction Material Lab, Inc.	Total
Lowland		13	9	0	22
Intermediate		0	22	12	34
Upland		3	2	5	10

### Groundwater data

Using the same procedure which we used to find the water level at each soil boring locations and project locations of Lake, Dyer, and Lauderdale counties (Cramer et al., 2019, 2020a, b), we developed a GWL contour map to estimate the GWL for the Tipton County boring logs.

The primary source for establishing the GWL contour map within the surface alluvial aquifer for Tipton County was the GWL contour map shown in Figure 15 that was developed by Schrader (2008).

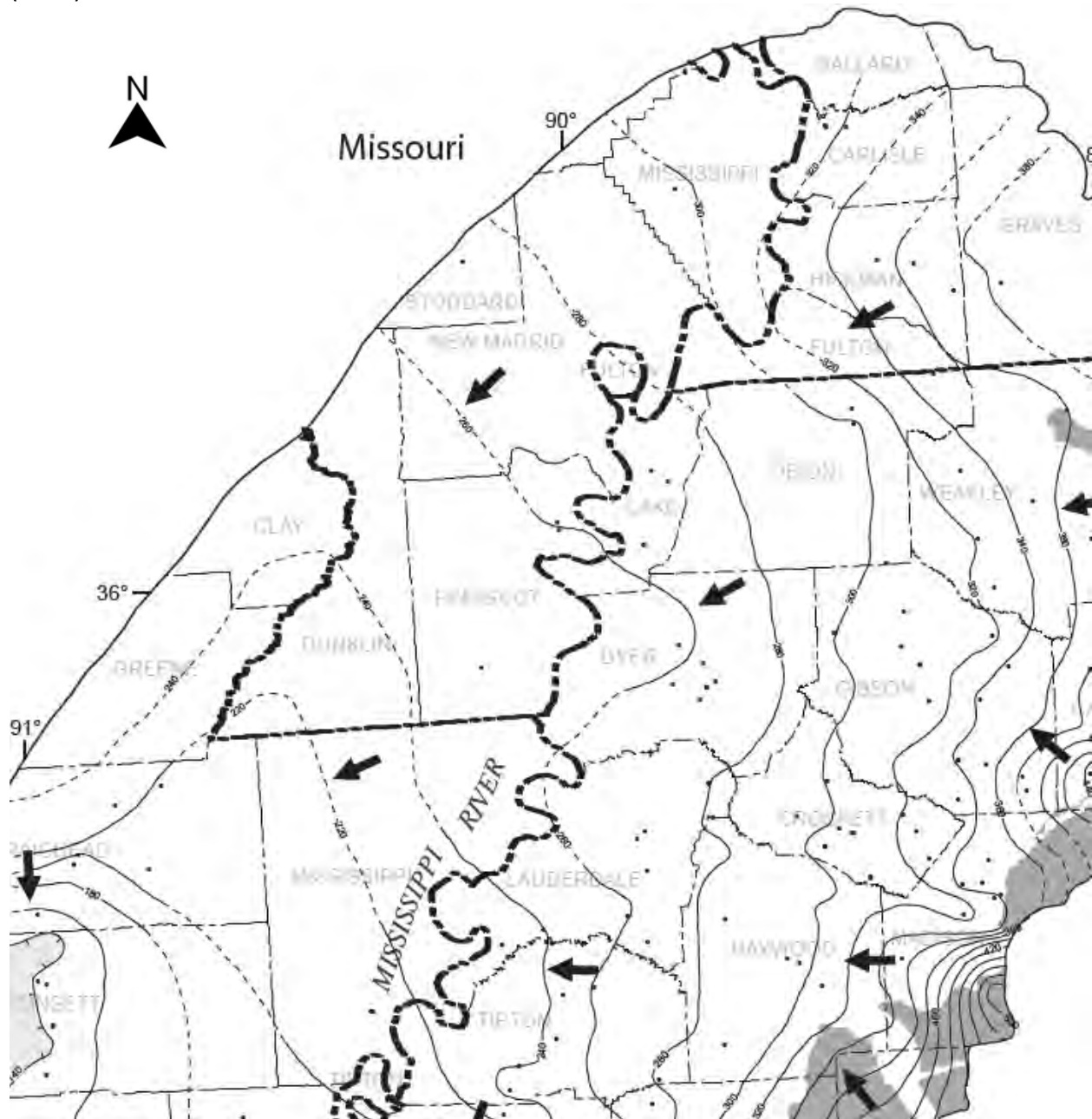


Figure 15: USGS groundwater level contour map (Schrader 2008).

We also reviewed more reports on the GWL condition of the Mississippi embayment, and according to the studies done by Clark (2011), and Clark and Hart (2009), we confirmed that Schrader's (2008) map is still the most updated GWL map for this area.

To establish the contour map of Tipton County, we also interpolated the contour lines from Lauderdale, Haywood, and Mississippi counties provided by Figure 15 (all contour lines are in

the format of ft.-NGVD 1929). Using ArcMap, we digitized the contour lines on a shapefile boundary of Tipton County (Figure 16) and the contour map was developed by the Inverse Distance Weighting (IDW) method. Figure 17 shows the GWL contour map of Dyer County that was used to develop the LPCs.

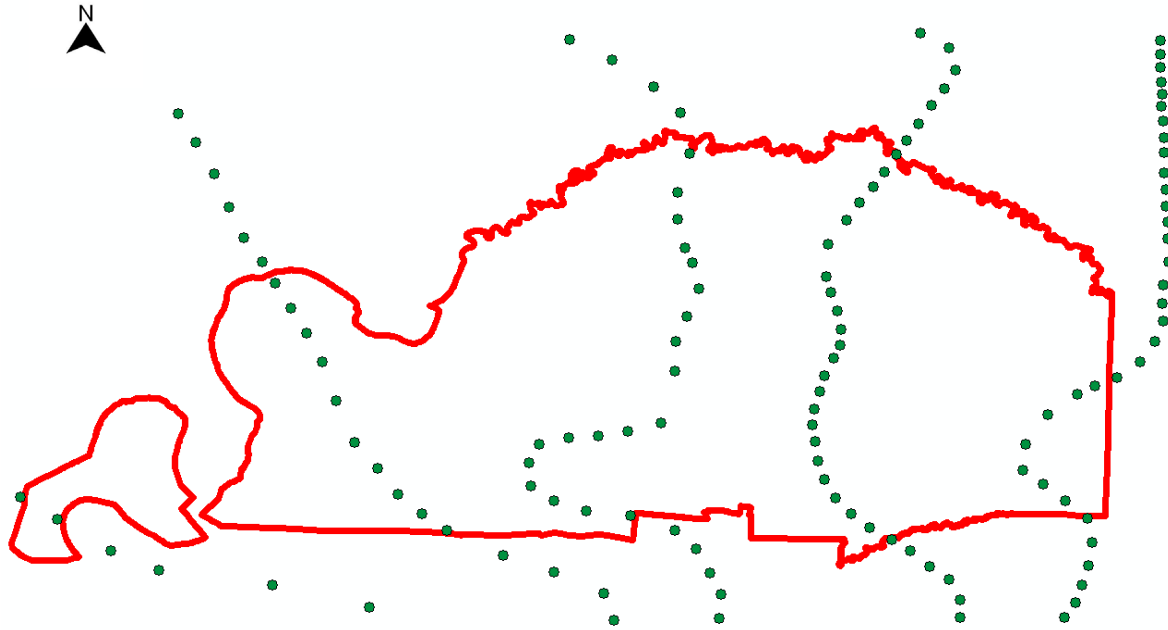


Figure 16: Digitized contour lines on Tipton County boundary shapefile in ArcMap.

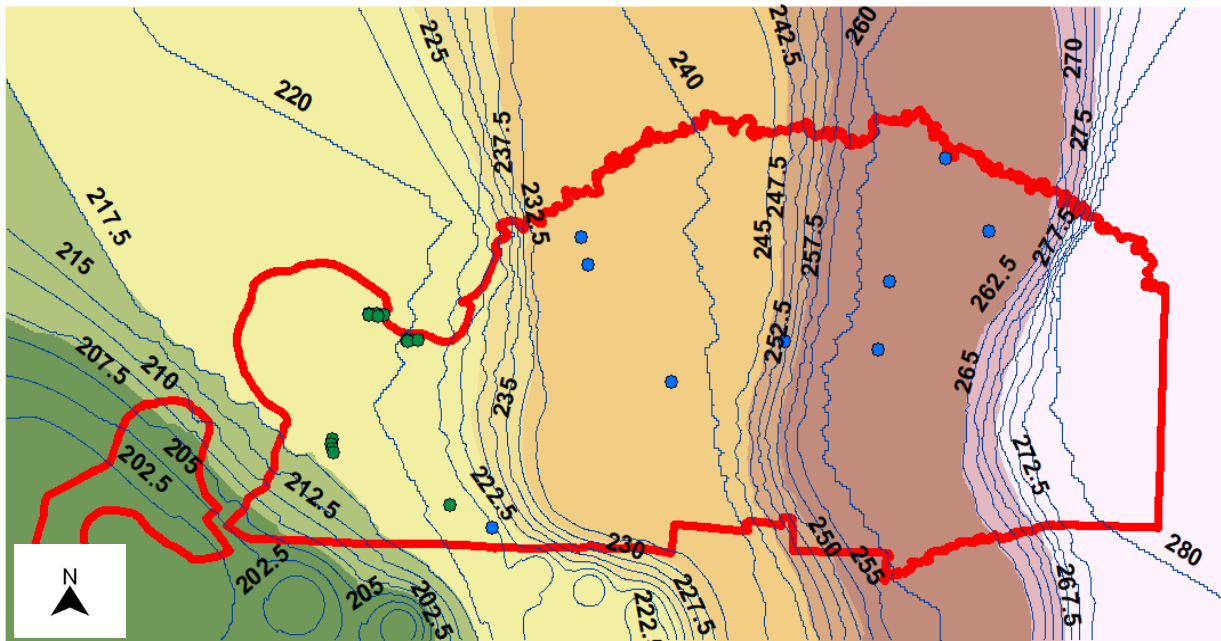


Figure 17: Groundwater level contour map for Tipton County.

For Lake, Dyer, and Lauderdale counties the accuracy of generated GWL based on Schrader’s map was verified by obtaining additional data for wells within Lake, Dyer, and Lauderdale County from the United States Geological Survey (USGS) groundwater data website (<https://maps.waterdata.usgs.gov>), but for Tipton County, as illustrated in Figure 18, there is only one inactive well available within Tipton County from the USGS database. Therefore, the GWL based on Schrader’s map could not be checked with current well data.

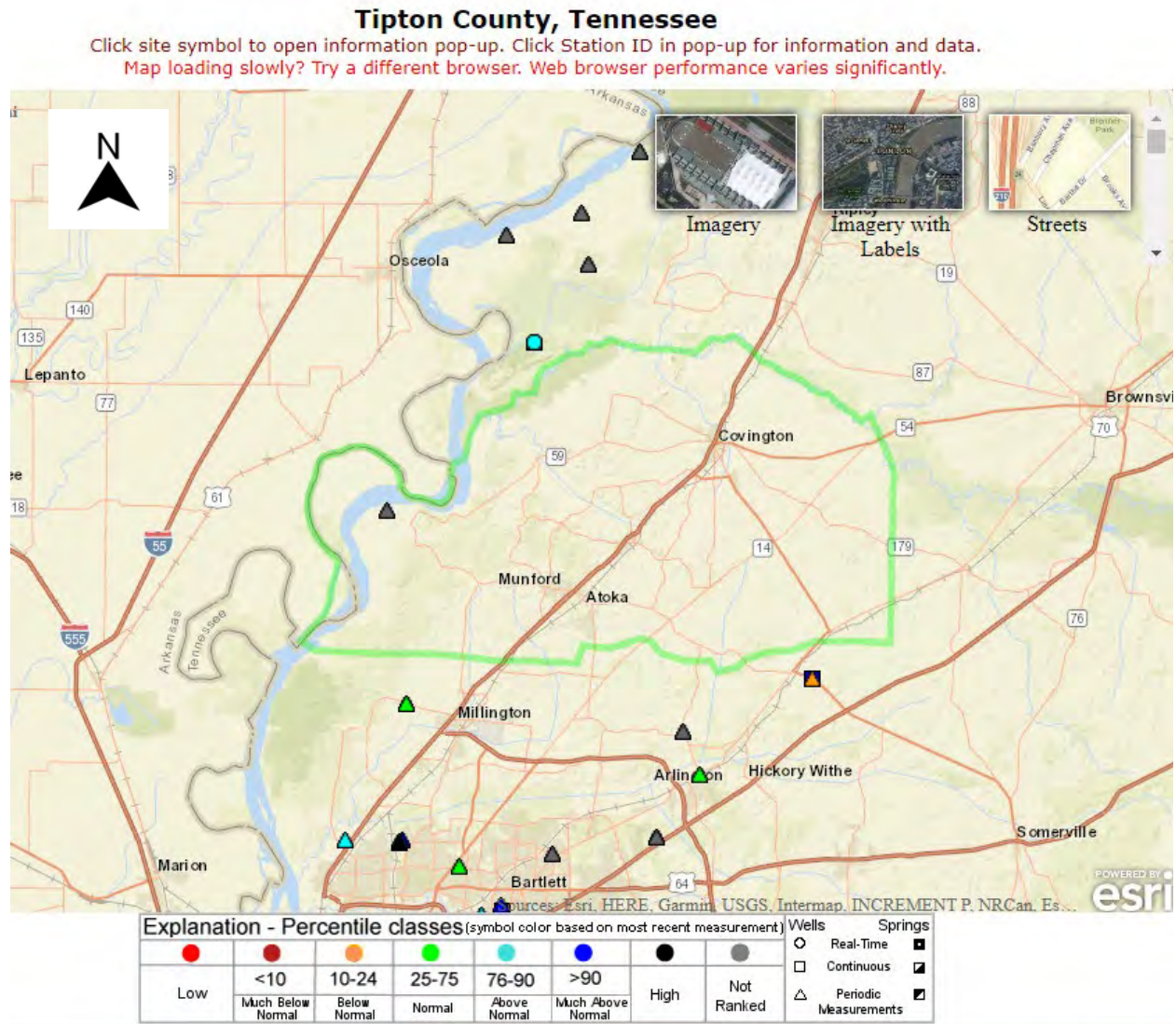


Figure 18: Location of the only USGS well in Tipton County.

### Methodologies Used to Develop Liquefaction Probability Curves

Using the same general procedure of developing LPCs used for Lake and Dyer, and Lauderdale counties (Cramer et al., 2019, 2020a, b), we generated the LPCs of Tipton County. To develop the LPCs of Tipton County, the following three general main steps were taken:

1. Calculating the factor of safety (FS) against liquefaction at a given depth in the soil profile of each soil boring using the simplified procedure (Seed and Idriss, 1971).

2. Calculating the liquefaction potential index (LPI and  $LPI_{ISH}$ ) of each soil boring location using:
  - Iwasaki et al. (1978, 1982) method or,
  - Maurer's (2015) framework denoted as the  $LPI_{ISH}$  method herein.
3. Developing LPCs for the probability of exceeding LPI of 5 and 15 and  $LPI_{ISH}$  of 5 for each primary surficial geologic unit.

Like Lauderdale County, for Tipton County due to the unavailability of any shear wave velocity data, LPCs of Tipton County have been developed based only on SPT field test data. The procedure of developing LPCs based on SPT data for each geologic unit is described in the subsequent section.

#### Liquefaction Probability Curves Based on the Standard Penetration Test (SPT)

Like Lake, Dyer, and Lauderdale counties, for Tipton County, the SPT boring logs were divided into 0.6 m (2 ft) increments, and each soil boring was summarized for SPT N values and USCS soil classifications to a depth of 20 meters (66 ft). Using the simplified procedure of Seed and Idriss (1971), initially, we computed the FS of every 0.6 m (2 ft) against liquefaction at each soil boring to a depth of 20 meters (66ft) and then using the two different approaches of LPI and  $LPI_{ISH}$  the probability of liquefaction surface manifestation was computed to develop LPCs. In both methods, the LPCs were developed for the same 10 Peak Ground Accelerations (PGA) of 0.1, 0.2, 0.3, 0.4, 0.5, 0.6, 0.7, 0.8, 0.9, and 1.0 and seven earthquake Magnitude ( $M_w$ ) of 5, 5.5, 6, 6.5, 7, 7.5, and 8 that we used in Dyer County and Lauderdale County studies (Cramer et al., 2020a, b). Thus, we determined the distribution of LPI and  $LPI_{ISH}$  for each of the 70 possible combinations of PGA and  $M_w$  using the same methodologies and equations that we utilized for Dyer County and Lauderdale County (Cramer et al., 2020a,b).

Details of LPI and  $LPI_{ISH}$  methods as well as the procedure of computing the probability of exceeding LPI values of 5 and 15 which are the lower bounds of "moderate" and "severe" liquefaction, respectively, based on the results of Iwasaki et al. (1978, 1982) and Toprak and Holzer (2003), can be found in the Lake, Dyer, and Lauderdale County studies (Cramer et al., 2019, 2020a, b), and  $LPI_{ISH}$  of 5 above which the liquefaction is occurring, according to Maurer (2015).

#### LPI-Based LPCs

The primary set of LPCs were developed based on Iwasaki's LPI approach in which it assumes that all liquefiable layers along the entire 20-meter (66 ft) soil profile contribute to the surficial manifestation of liquefaction without considering the impact of the non-liquefiable cap on liquefiable layers. Initially, the LPI-based LPCs were generated for three surficial geologic units of Lowland, Intermediate, and Upland separately. The total number of SPT soil borings that was utilized to develop LPI-based LPCs of Lowland, Intermediate, and Upland are 22, 34, and 10, respectively.

Figures 19, 20, and 21 show the LPCs for Lowland, Intermediate and Upland of the probability of exceeding LPI of 5 and 15 denoted as  $P[LPI>5]$  and  $P[LPI>15]$  versus the ratio of PGA over magnitude scaling factor (MSF).

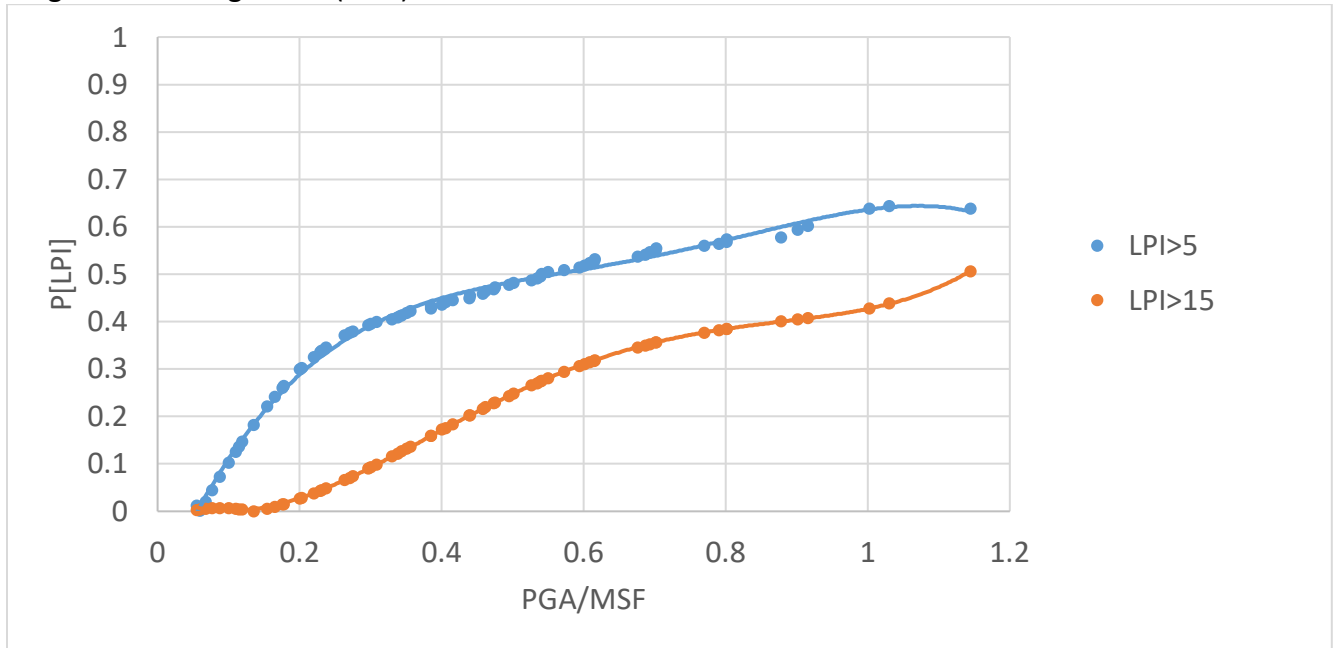


Figure 19: LPI-based Lowland LPCs from SPT data.

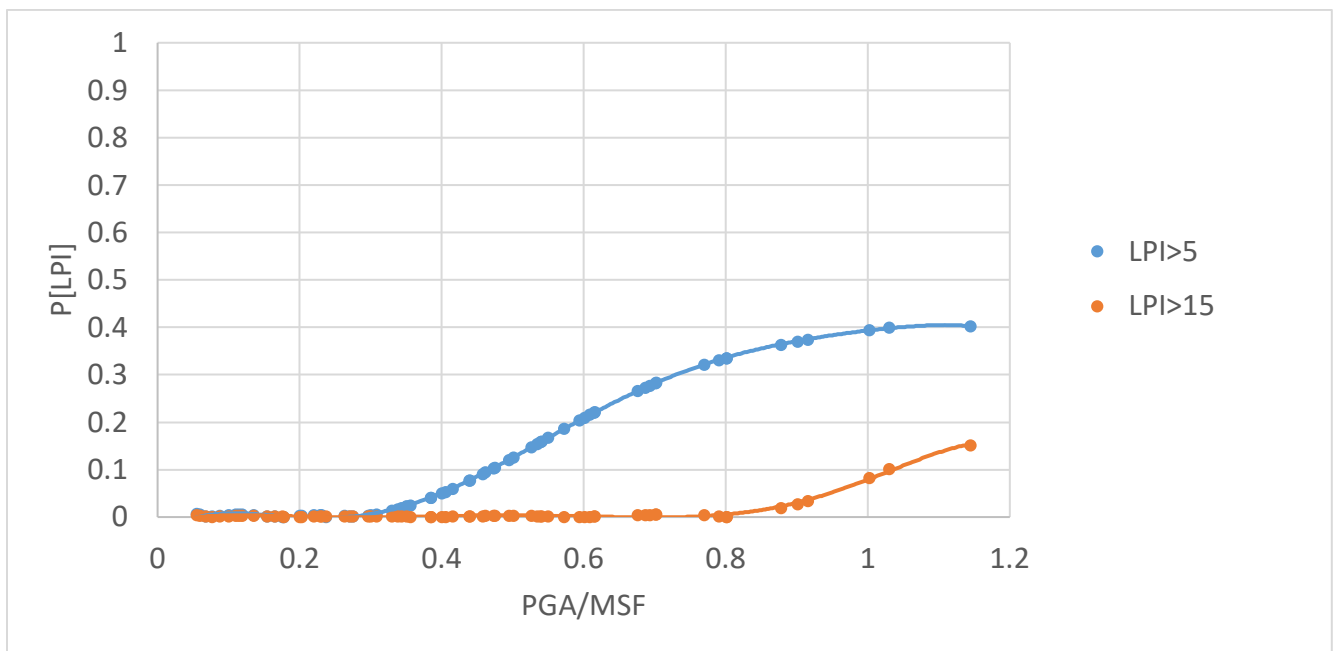


Figure 20: LPI-based Intermediate LPCs from SPT data.

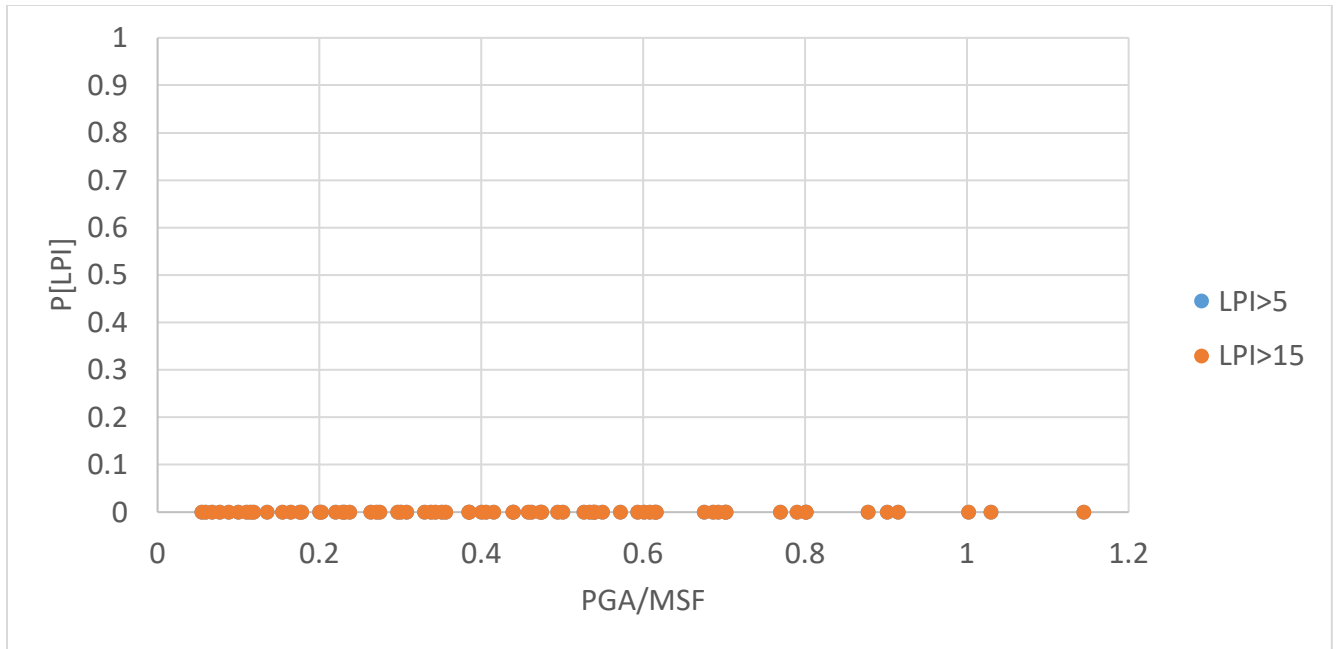


Figure 21: LPI-based Upland LPCs from SPT data.

As was expected Lowland LPCs are showing the highest probability of liquefaction because Lowlands are the most susceptible geologic units to liquefaction. The Uplands show a zero percent probability of liquefaction for the entire range of PGA/MSF for both LPI>5 and LPI>15. Table 3 provides the maximum probability of exceeding LPI>5 and LPI>15 for each geologic unit that was obtained from the LPCs at the highest ratio of PGA/MSF.

Table 3: the maximum probability of exceeding LPI>5 and LPI>15 at each geologic unit.

The maximum probability of exceeding	Lowland	Intermediate	Upland
P[LPI>5]	0.64 (64%)	0.40 (40%)	0.0 (0%)
P[LPI>15]	0.5 (50%)	0.15 (15%)	0.0 (0%)

As shown in Table 2, only 10 soil borings were obtained within the Upland geologic unit. Therefore, the SPT boring log data of Intermediate and Upland geologic units were combined to develop LPCs representing non-Lowlands as shown in Figure 22. The maximum probability of exceeding LPI>5 and LPI>15 at the highest ratio of PGA /MSF for the non-Lowland is 0.49 (49%) and 0.16 (16%), respectively. Therefore, comparing to the Intermediate and Upland maximum probabilities shown in Table 3, the overall probability of the combined Intermediate and Upland geologic units represented by the non-Lowland LPC increases because the Upland LPCs are completely zero percent for both LPI>5 and LPI>15.

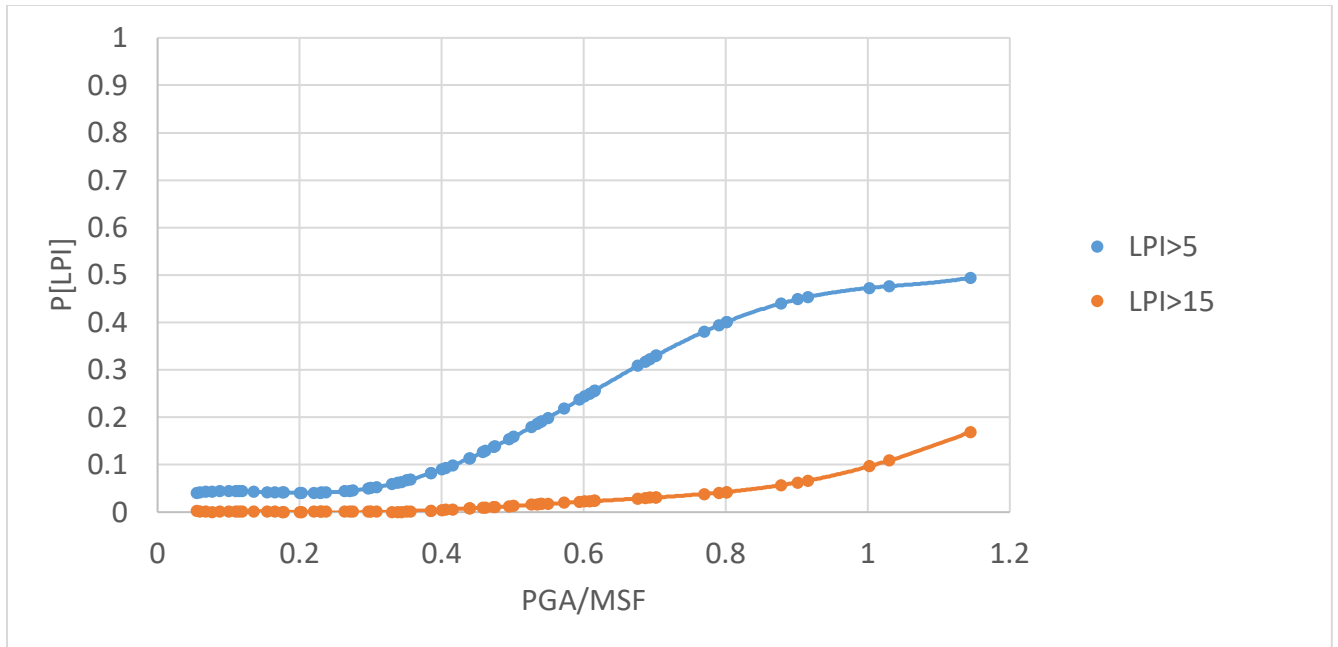


Figure 22: LPI-based non-Lowland LPCs from SPT data.

### LPI<sub>ISH</sub>-Based LPCs

Like Dyer and Lauderdale counties, additional LPCs for Tipton County were developed based on Maurer’s framework in which by using the LPI<sub>ISH</sub> index, the impact of non-liquefiable soil layers on surficial liquefaction manifestation is considered. The detail of Maurer’s framework is provided in the Seismic and Liquefaction Hazard Mapping of Dyer County report (Cramer et al., 2020a). However, the P[LPI<sub>ISH</sub>>15] was not determined for Tipton County because Maurer’s framework (Maurer, 2015) is based on only P[LPI<sub>ISH</sub>>5].

Similar to the LPI based LPCs, the LPI<sub>ISH</sub> based LPCs were generated for Lowland and non-Lowland geologic units and the non-Lowland represents a combination of the Intermediate and Upland geologic units. Figures 23 and 24 show the Lowland and non-Lowland LPCs, respectively.

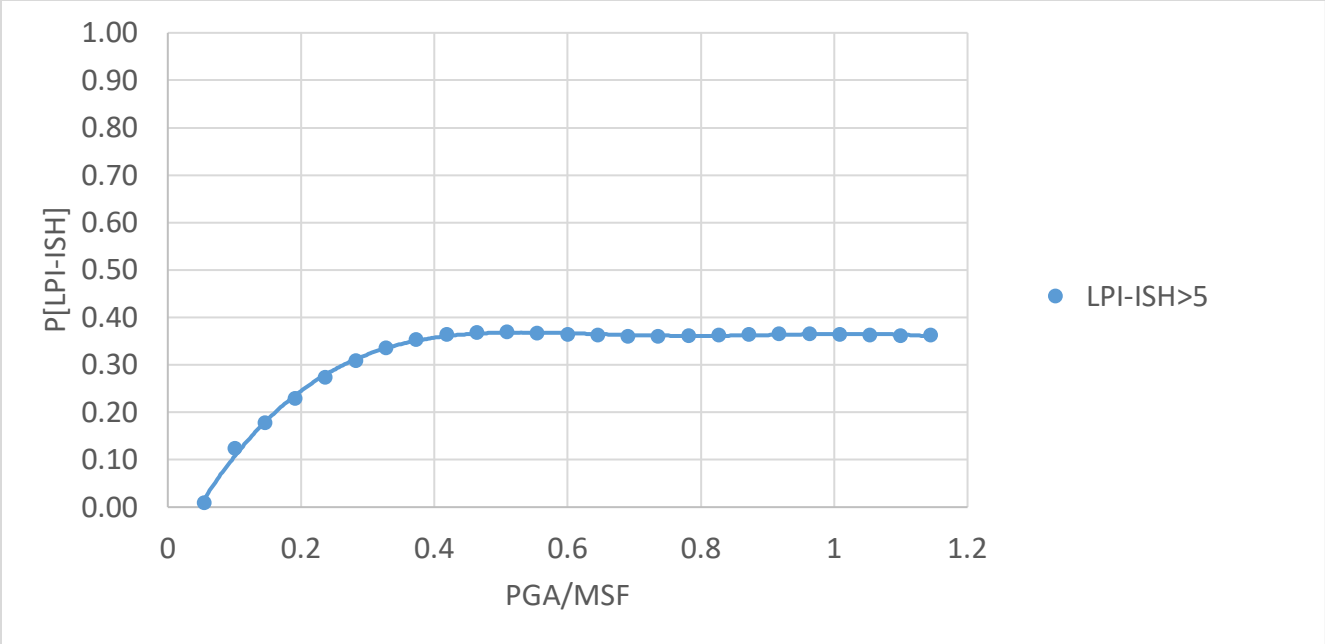


Figure 23: LPI<sub>ISH</sub> based LPCs of Lowland from SPT data.

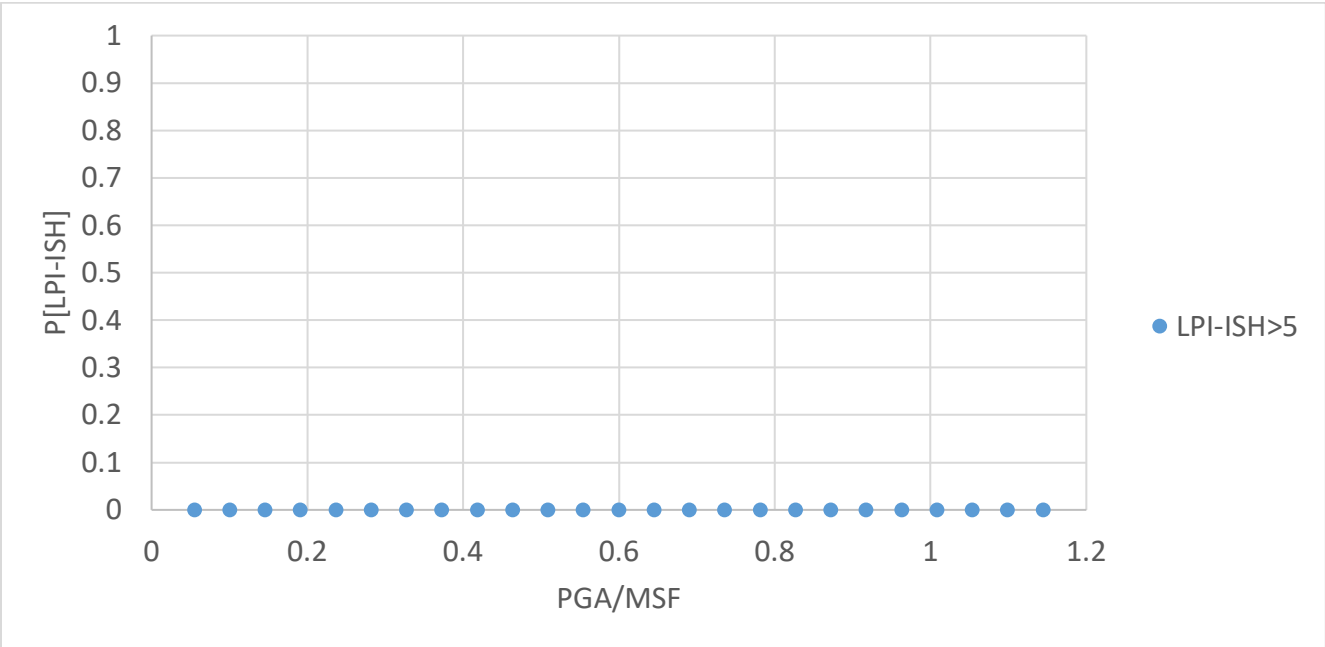


Figure 24: LPI<sub>ISH</sub> based LPCs of non-Lowland from SPT data.

For the Lowland, the LPI<sub>ISH</sub> based LPCs reach the maximum liquefaction probabilities of 36% for LPI<sub>ISH</sub>>5. However, the non-liquefiable layer impact is stronger for non-Lowlands because the LPC shows a zero percent probability of liquefaction for all 70 earthquake scenarios.

The results of the LPI- and LPI<sub>ISH</sub>- based methods are compared and discussed in the next section.

### Comparison of LPI- and LPI<sub>ISH</sub>-based LPCs

The LPI- LPI<sub>ISH</sub>-based LPCs of Lowland and non-Lowland for  $P[LPI-LPI_{ISH}>5]$  are compared in this section.

Figure 25 provides a comparison of LPCs for Lowland areas of Tipton County for  $P[LPI>5]$ . Figure 25 indicates that the probability of liquefaction provided by the LPCs based on the LPI<sub>ISH</sub> framework is significantly lower than the probability of liquefaction provided by the LPCs based on the LPI framework especially at higher ratios of PGA/MSF in which the maximum difference is about 28% for  $P[LPI>5]$ .

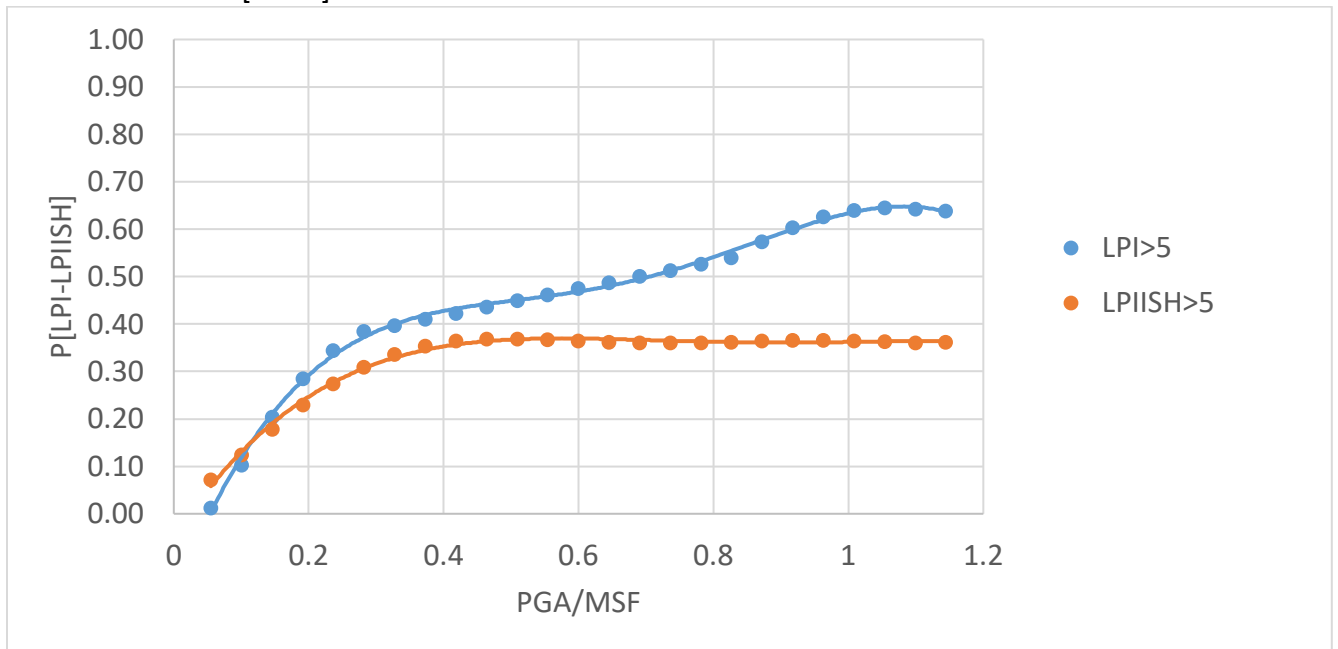


Figure 25: LPI- and LPI<sub>ISH</sub>-based Lowland LPCs for  $P[LPI>5]$ .

Figure 26 provides a comparison of LPCs for the non-Lowland areas of Tipton County for  $P[LPI>5]$ . Figure 26 indicates that the probability of liquefaction provided by the LPCs based on the LPI<sub>ISH</sub> framework is lower than the LPCs based on the LPI framework especially at higher ratios of PGA/MSF in which the maximum difference is about ~50% for moderate to severe liquefaction ( $LPI>5$ ).

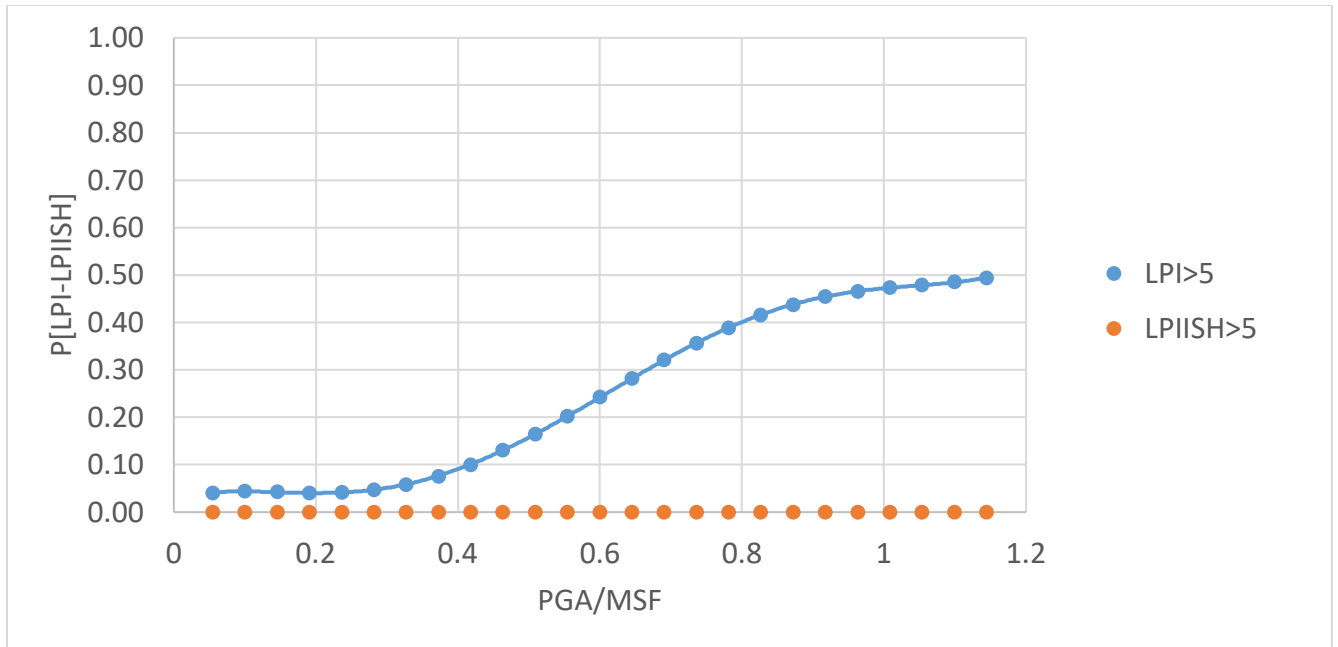


Figure 26: LPI- and LPI<sub>ISH</sub>-based non-Lowland LPCs for P[LPI>5].

As mentioned previously, the effect of upper non-liquefiable soil layers on the surface manifestation of liquefiable soil layers is the most notable difference between LPI and LPI<sub>ISH</sub> methods. LPI does not consider the impact of non-liquefiable soil layers while LPI<sub>ISH</sub> considers it. Thus, considering the impact of non-liquefiable layers causes the LPI<sub>ISH</sub> based LPCs to show lower liquefaction probability than LPI-based LPCs. Also, it should be noted that the weighting function in LPI and LPI<sub>ISH</sub> equations are different which causes assigning different weights to the liquefiable layers, consequently different LPI and LPI<sub>ISH</sub> values for the same soil layer. Further information regarding the weighting functions of LPI and LPI<sub>ISH</sub> methods can be found in Cramer et al. (2020a and 2020b). For a better understanding of the reason for differences between LPI and LPI<sub>ISH</sub> based LPCs especially for Lowlands, we conducted more detailed analyses of soil boring logs of Lowland areas of Tipton County as far as percentage and depth of liquefiable and non-liquefiable layers that are presented herein.

Each of the 22 soil boring profiles of the Lowland region was divided into 0.6 m (2 ft) increment to the maximum depth of 20 meters (66 ft) This provided a total of 726 soil layers. Of the 726 soil layers, 18% percent are liquefiable (saturated loose sand with less than 35% fines) and 82% of the layers are non-liquefiable layers. Thus, most soil layers are non-liquefiable as shown in Figure 27.

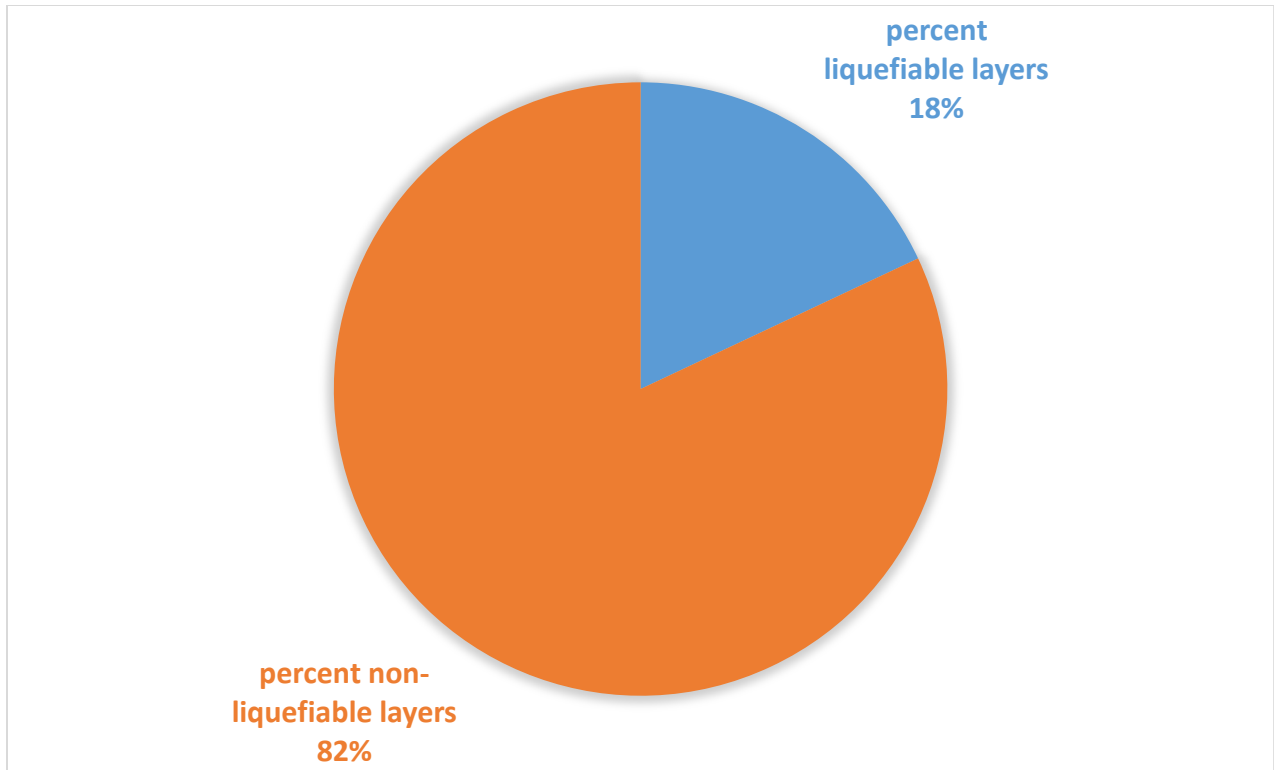


Figure 27. Percent liquefiable and non-liquefiable layers.

Both methods give more weight to the shallower liquefiable layers than deeper layers, however, in the  $LPI_{ISH}$  method the weighting function is based on power-law, and in the LPI method, the weighting function is linear (details are provided in Dyer County study, Cramer et al., 2020a). Figure 28 shows the distribution of liquefiable and non-liquefiable layers of 22 Lowland soil borings within the various depths to the first 10 meters. Most of the layers of the first 10 meters of soil borings are non-liquefiable. Therefore, since most of the soil layers from 0 to 10 m depth are non-liquefiable, by considering the impact of non-liquefiable layers on liquefaction potential of liquefiable layers in the  $LPI_{ISH}$  method, the probability of liquefaction surface manifestation decreases and the  $LPI_{ISH}$  based LPCs show lower probability surface manifestation of liquefaction than LPI based LPCs.

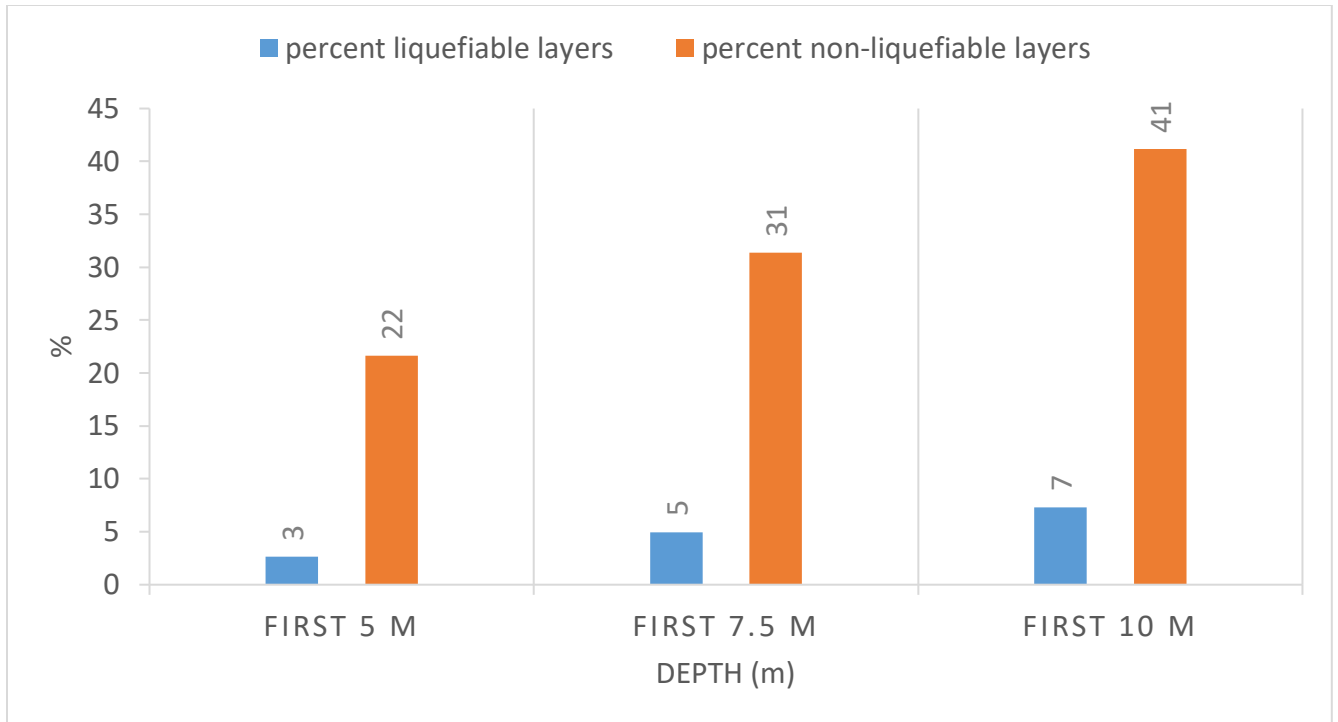


Figure 28. distribution of liquefiable and non-liquefiable layers along 20 meters depth.

#### Liquefaction Probability Curves Based on the Shear Wave Velocity ( $V_s$ )

For Tipton County, due to time overlap with the COVID-19 situation, the geophysics team was not able to conduct shear wave velocity tests, hence, we could not perform liquefaction potential analysis based on  $V_s$  data.

#### LPCs for liquefaction hazard maps of Tipton County

In this section, we discuss the recommended LPCs for Lowland and non-Lowland parts of Tipton County that are used to develop liquefaction hazard maps of Tipton County.

#### Lowland LPCs Recommendation

For the Lowland surficial geologic unit of Tipton County, the LPCs were developed based on SPT data of 22 soil boring logs. Using two different approaches of LPI and  $LPI_{ISH}$ , the LPCs were developed for Lowlands of Tipton County for two index thresholds of 5 and 15 based on the LPI approach and index threshold of 5 for the  $LPI_{ISH}$  approach. The main and the most significant difference between the two approaches is that LPI does not consider the impact of upper non-liquefiable soil layers on liquefaction surface manifestation at a soil profile while  $LPI_{ISH}$  does. Thus, the  $LPI_{ISH}$  based LPCs provide significantly lower LPCs than LPI-based LPCs for  $P[LPI - LPI_{ISH} > 5]$  because there is a significant proportion of non-liquefiable soil layers compared to liquefiable layers as shown in Figure 27 especially near the soil surface as shown in Figure 28.

Thus, to consider the influence of non-liquefiable soil layers on liquefaction hazard maps, it is suggested that the liquefaction hazard maps of the Lowland part of Tipton County be based on the LPCs of both frameworks of Iwasaki and Maurer as presented in Figures 19 and 23, respectively.

#### Non-Lowland LPCs Recommendation

For the non-Lowland parts of the county which are the combination of Intermediate and Upland surficial geologic units, the LPCs were also developed based on both frameworks of Iwasaki's LPI and Maurer's  $LPI_{ISH}$  using SPT data from 37 soil borings. As noted in the Comparison of LPI- and  $LPI_{ISH}$ -based LPCs section of this report, the LPI-based LPCs show a higher trend than  $LPI_{ISH}$ -based LPCs due to the impact of non-liquefiable soil layers on liquefaction surface manifestation. For the non-Lowland areas of Tipton County, it is suggested that the liquefaction hazard maps be developed based on both sets of Iwasaki and Maurer LPCs as provided in Figures 22 and 24, respectively.

#### Geotechnical summary

Using the same general procedure that we utilized to develop LPCs for Lake, Dyer, and Lauderdale counties (Cramer et al., 2019, 2020a, 2020b), we generated the LPCs of Tipton County. Due to the COVID-19 situation, the  $V_s$  field test data were not obtained and the LPCs for Tipton County were developed based only on SPT boring logs data.

The surficial geology of Tipton County consists of three primary units of Lowland, Intermediate, and Upland. A total of 22, 27, and 10 SPT soil borings were selected from within each of these geologic units, respectively, from the total of 113 total borings obtained using the boring selection criteria summarized in the SPT Data section.

The LPCs of Tipton County were developed based on both the Iwasaki's LPI approach and Maurer's  $LPI_{ISH}$  framework. Initially, the LPI-based LPCs were generated for Lowland, Intermediate, and Uplands that were shown in Figures 19, 20, and 21, respectively. For each geologic unit, the LPCs were developed for  $P[LPI>5]$  and  $P[LPI>15]$  which represent the "moderate to severe" and "severe" probability of liquefaction, respectively. However, only 10 soil borings were obtained within the Upland geologic unit. Therefore, the SPT boring log data of Intermediate and Upland geologic units were combined to develop LPCs representing non-Lowlands as shown in Figure 22. In summary, LPCs were developed for Lowland and non-Lowland geologic units.

Additionally, for the Lowlands and the non-Lowlands parts of Tipton County, another set of LPCs was developed based on Maurer's (2015)  $LPI_{ISH}$  framework. The  $LPI_{ISH}$  based Lowland and non-Lowland LPCs are illustrated in Figures 23 and 24, respectively. The  $LPI_{ISH}$  based LPCs are for  $LPI_{ISH}>5$ .

A comparison was made between the Lowland and non-Lowland LPI and LPI<sub>ISH</sub> based LPCs of Tipton County in Figures 25 and 26. For both the Lowland and non-Lowland areas of Tipton County, the probability of liquefaction provided by the LPCs based on the LPI<sub>ISH</sub> framework are significantly lower than the LPCs based on the LPI framework especially at higher ratios of PGA/MSF.

For the Lowland parts of Tipton County, it is suggested that the liquefaction hazard maps be based on both LPI- and LPI<sub>ISH</sub>-based LPCs developed from SPT data of 22 soil borings. For the Lowland parts of Tipton County, the LPI- and LPI<sub>ISH</sub>-based LPCs are presented in Figures 19 and 23, respectively. For the non-Lowland areas, it is recommended that the LPCs of LPI and LPI<sub>ISH</sub> based approaches that were developed based on the SPT data of 37 boring logs within the Intermediate and Upland parts of the county be used to develop liquefaction hazard maps. The non-Lowland LPI- and LPI<sub>ISH</sub>-based LPCs are provided in Figures 22 and 24, respectively.

It is also recommended that as additional soil boring data becomes available within Tipton County, that the LPCs be updated.

### Seismic Measurements

No seismic measurements were made in Tipton County as part of this project. It was deemed unnecessary to make seismic measurements like was done in Lake, Dyer, and Lauderdale Counties because the geology was not significantly different in Tipton County and the measurements made in Lauderdale County were not significantly different from those in Dyer County. We adopted the lowlands and non-lowlands Quaternary reference Vs profiles from the Dyer and Lauderdale County studies (Figure 29).

We compare in Figure 29 the two Lauderdale County representative velocity profiles with the uplands average profile of Romero and Rix (2001) and a representative uplands site velocity profile for Shelby County. At shallower depths less than 20 m, the uplands profiles agree quite well. In Tipton County the top of the faster velocity Eocene sediments can be as shallow as 20 m or less, which can start biasing the MASW profiles to faster velocities especially below 30 m. In Lauderdale County in the non-lowland areas, the top of the Eocene is typically 30 m. A check of the estimated depth to the top of the Eocene at MASW sites from the geology model with the depth at which the Vs exceeds 500 m/s (estimated Eocene Vs) in the MASW profiles shows a fairly good correlation both in Dyer and Lauderdale Counties.

# DyLa Co Vs Profiles

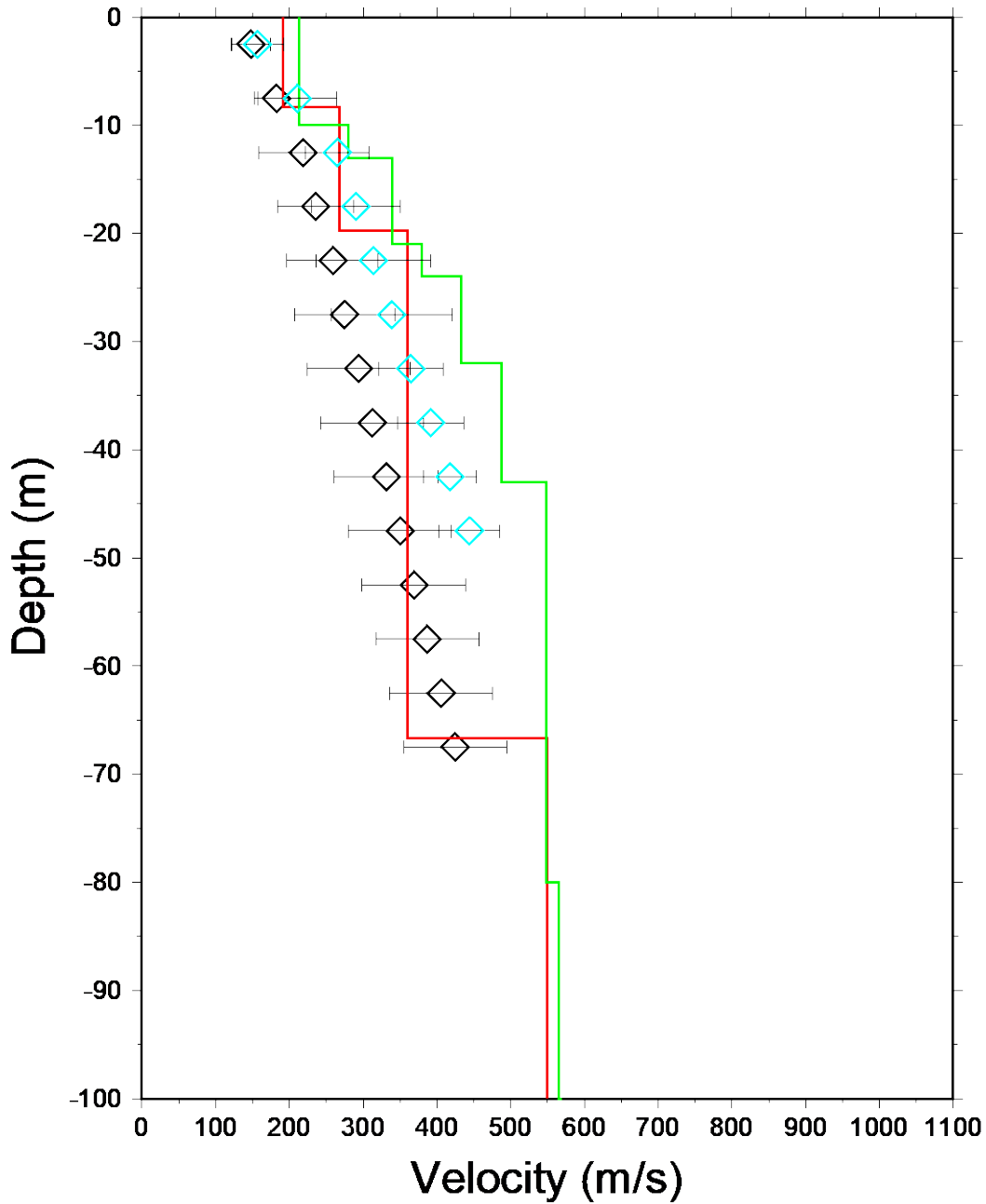


Figure 29: Comparison of adopted lowlands (black) and non-lowlands (cyan) velocity profiles for Tipton County with the Romero and Rix (2001) uplands average profile (green line) and typical velocity profile (red line) in Shelby County.

## Hazard Maps Development

### Methodology

A standard methodology for including the effects of local geology in seismic and liquefaction hazard estimates was used in this study. We followed the approach of Cramer et al. (2006, 2008, 2014, 2017, and 2018a) of developing site amplification distributions on a grid, applying those distributions to modify hard rock hazard curves to geology-specific hazard curves and develop seismic hazard maps, and then applying geology-specific liquefaction probability curves to develop liquefaction hazard maps. The site amplification distributions are based on the 3D geological, geotechnical, and seismological models developed above for Tipton County. The 2014 U.S. Geological Survey (USGS) National Seismic Hazard Project's seismic hazard model (seismic sources and ground motion attenuation model of Petersen et al., 2014) for hard rock was modified using our Tipton County site amplification distributions. Probabilistic seismic hazard maps were generated from the USGS probabilistic model and scenario (deterministic) seismic hazard maps were generated using selected scenario fault ruptures (earthquakes) and the USGS ground motion attenuation model. The resulting peak ground acceleration (PGA) seismic hazard maps were then modified using appropriate Tipton County liquefaction probability curves (discussed above) to generate liquefaction hazard maps (both probabilistic and scenario).

### Tipton County Shear-wave Velocity Model

Seismic hazard maps with the effects of local geology depend on developing site amplification distributions on a grid for the 3D geology of the study area. The 3D geology is converted to geologic (sediment) profiles on a uniform grid. The geology layers are converted to shear-wave velocity ( $V_s$ ) profiles at each grid point and input to a geotechnical soil response program (SHAKE91), along with appropriate geotechnical properties, to develop site response distributions at each grid point using the University of Memphis High Performance Computing (HPC) facility. The site amplification distributions model frequency and amplitude dependent amplification/deamplification at the surface of hard rock ground motions input at the bottom of the sediment profile.

The Tipton County representative velocity models used were developed from published and measured  $V_s$  profiles in and near the county as described above. Three separate models were developed for Lauderdale County, two for the Quaternary sediments above the top of the Eocene deposits and one for the geologic layers from the Eocene to the Paleozoic. The two Quaternary representative velocity models were divided between lowlands and non-lowlands as shown in Figure 29 above.

The Quaternary  $V_s$  models are a step-wise gradient model developed from the shallow  $V_s$  observations with different gradients for lowlands and non-lowlands models. The depth to the top of the Eocene layer varies for each profile between less than 30 m and 70 m depth so the gradient trend was projected downward from the all Quaternary sediment trend above 30 m to

50 -70 m in 5 m depth steps. The Eocene Vs jumps to 515 m/s at the top of that layer. Appropriate uncertainties based on the statistics (standard deviation) of the profile averaging at each depth interval were developed and applied in the sediment profile randomization process employed in the development of the site amplification distributions at each grid point.

The Eocene to Paleozoic Vs model is the same as developed for Lake County (Cramer et al., 2019). It was developed from the CUSSO deep hole site in Kentucky (Woolery et al., 2016) and published deeper embayment measurements in and near Lake County plus Vs models from Shelby County (Cramer et al., 2006). The borehole geological information mainly constrained the depths to the top of the Eocene, Cretaceous, and Paleozoic (bedrock) layers. In Lake County, very limited observations were available for other intermediate geological layers such as the top of the Memphis Sand, Flour Island clay, Fort Pillow sand, and Old Breastworks clay. The depth to the top of these four geological layers are needed to define the geology and Vs profiles beneath Tipton County. Using the limited observations in Lake County for these four layers and the better constrained isopachs for the top of the Eocene and Cretaceous, we developed a scheme to estimate the depth to the tops of the four intermediate layers between the Eocene and Cretaceous layers. Taking the depth difference between the tops of the Eocene and Cretaceous layers as unity, statistical estimates (average and standard deviation) were determined from the few available measurements for the depth difference between the top of the Eocene and the tops of each intermediate layer. The results in Table 4 are in fraction of the distance between the tops of the Eocene and Cretaceous. We then used these averages and standard deviations to estimate the depth with uncertainty to the top of the intermediate layers at each grid point. Vs values and uncertainties assigned to each intermediate layer was determined from the CUSSO Vs profile and checked and adjusted with available deeper Vs profile observations in Lake County and from the Shelby Co model. Because the geology model for Tipton County also included the depth to the top of the Memphis Sand within the county (Figure 6), we used the actual geology model values instead of the estimated values just described for the top of the Memphis Sand. Figure 30 and Tables 5 and 6 show the resulting deeper Vs model and uncertainties used in the site amplification distribution calculations at each grid point for lowlands and non-lowlands, respectively.

As a further check on the intermediate Vs profile model developed for Lake County, we compared our model and available observations with the Vs profile from ambient noise (surface-waves) based Vs profile by Chunyu Liu (Figure 31). Liu's results are from the Non-Volcanic Tremor (NVT) L-shaped array of 19 broadband stations with a 60m spacing (600 m on a side). The NVT array was located near Mooring in Lake County. Clearly in Figure 31 below 150 m depths the Liu profile agrees with our model and other observations within the uncertainty. Above 150 m the Liu profile estimates of Vs are lower, but still within uncertainty, although with a loss of resolution in Liu's profile above 50 m. Liu did find an Vs anisotropy between 100 and 140 m depths.

# Lake Co Vs Profiles

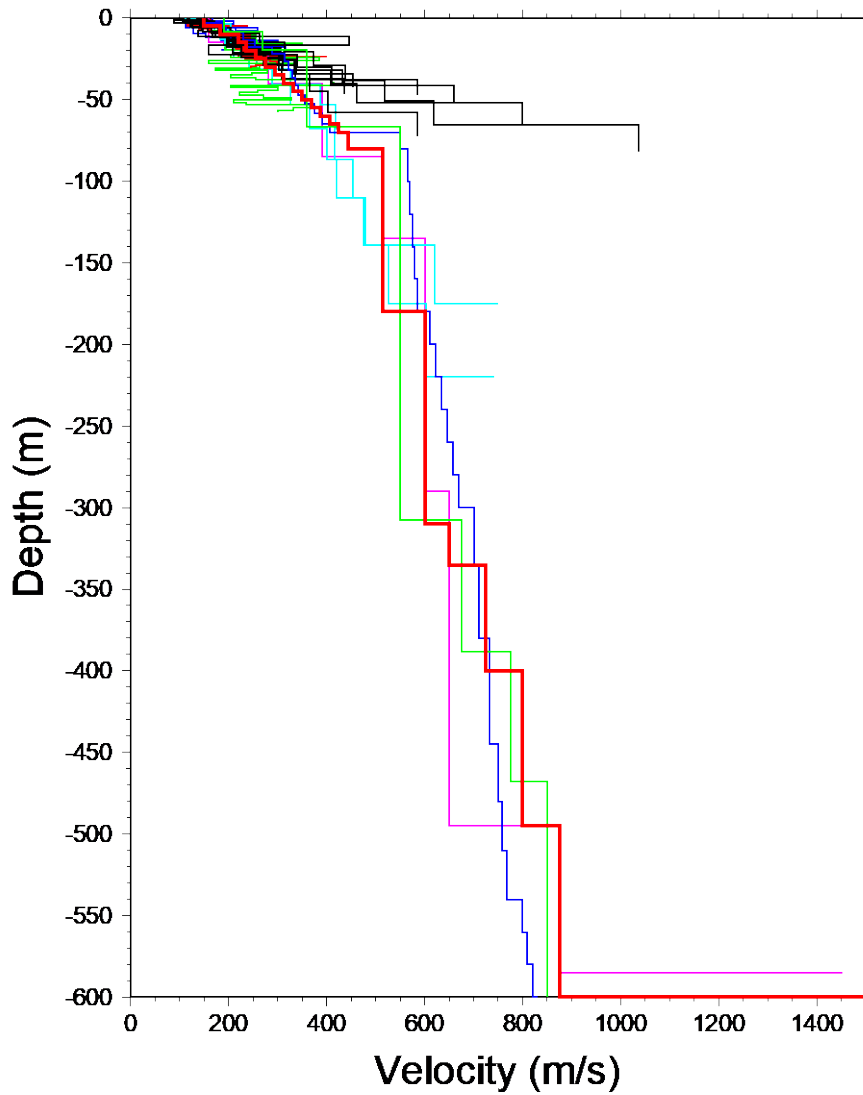


Figure 30: Vs profiles down to 600 m depth with Lake County Quaternary Vs model shown in heavy red line. Thin colored lines are published Vs profiles. Thin black lines are MASW profiles measured as a part of the Lake County study. The magenta profile is the CUSSO (Kentucky) deephole profile. The deeper green profile is the Shelby County reference profile. The blue profile is the Romero and Rix (2001) profile.

Table 4: Intermediate layer statistics in fraction of Cretaceous-Eocene depth difference.

Top of Formation	Fractional Distance	Fractional Std. Deviation	# of Observations
Memphis Sand	0.234	±0.029	6
Flour Island (clay)	0.546	±0.034	6
Fort Pillow (sand)	0.611	±0.048	5
Old Breastworks (clay)	0.771	±0.035	5

Table 5: Lowlands geotechnical profile used in 3D geology hazard model. Uncertainties are one std. deviation.

Formation	DepthToTop(m)	Damping	Density(g/cc)	Velocity(m/s)
Alluvium	0.	0.05	2.00	148±13
	5.±0.75	0.05	2.00	183±15
	10.±0.75	0.03	2.00	219±30
	15.±0.75	0.03	2.00	236±26
	20.±0.75	0.03	2.00	259±31
	25.±0.75	0.03	2.00	275±34
	30.±0.75	0.02	2.00	294±35
	35.±0.75	0.02	2.00	312±35
	40.±0.75	0.02	2.00	331±35
	45.±0.75	0.02	2.00	350±35
	50.±0.75	0.02	2.00	369±35
	55.±0.75	0.02	2.00	387±35
	60.±0.75	0.02	2.00	406±35
	65.±0.75	0.02	2.00	425±35
70.±0.75	0.02	2.00	444±35	
Eocene	80.±1.00	0.02	2.00	515±127
Memphis Sand	180±12	0.02	2.00	600±50
Flour Island	310±7.5	0.02	2.00	650±25
Fort Pillow	335±15	0.01	2.00	725±15
Old Breastworks	400±13	0.01	2.00	800±25
Cretaceous	495±13	0.01	2.50	875±63
Paleozoic	600±13	0.001	2.80	2800

Table 6: Non-lowlands geotechnical profile used in 3D geology hazard model. Uncertainties are one std. deviation.

Formation	DepthToTop(m)	Damping	Density(g/cc)	Velocity(m/s)
Alluvium	0.	0.05	2.00	157±13
	5.±0.75	0.05	2.00	211±15
	10.±0.75	0.03	2.00	265±30
	15.±0.75	0.03	2.00	290±26
	20.±0.75	0.03	2.00	314±31
	25.±0.75	0.03	2.00	339±34
	30.±0.75	0.02	2.00	365±35
	35.±0.75	0.02	2.00	392±35
	40.±0.75	0.02	2.00	418±35
	45.±0.75	0.02	2.00	444±35
	50.±0.75	0.02	2.00	470±35
	55.±0.75	0.02	2.00	496±35
	Eocene	70.±1.00	0.02	2.00
Memphis Sand	180±12	0.02	2.00	600±50
Flour Island	310±7.5	0.02	2.00	650±25
Fort Pillow	335±15	0.01	2.00	725±15
Old Breastworks	400±13	0.01	2.00	800±25
Cretaceous	495±13	0.01	2.50	875±63
Paleozoic	600±13	0.001	2.80	2800

# Lake Co Vs Profiles

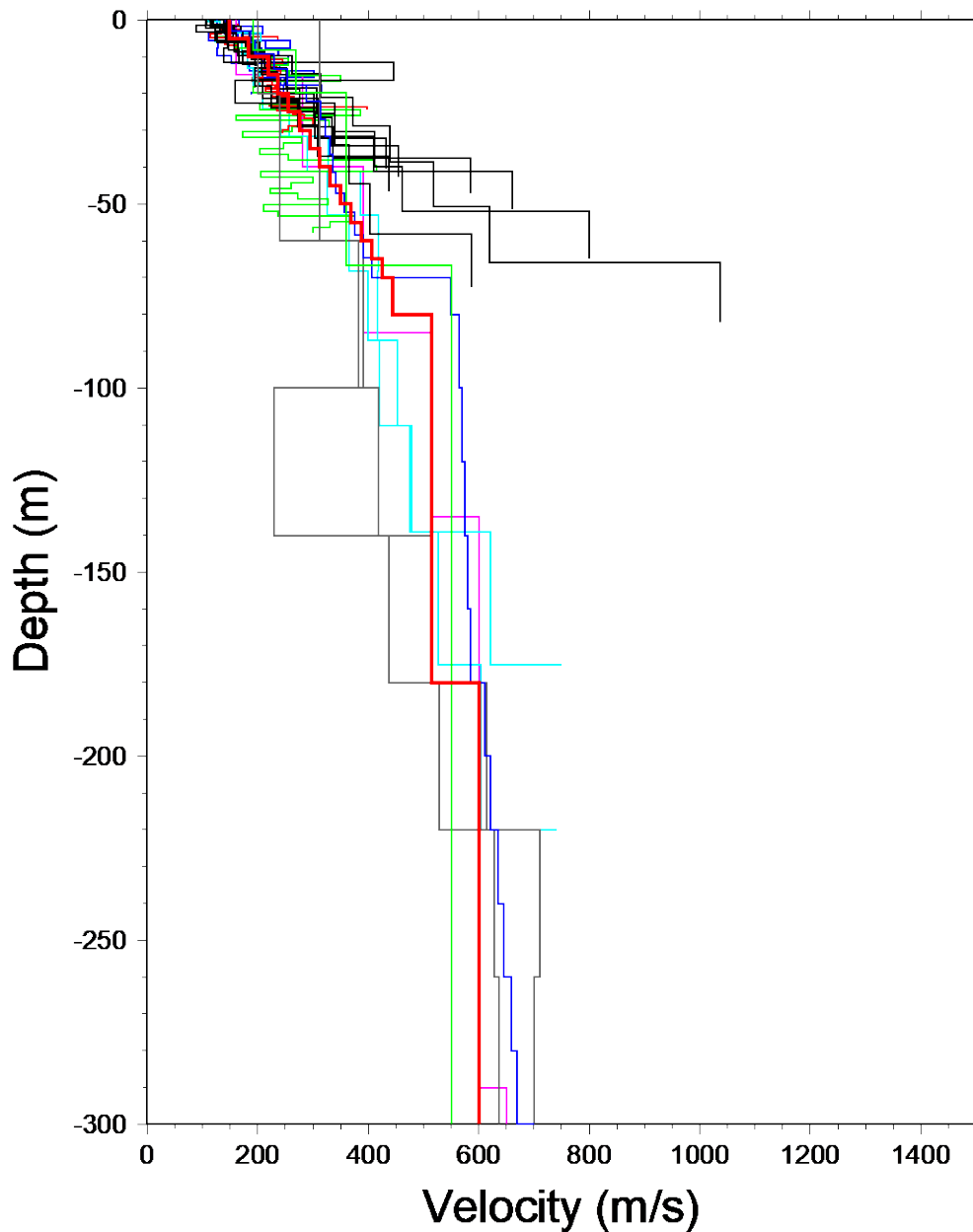


Figure 31: Vs profiles down to 300 m depth with Lake County Quaternary Vs model shown in heavy red line. The grey lines are Chunyu Liu's NVT profiles. The other profiles are colored as indicated in Figure 30.

## Grids

There is one grid size used in our Tipton County study. The 3D geology for the depth to the top of the Eocene, Memphis Sand, Cretaceous and Paleocene layers were provided on a 0.005-degree grid (~500 m). These geology inputs were combined using the Quaternary and deeper Vs models discussed above for site amplification distribution and seismic hazard calculations. The final seismic and liquefaction hazard maps use this 0.005-degree grid spacing.

## Time History Database

The site amplification distribution calculations use a suite of input time histories (seismograms) at the bedrock/sediment interface to estimate sediment response. Time histories are required by soil response computer programs to estimate site response. The time histories used are listed in Table 7 and have been used by Cramer et al. (2006, 2017, and 2018a) in similar seismic hazard analyses. At each grid point, the time history used is randomly selected for each iteration in the soil profile randomization to properly include uncertainty in the site amplification distribution calculations.

Table 7: Strong motion time series on rock used in the analysis (Cramer, 2006).

Earthquake	Station	Components
1989 <b>M</b> 6.9 Loma Prieta, California	G01	E, N
1992 <b>M</b> 7.1 Cape Mendocino, California	CPM	E, N
1992 <b>M</b> 7.3 Landers, California	JOS	E, N
1995 <b>M</b> 6.9 Kobe, Japan	KJM	E, N
1999 <b>M</b> 7.4 Kocaeli, Turkey	GBZ	W
	IZT	S
1999 <b>M</b> 7.6 Chi-Chi, Taiwan	TCU	N, W
1999 <b>M</b> 7.1 Duzce, Turkey	1060	E, N
Atkinson and Beresnev (2002)	<b>M</b> 7.5 and <b>M</b> 8.0 at Memphis, Tennessee	

## Hazard Maps

Seismic and liquefaction hazard maps have been developed for both probabilistic and scenario cases. Probabilistic hazard maps have been generated for 10%, 5%, and 2% probability of exceedance in 50 years. The 2%-in-50-year maps correspond to current building code standards and represent up to the 80 percentile New Madrid seismic ground motions. 5%-in-50-year maps are similar to median scenario ground motion maps for the **M**7 earthquakes in the New Madrid seismic zone and represent up to 60 percentile ground motions. The 10%-in-50-year maps correspond to an older design standard and only represent up to 35 percentile ground motions from the New Madrid seismic zone (NMSZ) sources. The 10%-in-50-year maps do not adequately represent expected median ground motions from New Madrid 1811-1812

earthquakes, are no longer recommended for design purposes by regulatory agencies, and are not presented here.

Median ground motion scenario (deterministic) hazard maps have been generated for seven scenario earthquakes (Table 8 and Figure 32A,B) and represent median expected ground motions from those earthquakes. The scenarios are for the largest earthquakes from the 1811-1812 New Madrid sequence, a **M6** earthquake in 1843, and for a hypothetical **M5.8** earthquake in Tipton County near Covington. Because of its distance from Tipton County and low expected ground motions, the historical **M6** in 1895 earthquake is not included in our collection of scenarios for Tipton County. The **M5.8** scenario represents the effects of recent **M5.5-6.0** Central and Eastern North American earthquakes if a similar size earthquake were to occur in Tipton County.

The ground motion periods represented in the Tipton County seismic hazard maps are peak ground acceleration (PGA), 0.2 s, and 1.0 s. 0.3 s maps have also been generated for compatibility with HAZUS, a risk and loss assessment package commonly used in loss analysis. The 0.2 and 0.3 s hazard maps are similar so the 0.3 s hazard maps are not shown in this report.

Table 8: Scenario earthquakes used in Tipton County study.

- M 7.7** on the Reelfoot Thrust (central segment)
- M 7.5 on the Cottonwood Grove Fault (SW segment)
- M 7.3 on the New Madrid North Fault (NE segment)
- M 6.9 “Dawn” Aftershock (2 alternatives)
- M 6.2 near Marked Tree, Arkansas (1843 earthquake)
- Hypothetical M 5.8 earthquake near Covington (recent CEUS earthquakes)

# Tipton Co Scenario Eqqs

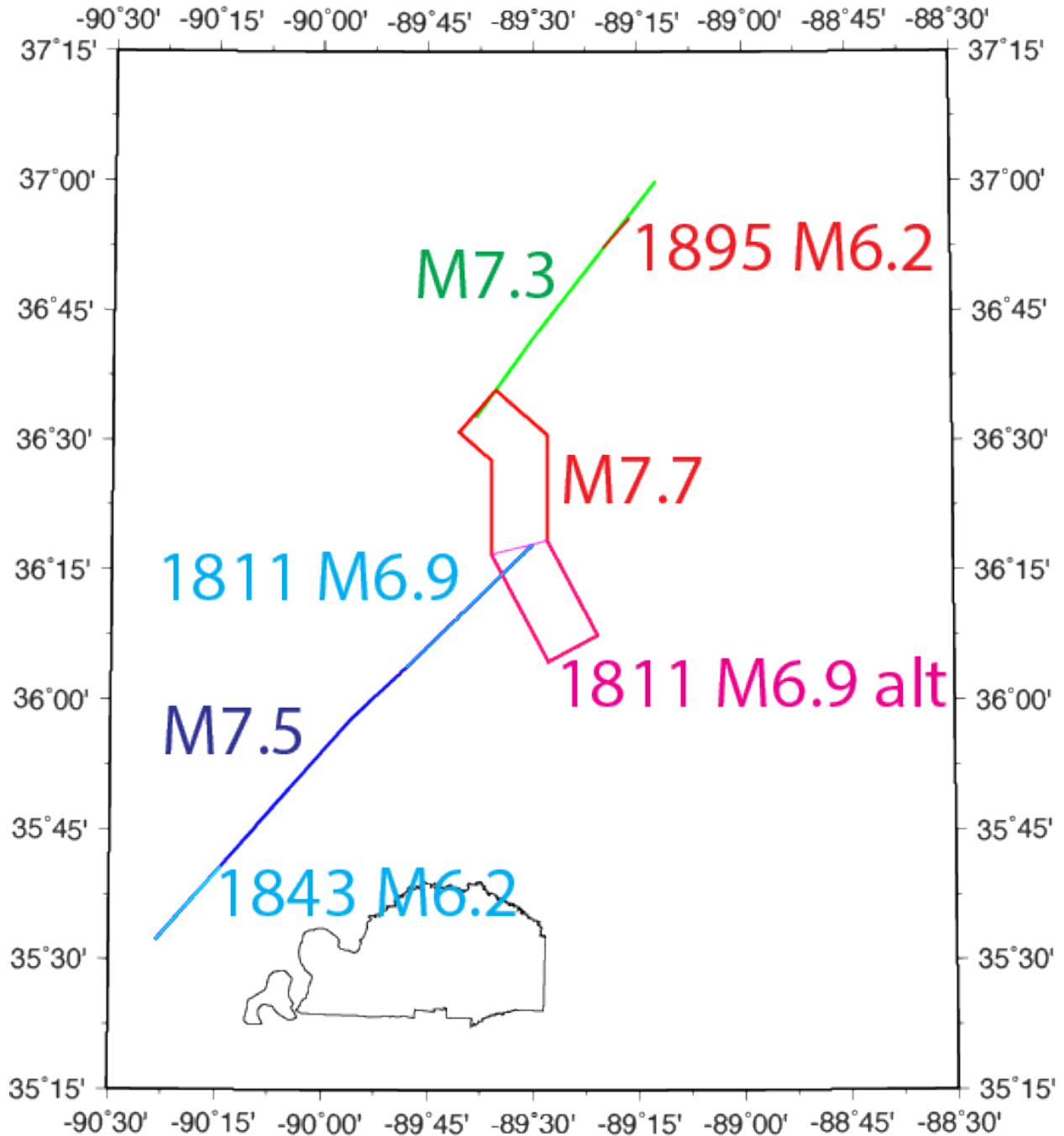


Figure 32A: Potential scenario ruptures for Tipton County. 1811–1812 **M7** ruptures indicated by **M7.5**, **M7.3**, and **M7.7**. 1811 **M6.9**s indicate two alternative “Dawn” aftershock ruptures. 1843 and 1895 **M6.2**s indicate historic end of seismic zone ruptures.

# Tipton Co Scenario Eqks

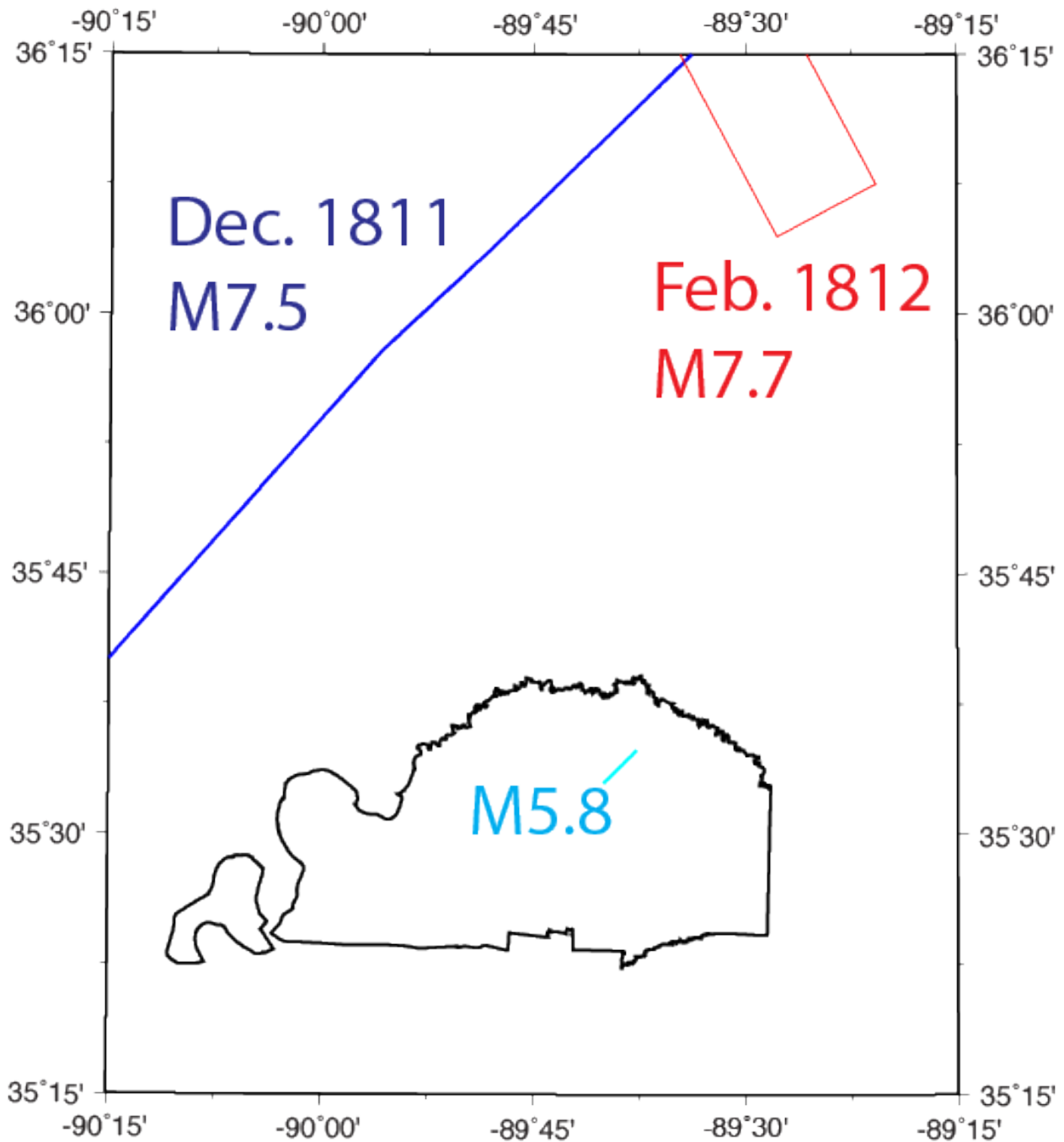


Figure 32B: Scenario ruptures close to Tipton County. The Dec. 1811 is strike-slip mainshock rupture extending out of the map view. The Feb. 1812 is thrust mainshock rupture mostly out of map view. The **M5.8** is a hypothetical earthquake in Tipton County near Covington.

## Seismic Hazard Maps

Figures 33 - 35 show the 5%-in-50-year probabilistic seismic hazard maps for Tipton County for PGA, 0.2 s, and 1.0 s. The background maps are the equivalent USGS national seismic hazard maps for B/C boundary conditions ( $V_{s30} = 760$  m/s). At short periods (PGA and 0.2 s) the Lauderdale County range of values is 0.3 – 0.6 g (g is the acceleration of gravity at the earth's surface – 9.80665 m/s). At long periods (1.0 s) the range is 0.3 – 0.5 g. Short period seismic hazard is for 1-2 story buildings, while long period hazard is for ~10 story buildings.

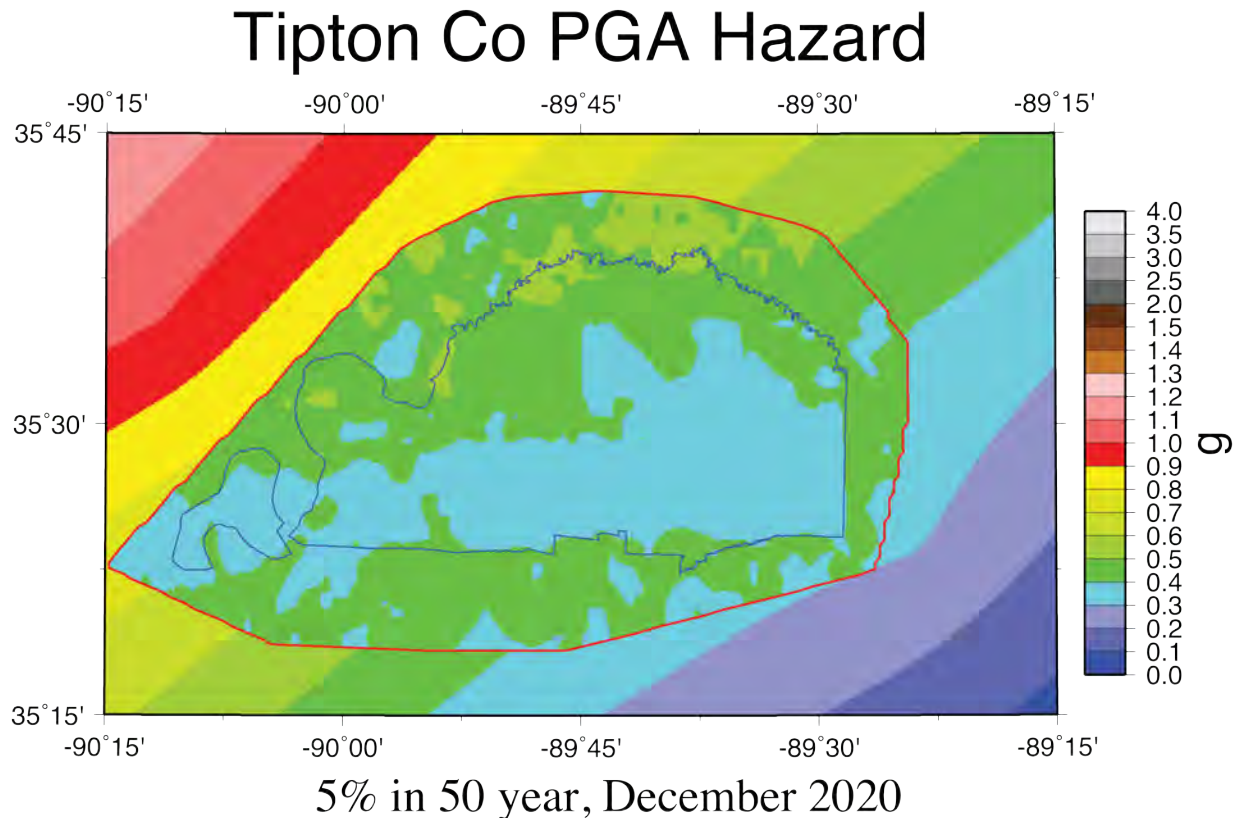


Figure 33: 5%-in-50-year PGA hazard map for Tipton County with the effects of local geology inset on the U.S. Geological Survey's national seismic hazard map for BC boundary conditions.

# Tipton Co 0.2s Hazard

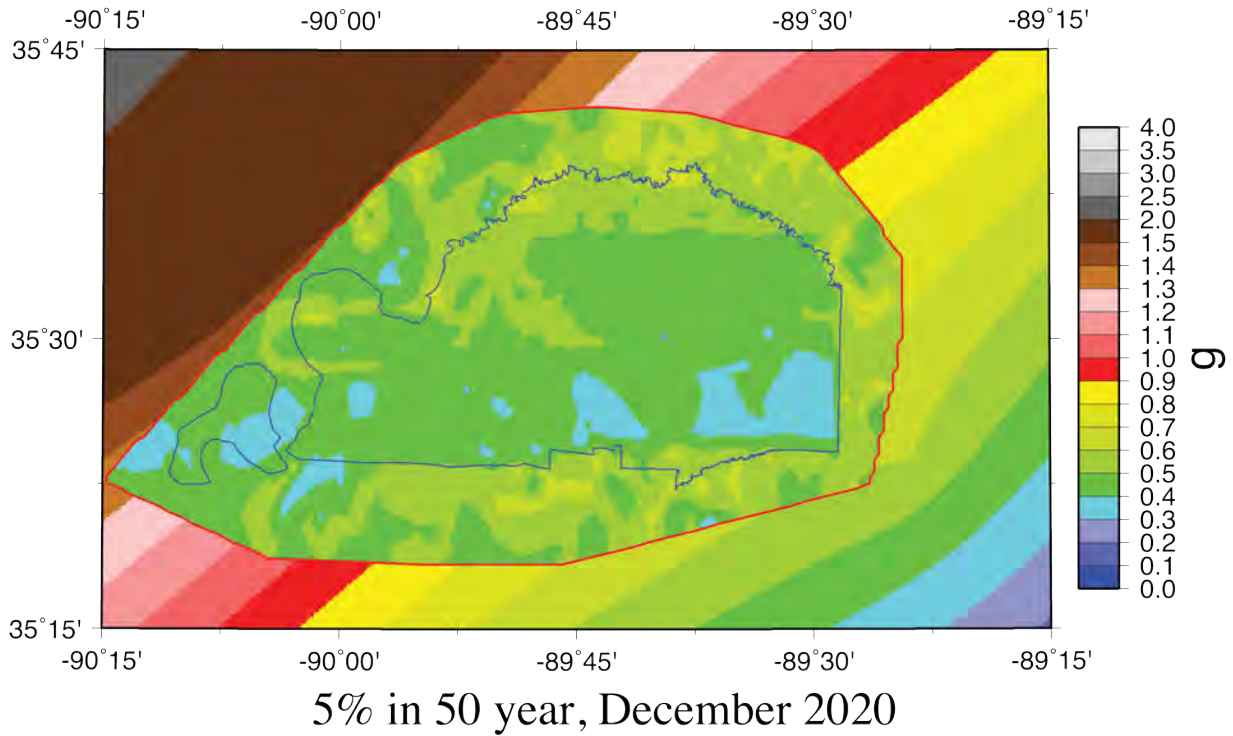


Figure 34: 5%-in-50-year 0.2 s hazard map for Tipton County with the effects of local geology inset on the U.S. Geological Survey's national seismic hazard map for BC boundary conditions.

# Tipton Co 1.0s Hazard

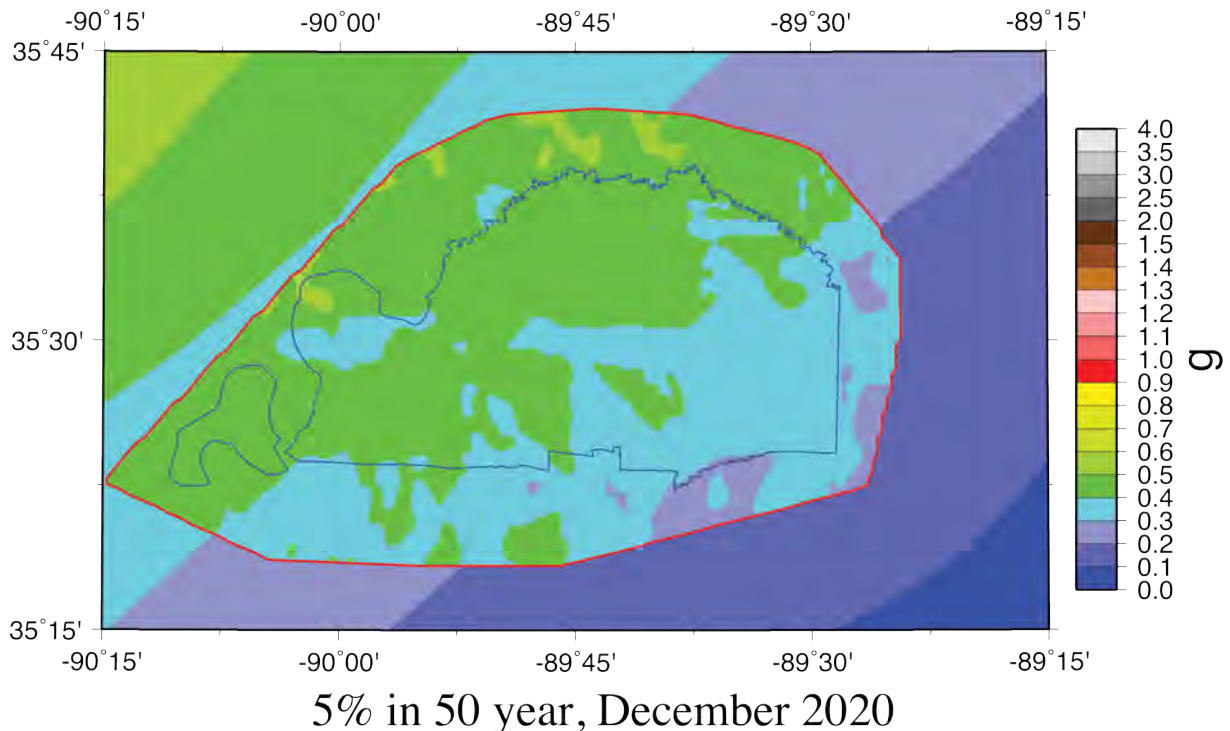


Figure 35: 5%-in-50-year 1.0 s hazard map for Tipton County with the effects of local geology inset on the U.S. Geological Survey's national seismic hazard map for BC boundary conditions.

Figures 36 - 38 show the 2%-in-50-year probabilistic seismic hazard maps for Lauderdale County. The hazard range is higher than the 5%-in-50-year maps: 0.4 – 0.8 g for PGA, 0.5 – 1.0 g for 0.2 s, and 0.5 – 0.9 g for 1.0 s.

The probabilistic seismic hazard maps with the effect of local geology show a short period reduction of 10% to 50% and a long period amplification of 10% to 100% relative to the USGS national seismic hazard maps at the same periods. The short period reduction is due to estimated ground motion nonlinear soil effects strongly reducing the high ground motions expected near the earthquake sources. The long period amplification is due to the reduced nonlinear effects and increase dominance of soil column resonant effects amplifying ground motions. As we progress further from the earthquake sources the ground motion level decreases, the nonlinear effects decrease, and the dominance of resonance effects increases. In Shelby County, about 50 km from the New Madrid earthquake sources, Cramer et al. (2018a) show Shelby County seismic hazard maps with 40 – 60% decreases at short period and 50 – 100 % increases at long period over the USGS national seismic hazard maps. Another feature of the probabilistic seismic hazard maps is the lower ground motion estimates in the southern portion of the county, particularly at short periods. These lower estimates are due to the presence of thicker Quaternary sediments in that part of Tipton County, which cause more nonlinear

deamplification. This southern county region is also a little farther from the earthquake sources in the model.

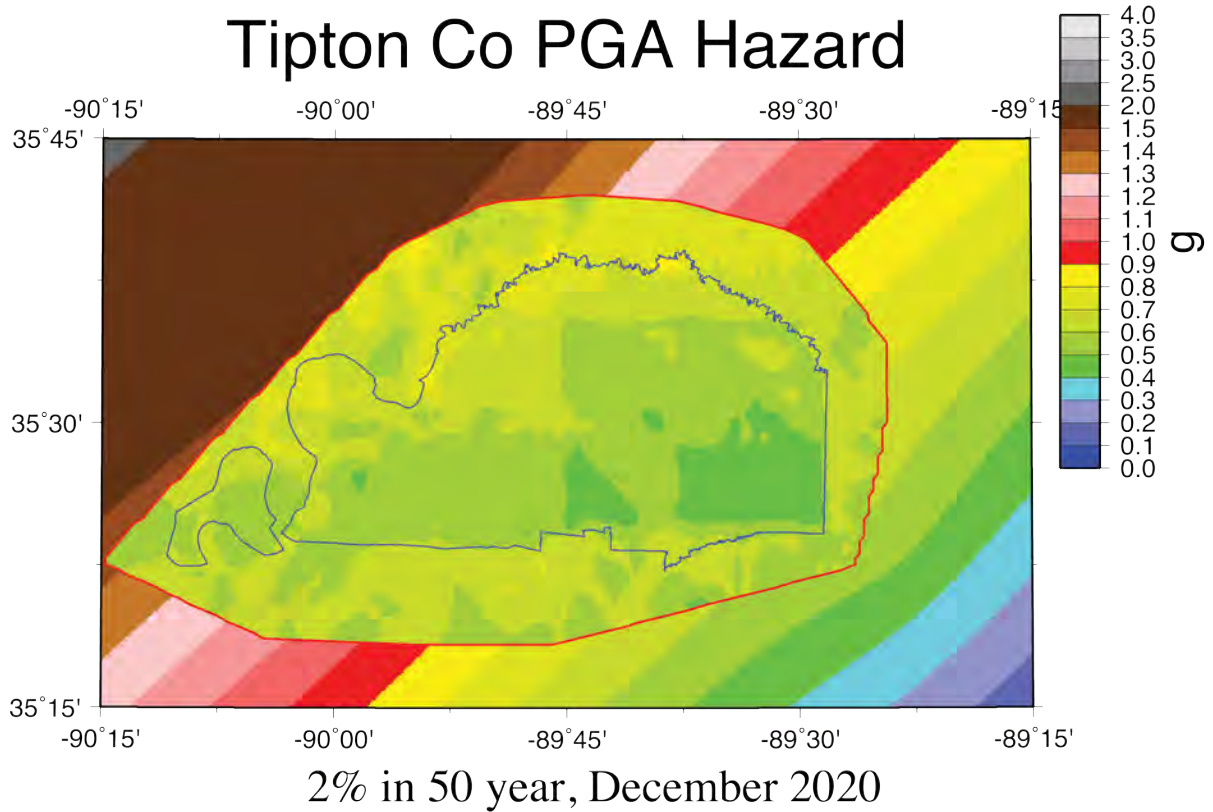


Figure 36: 2%-in-50-year PGA hazard map for Tipton County with the effects of local geology inset on the U.S. Geological Survey's national seismic hazard map for BC boundary conditions.

# Tipton Co 0.2s Hazard

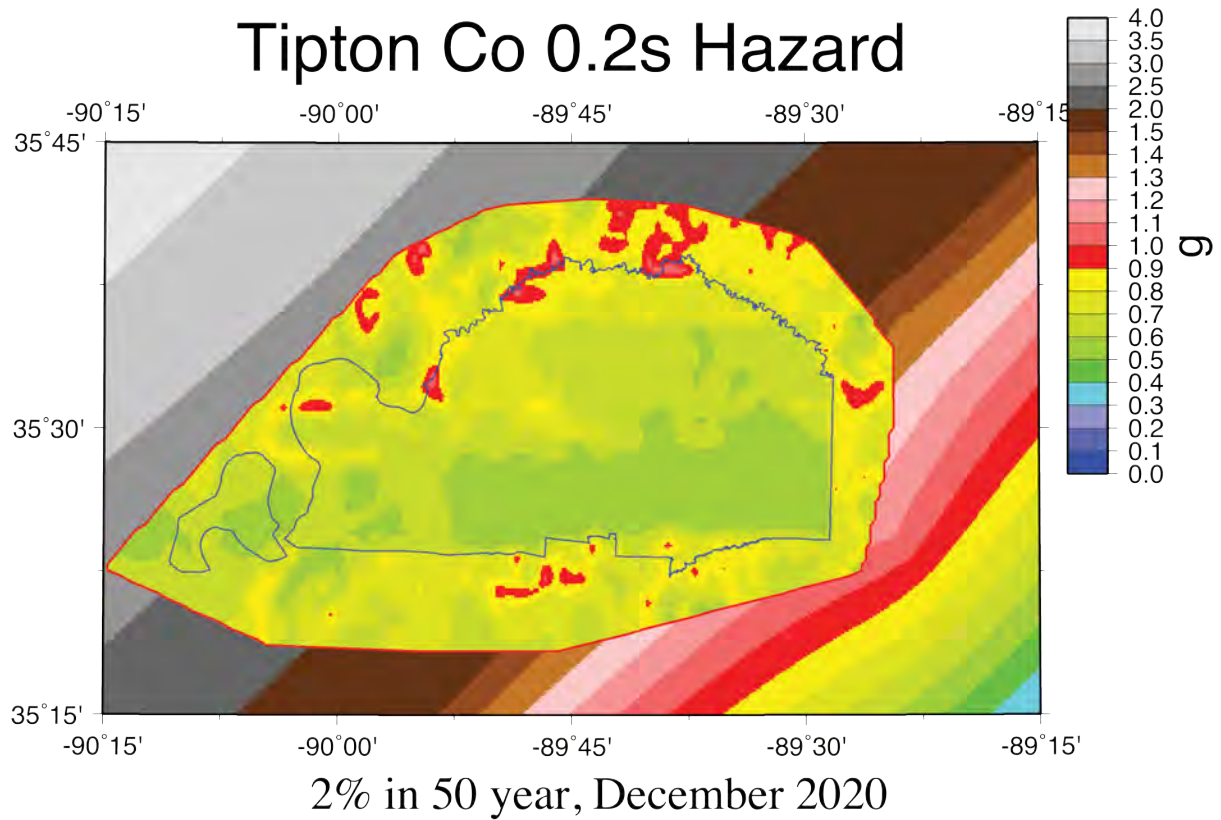


Figure 37: 2%-in-50-year 0.2 s hazard map for Tipton County with the effects of local geology inset on the U.S. Geological Survey's national seismic hazard map for BC boundary conditions.

# Tipton Co 1.0s Hazard

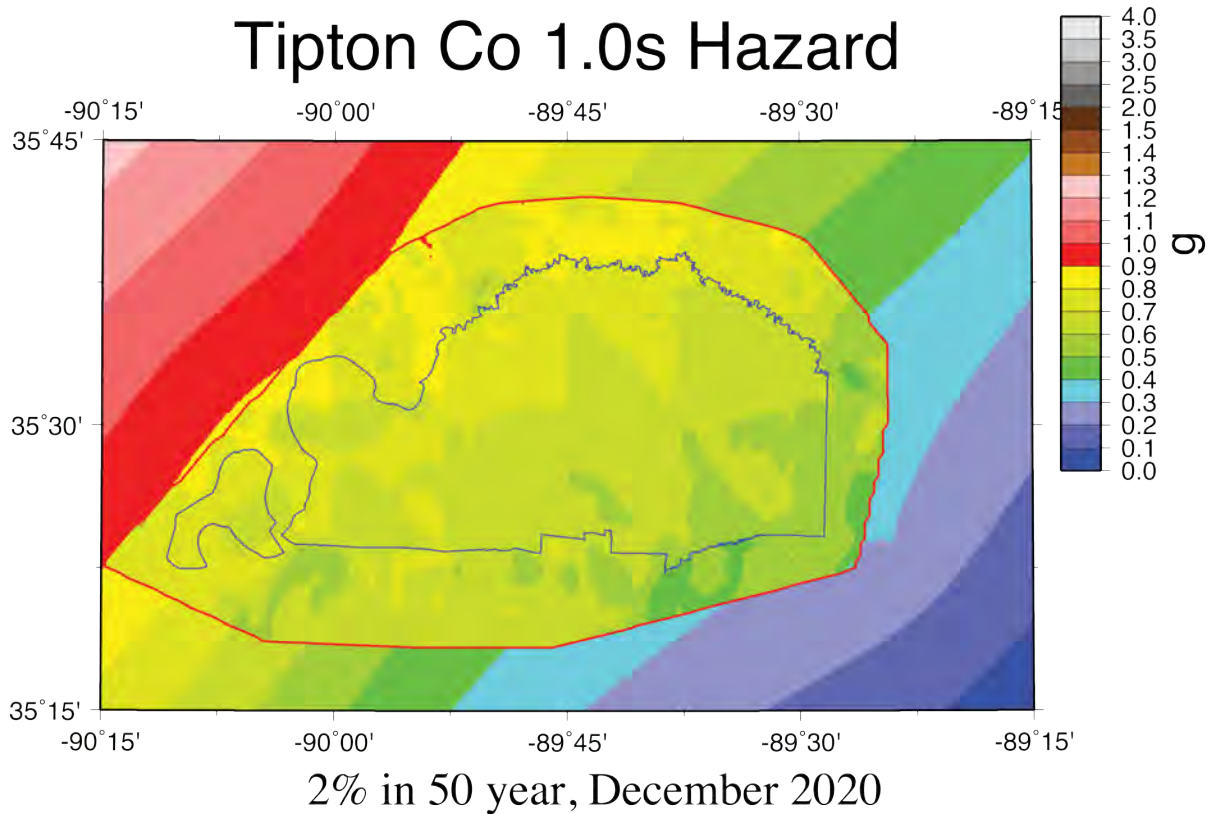
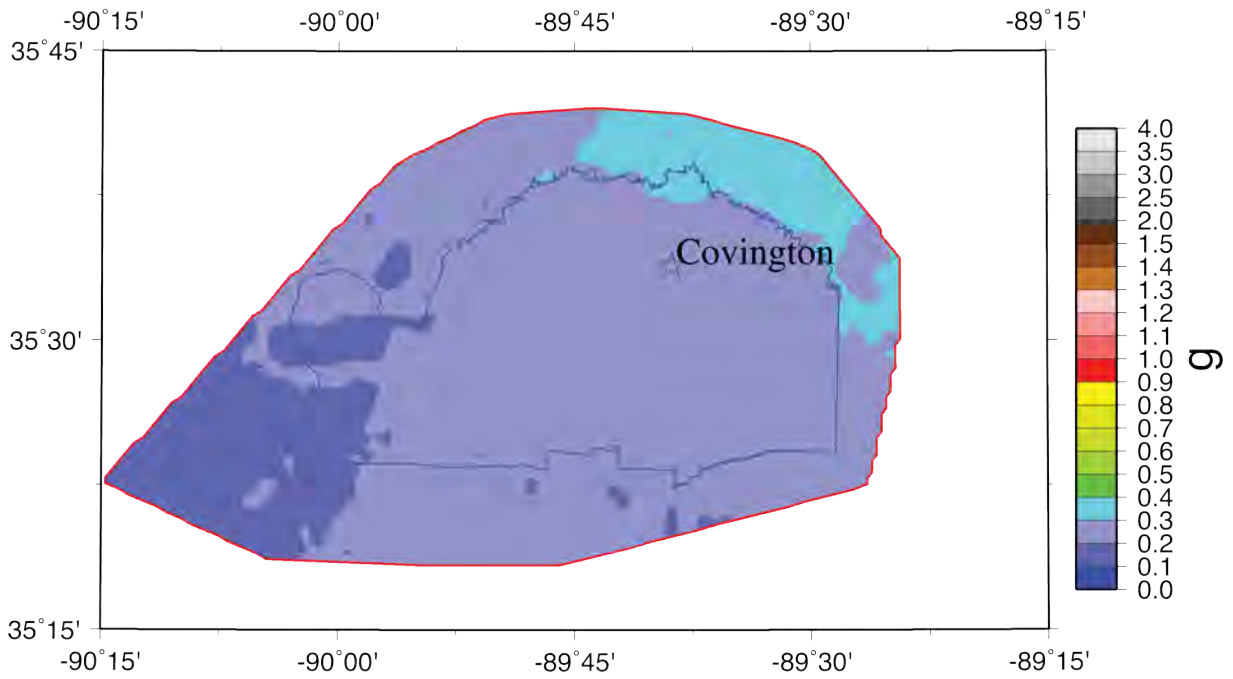


Figure 38: 2%-in-50-year 1.0 s hazard map for Tipton County with the effects of local geology inset on the U.S. Geological Survey's national seismic hazard map for BC boundary conditions.

Figures 39 - 45 present the PGA, 0.2 s, and 1.0 s seismic hazard maps for the seven scenarios of Table 8. There are no equivalent comparisons to the USGS probabilistic maps for these scenarios. At all periods shown, the M7 New Madrid scenario hazard maps range from 0.2 to 0.5 g for a repeat of the M7.7 February 1812 earthquake, from 0.2 to 0.5 g for the repeat of the M7.5 December 1811 earthquake, and 0.1 to 0.4 g for the repeat of the M7.3 January 1812 earthquake. The M6.9 largest aftershock hazard map alternatives range from 0.1 to 0.4 g if on the northern end of the SW arm and 0.1 to 0.4 g if on the east end of the Reelfoot thrust. The M6.2 1843 scenario ground motions are 0.1 to 0.3 g, and the M5.8 hypothetical Tipton County earthquake ground motions ranges from 0.1 – 0.6 g. Thus, both the scenario and probabilistic seismic hazard maps show similar ground motion levels at short and long periods due to the close proximity of ruptures and the effect of soils of the Mississippi embayment. These scenarios continue to show the lower hazard in the southern portion of the county seen in the probabilistic hazard maps, due to the thicker upland Quaternary sediment. For the M6.2 Marked Tree scenario and at PGA and 1.0 s for the M7.5 SW arm scenario, the higher ground motions are in the western portion of the county.

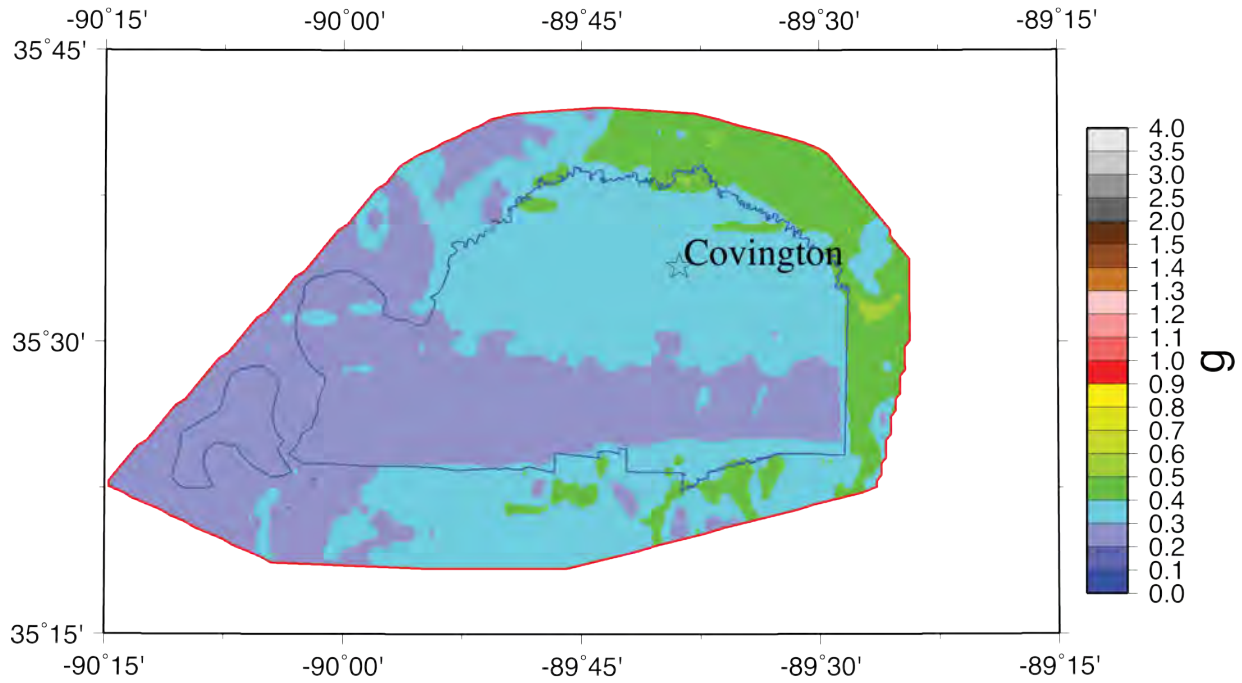
# Tipton Co PGA Hazard



NMRT M7.7, Dec 2020

Figure 39A: Scenario PGA hazard map for a M7.7 earthquake on the Reelfoot Thrust (central segment of NMSZ) for Tipton County with the effects of local geology.

# Tipton Co 0.2s Hazard



NMRT M7.7, Dec 2020

Figure 39B: Scenario 0.2 s hazard map for a M7.7 earthquake on the Reelfoot Thrust (central segment of NMSZ) for Tipton County with the effects of local geology.

# Tipton Co 1.0s Hazard

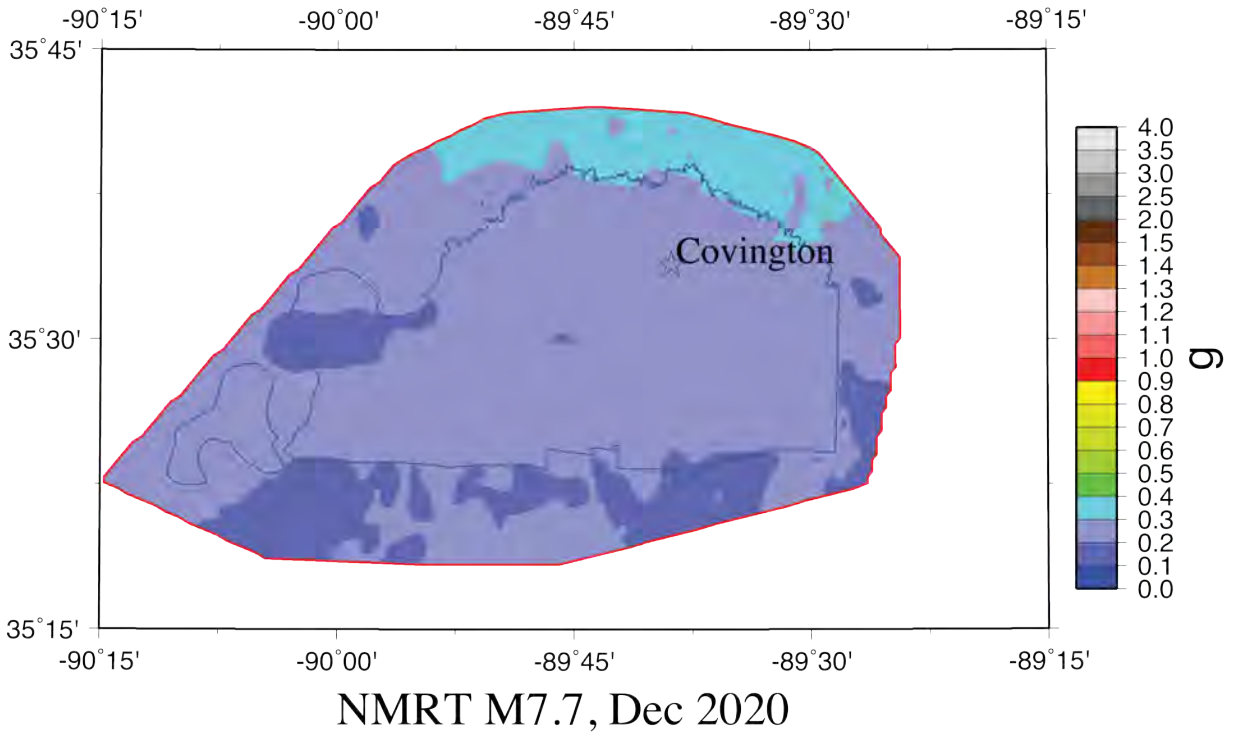


Figure 39C: Scenario 1.0 s hazard map for a M7.7 earthquake on the Reelfoot Thrust (central segment of NMSZ) for Tipton County with the effects of local geology.

# Tipton Co PGA Hazard

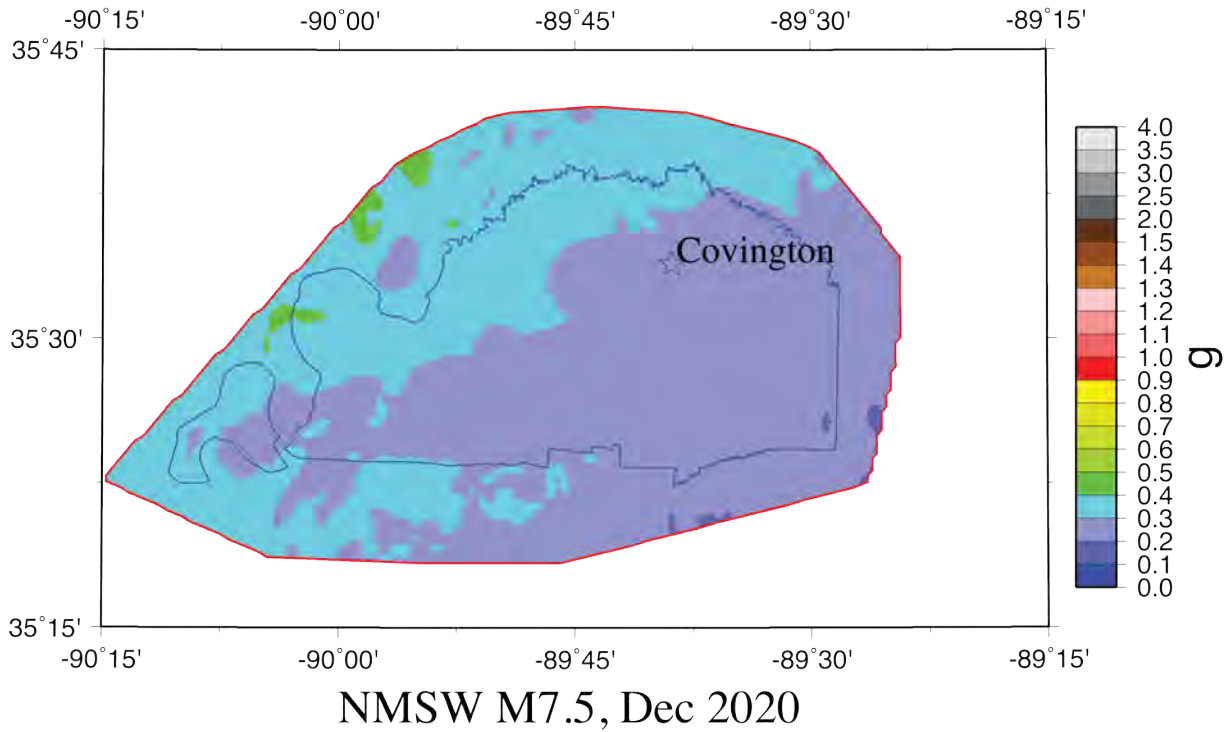
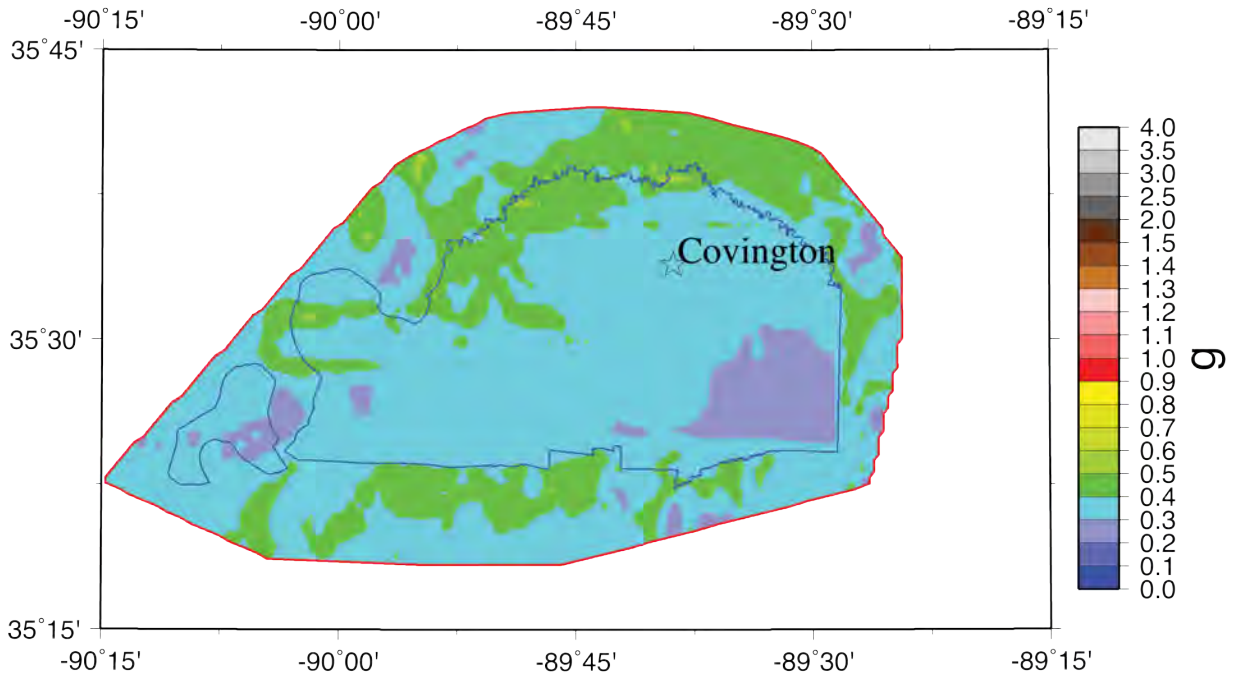


Figure 40A: Scenario PGA hazard map for a M7.5 earthquake on the Cottonwood Grove Fault (SW segment of NMSZ) for Tipton County with the effects of local geology.

# Tipton Co 0.2s Hazard



NMSW M7.5, Dec 2020

Figure 40B: Scenario 0.2 s hazard map for a M7.5 earthquake on the Cottonwood Grove Fault (SW segment of NMSZ) for Tipton County with the effects of local geology.

# Tipton Co 1.0s Hazard

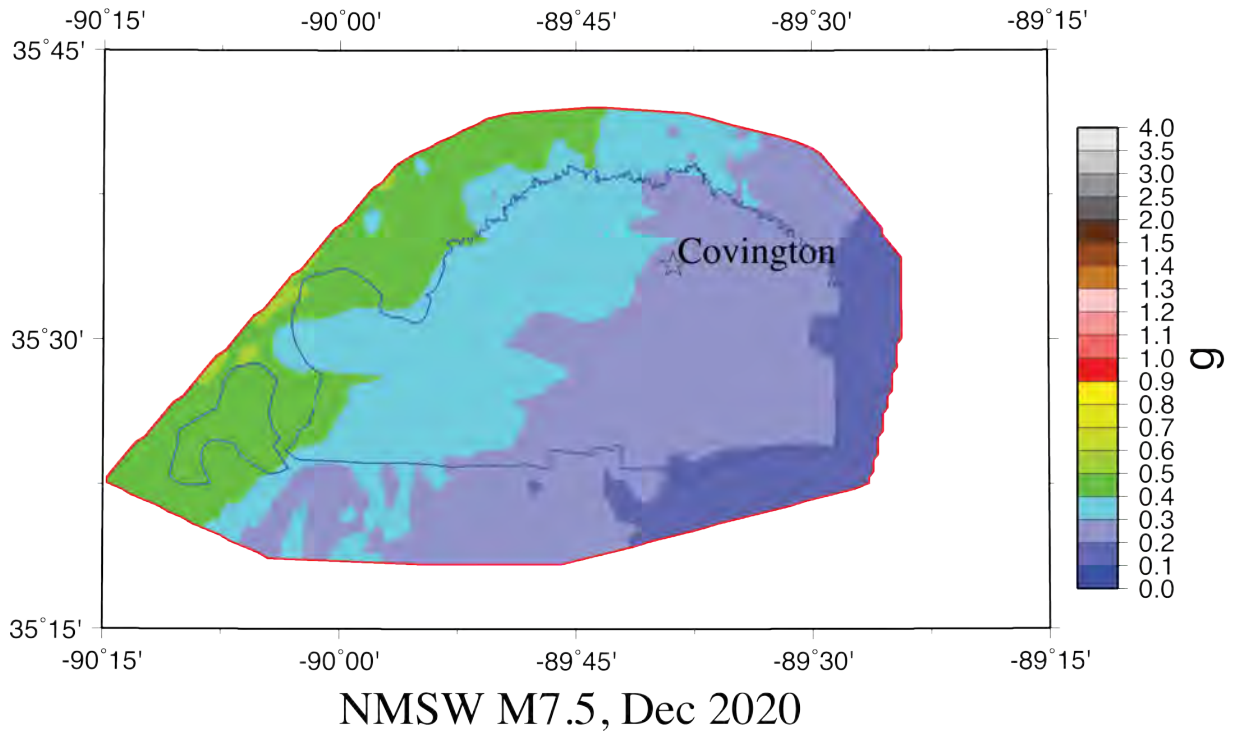
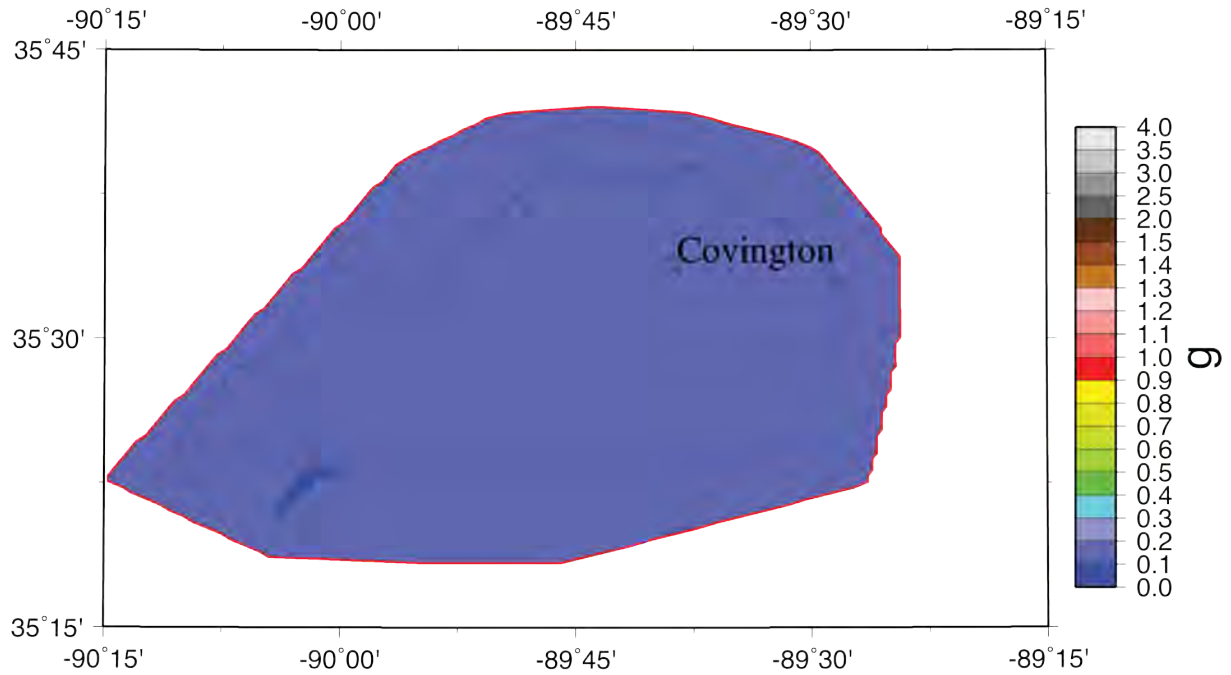


Figure 40C: Scenario 1.0 s hazard map for a M7.5 earthquake on the Cottonwood Grove Fault (SW segment of NMSZ) for Tipton County with the effects of local geology.

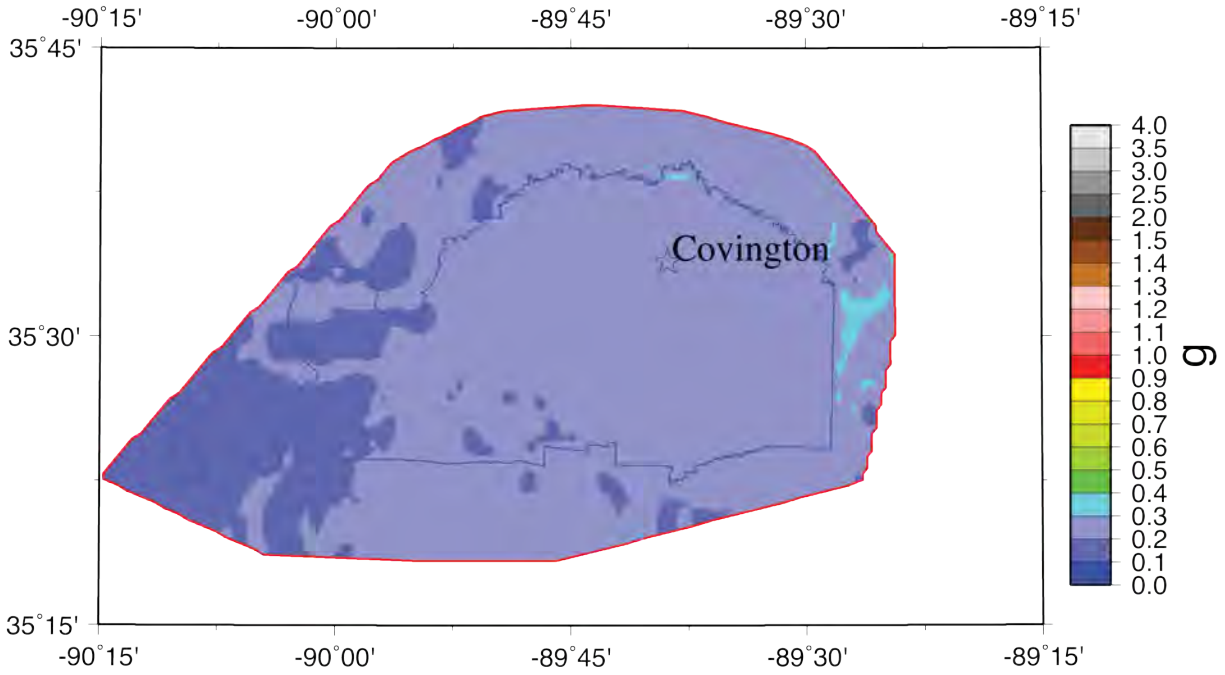
# Tipton Co PGA Hazard



NMNE M7.3, Dec 2020

Figure 41A: Scenario PGA hazard map for a M7.3 earthquake on the New Madrid North Fault (NE segment of NMSZ) for Tipton County with the effects of local geology.

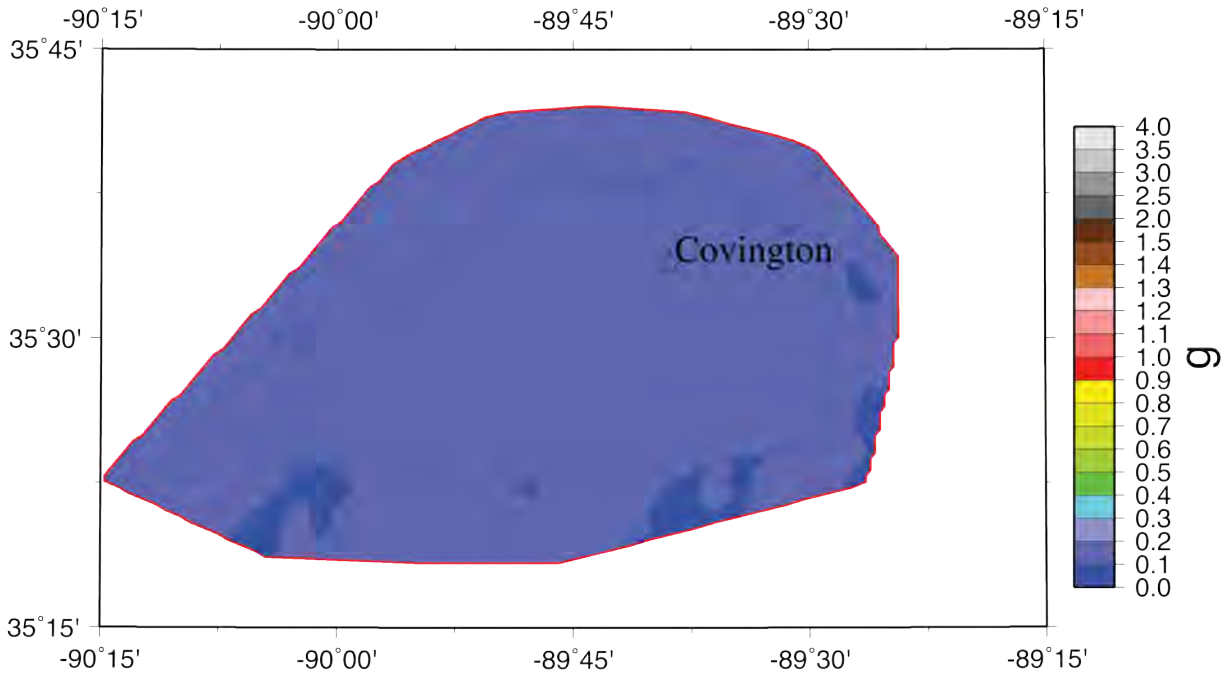
# Tipton Co 0.2s Hazard



NMNE M7.3, Dec 2020

Figure 41B: Scenario 0.2 s hazard map for a M7.3 earthquake on the New Madrid North Fault (NE segment of NMSZ) for Tipton County with the effects of local geology.

# Tipton Co 1.0s Hazard



NMNE M7.3, Dec 2020

Figure 41C: Scenario 1.0 s hazard map for a M7.3 earthquake on the New Madrid North Fault (NE segment of NMSZ) for Tipton County with the effects of local geology.

# Tipton Co PGA Hazard

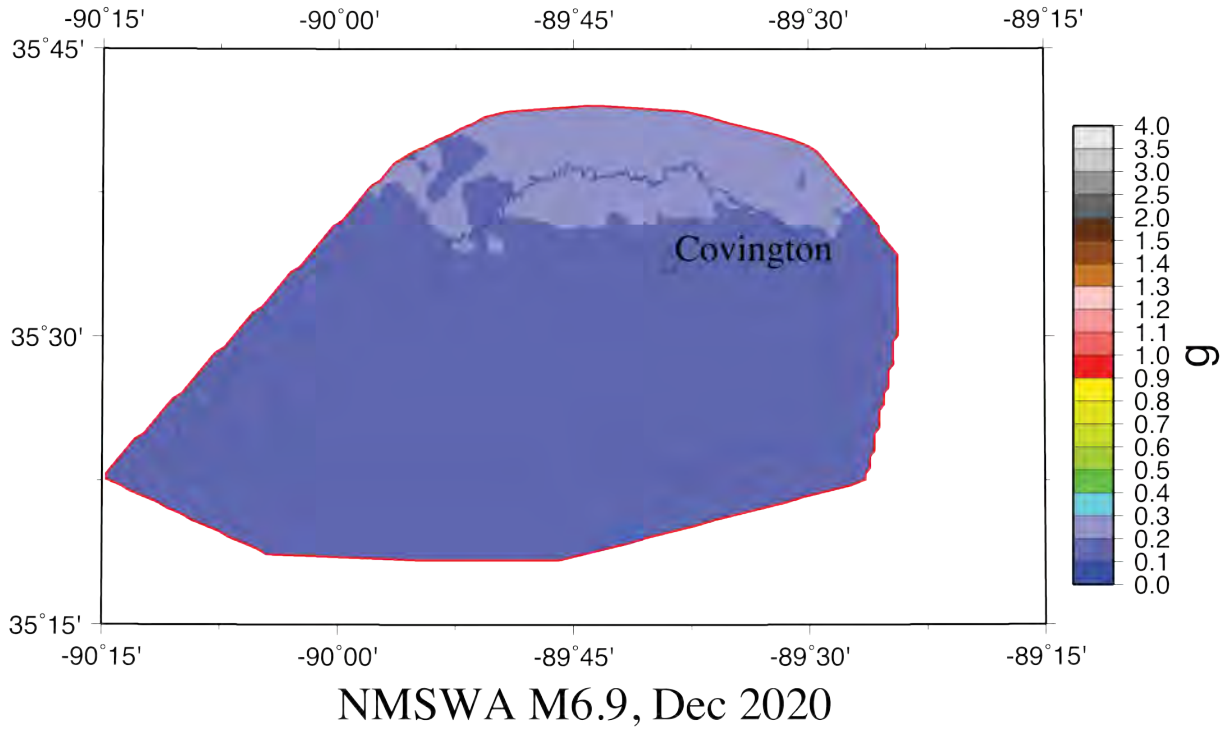


Figure 42A: Scenario PGA hazard map for a M6.9 “Dawn” aftershock (alt. 1) on the Cottonwood Grove Fault (SW segment of NMSZ) for Tipton County with the effects of local geology.

# Tipton Co 0.2s Hazard

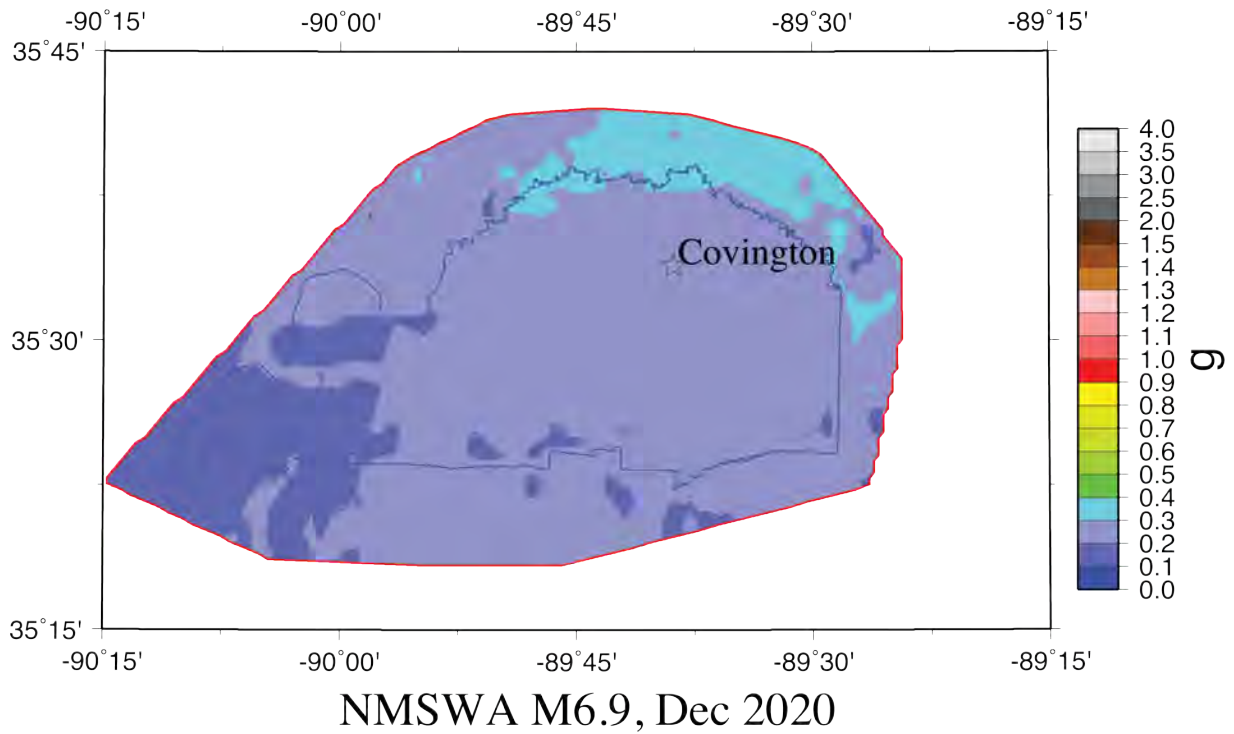


Figure 42B: Scenario 0.2 s hazard map for a M6.9 “Dawn” aftershock (alt. 1) on the Cottonwood Grove Fault (SW segment of NMSZ) for Tipton County with the effects of local geology.

# Tipton Co 1.0s Hazard

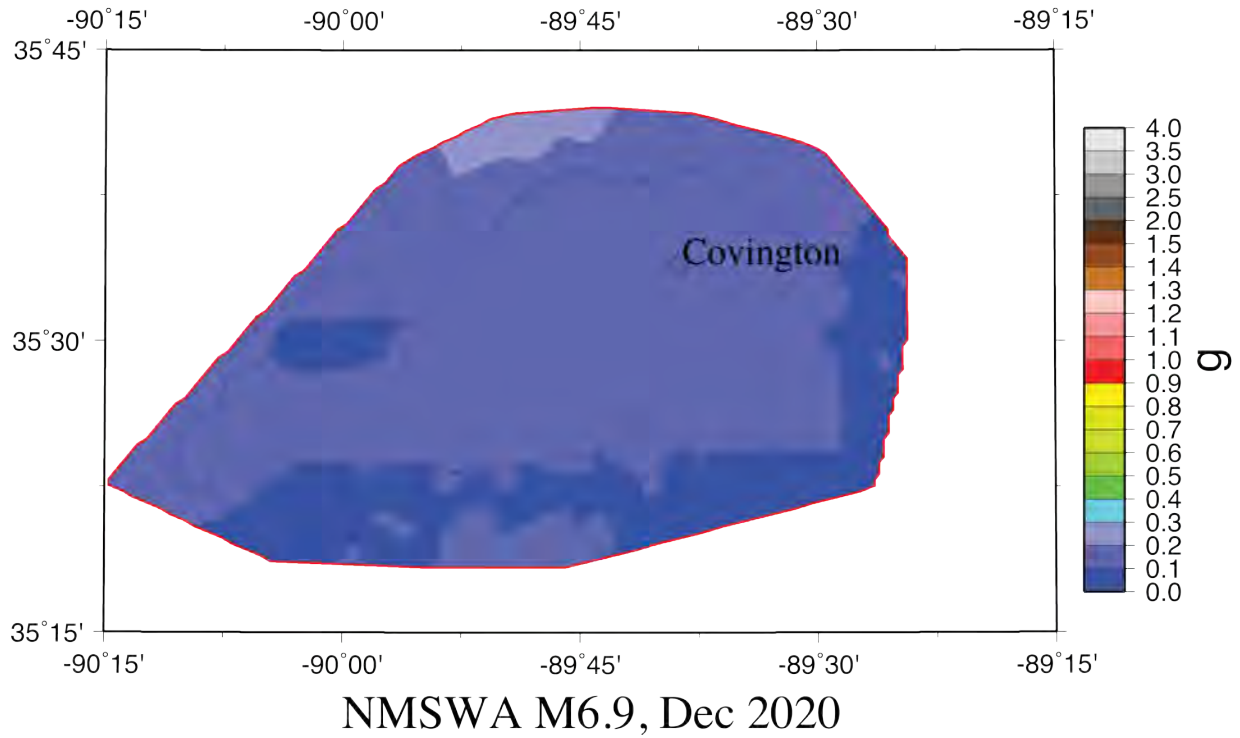


Figure 42C: Scenario 1.0 s hazard map for a M6.9 “Dawn” aftershock (alt. 1) on the Cottonwood Grove Fault (SW segment of NMSZ) for Tipton County with the effects of local geology.

# Tipton Co PGA Hazard

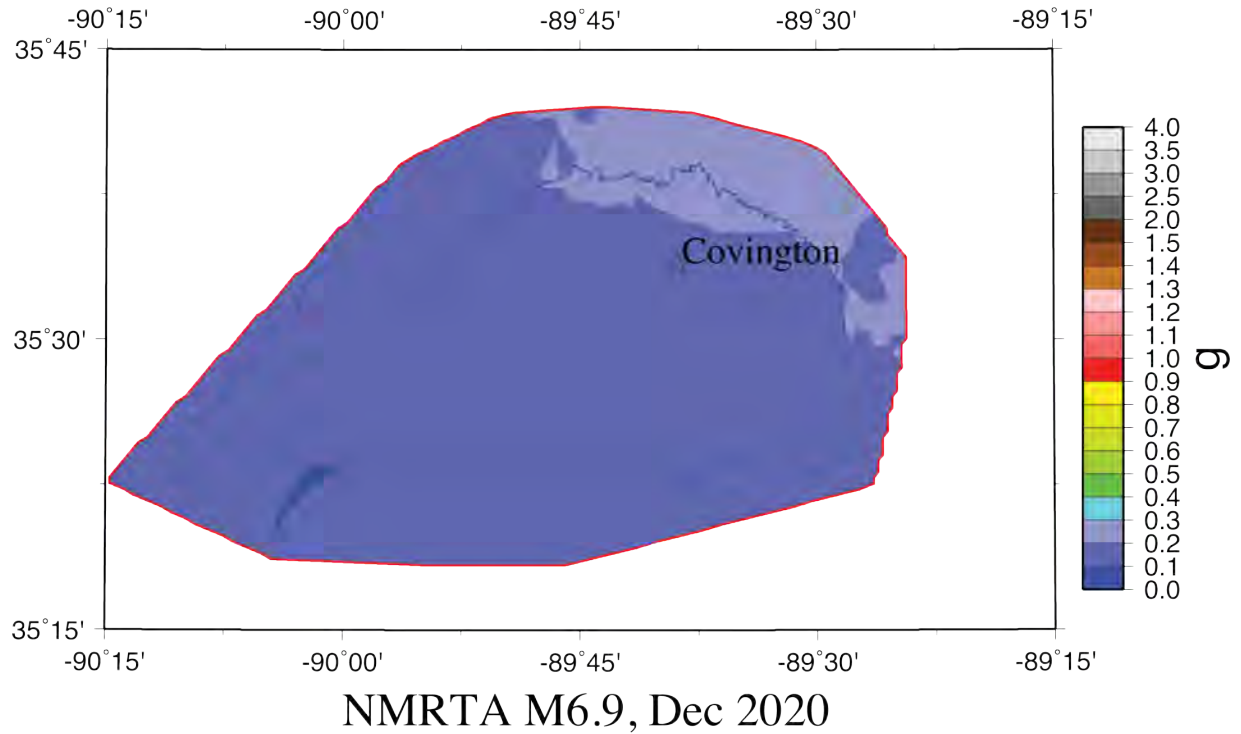
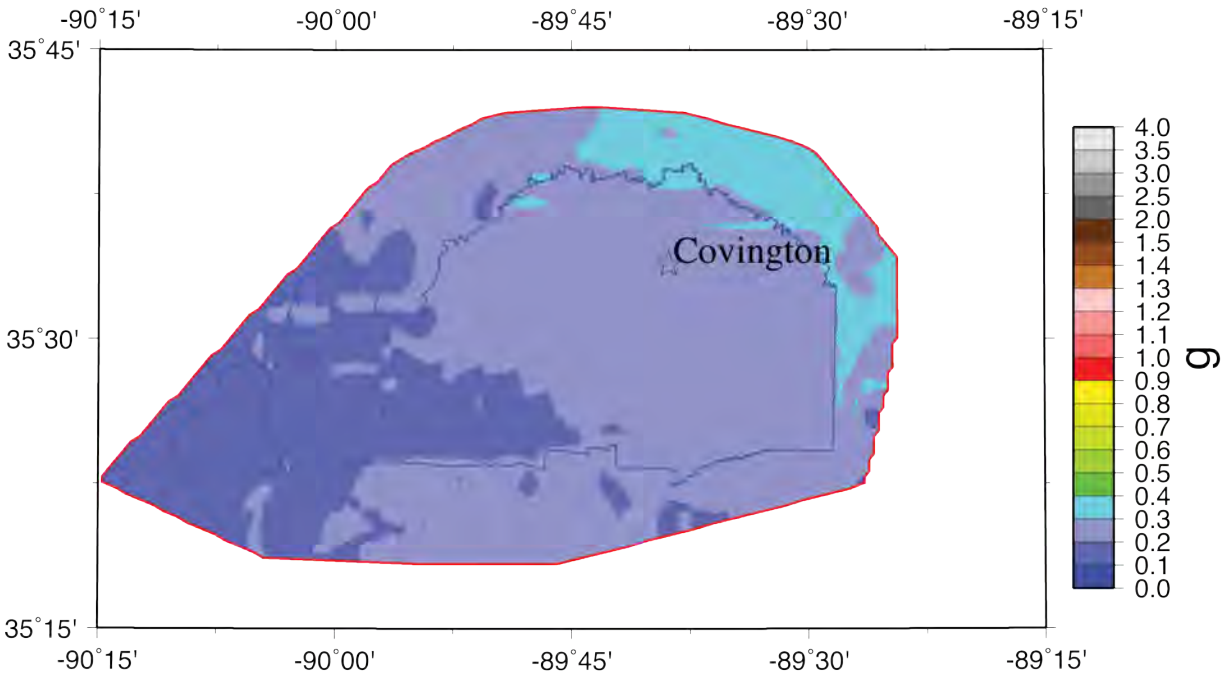


Figure 43A: Scenario PGA hazard map for a M6.9 “Dawn” aftershock (alt. 2) on the Reelfoot Thrust (central segment of NMSZ) for Tipton County with the effects of local geology.

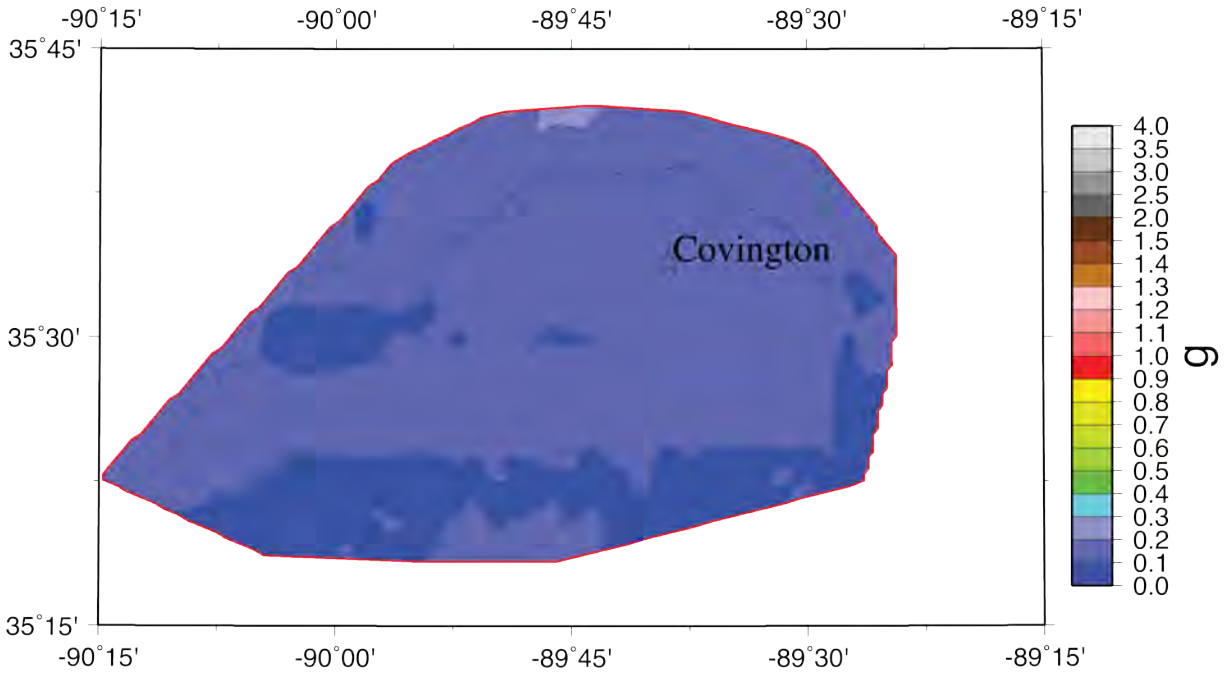
# Tipton Co 0.2s Hazard



NMRTA M6.9, Dec 2020

Figure 43B: Scenario 0.2 s hazard map for a M6.9 “Dawn” aftershock (alt. 2) on the Reelfoot Thrust (central segment of NMSZ) for Tipton County with the effects of local geology.

# Tipton Co 1.0s Hazard



NMRTA M6.9, Dec 2020

Figure 43C: Scenario 1.0 s hazard map for a M6.9 “Dawn” aftershock (alt. 2) on the Reelfoot Thrust (central segment of NMSZ) for Tipton County with the effects of local geology.

# Tipton Co PGA Hazard

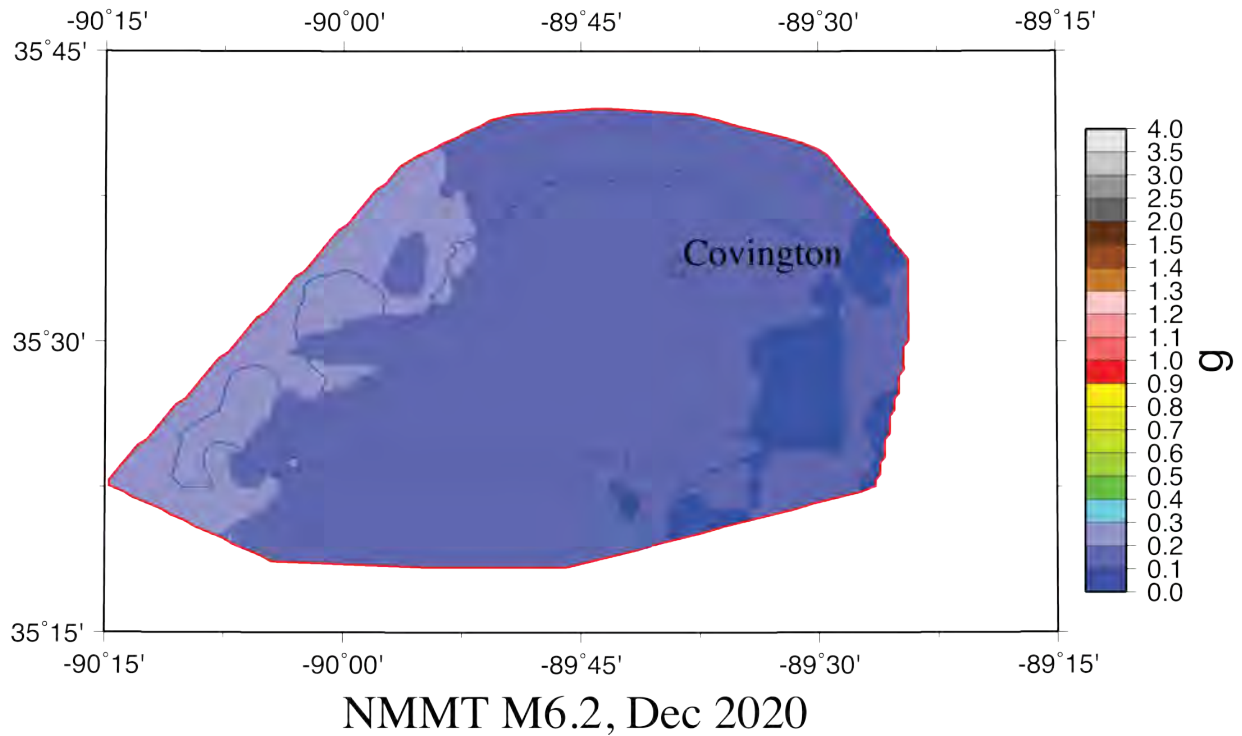
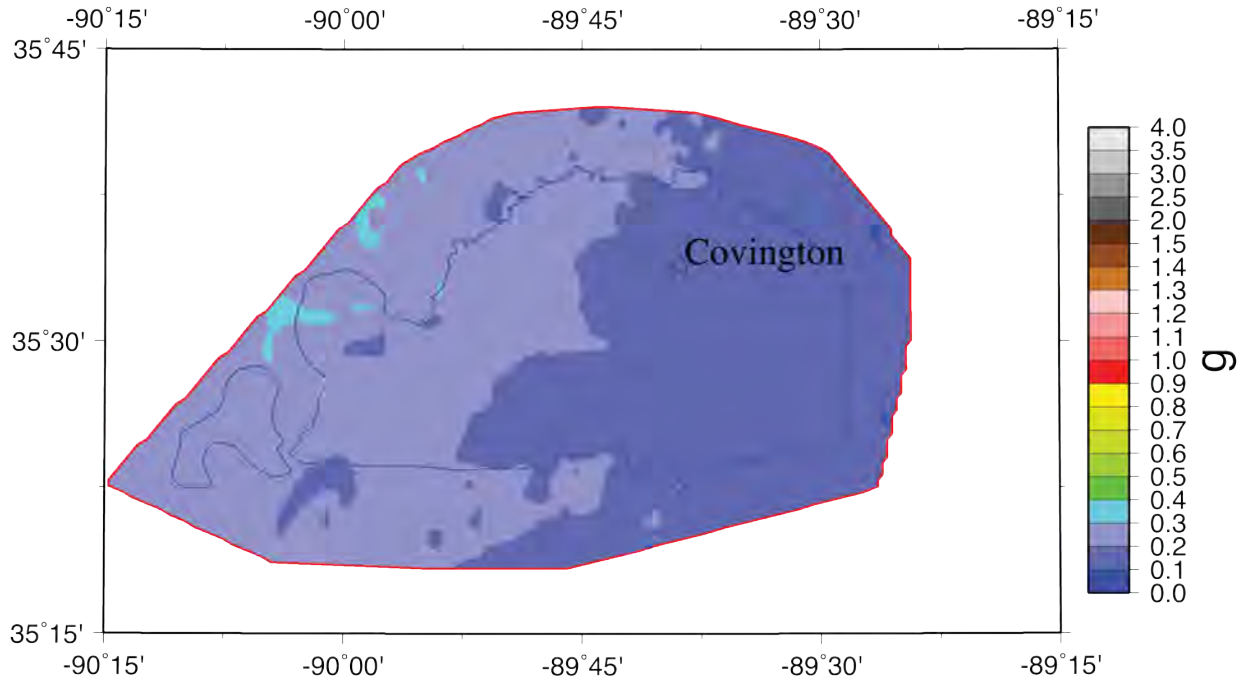


Figure 44A: Scenario PGA hazard map for a M6.2 on the Cottonwood Grove Fault (1843 Marked Tree – SW segment of NMSZ) for Tipton County with the effects of local geology.

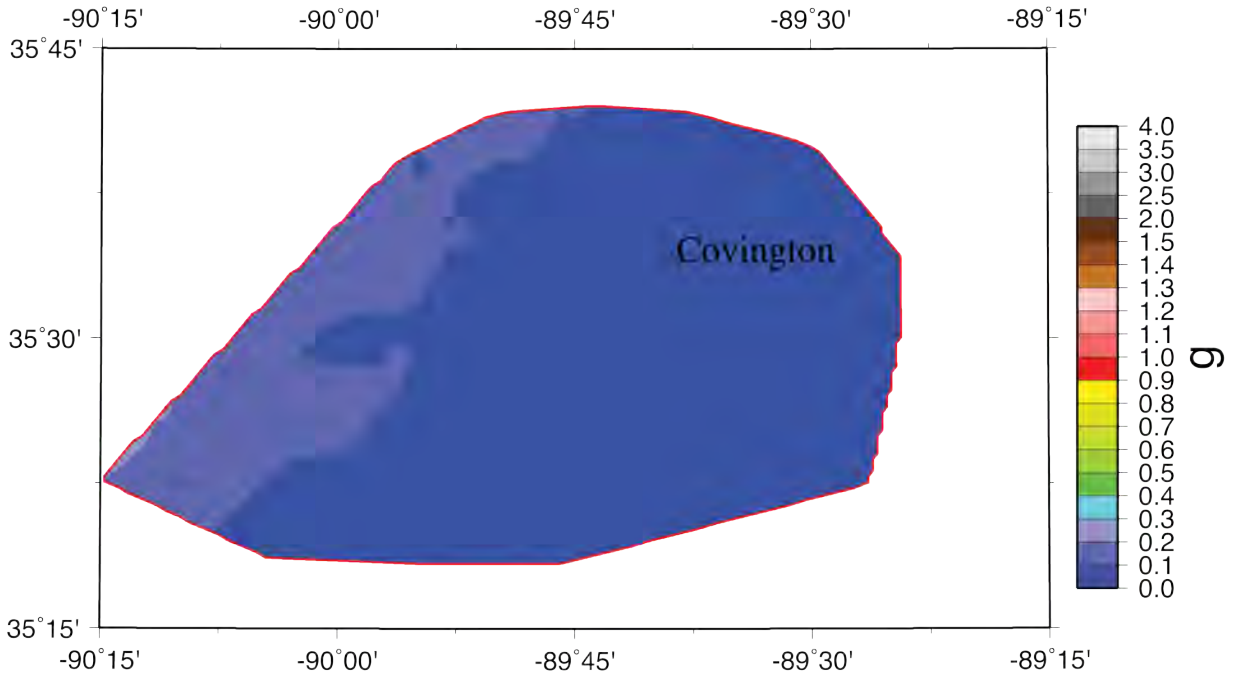
# Tipton Co 0.2s Hazard



NMMT M6.2, Dec 2020

Figure 44B: Scenario 0.2 s hazard map for a M6.2 on the Cottonwood Grove Fault (1843 Marked Tree – SW segment of NMSZ) for Tipton County with the effects of local geology.

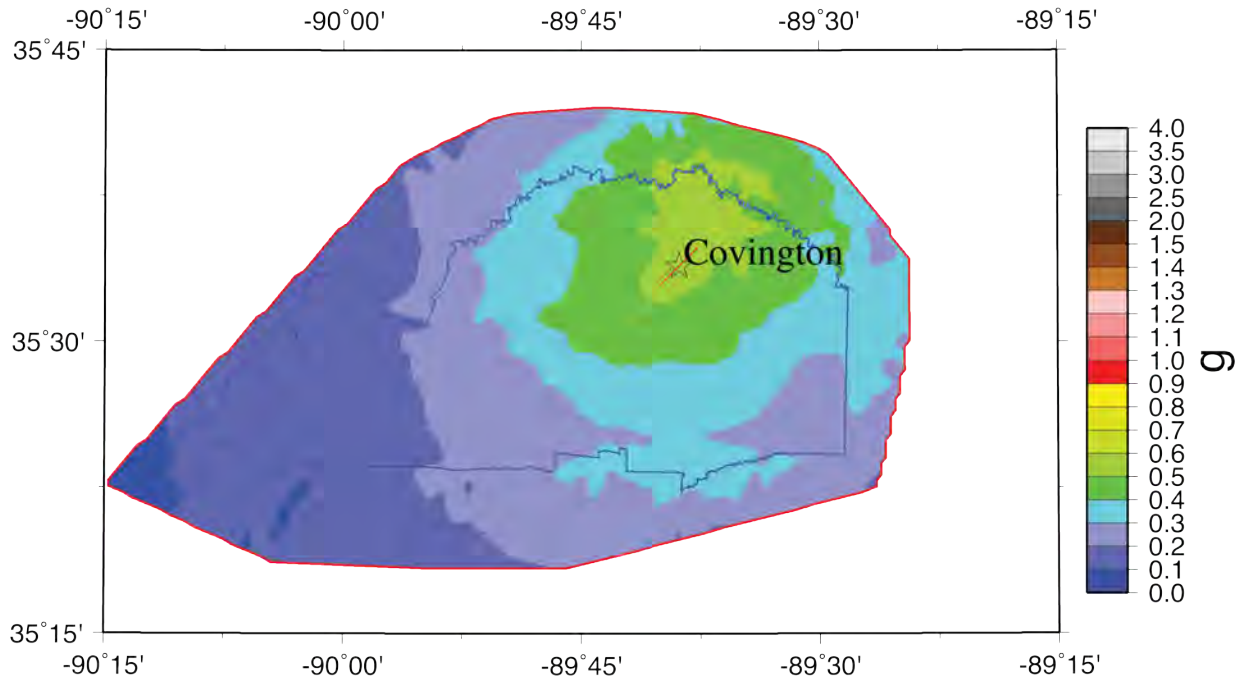
# Tipton Co 1.0s Hazard



NMMT M6.2, Dec 2020

Figure 444C: Scenario 1.0 s hazard map for a M6.2 on the Cottonwood Grove Fault (1843 Marked Tree – SW segment of NMSZ) for Tipton County with the effects of local geology.

# Tipton Co PGA Hazard



TIP M5.8, Dec 2020

Figure 45A: Scenario PGA hazard map for a M5.8 hypothetical earthquake for Tipton County with the effects of local geology. Red line indicates location of source fault.

# Tipton Co 0.2s Hazard

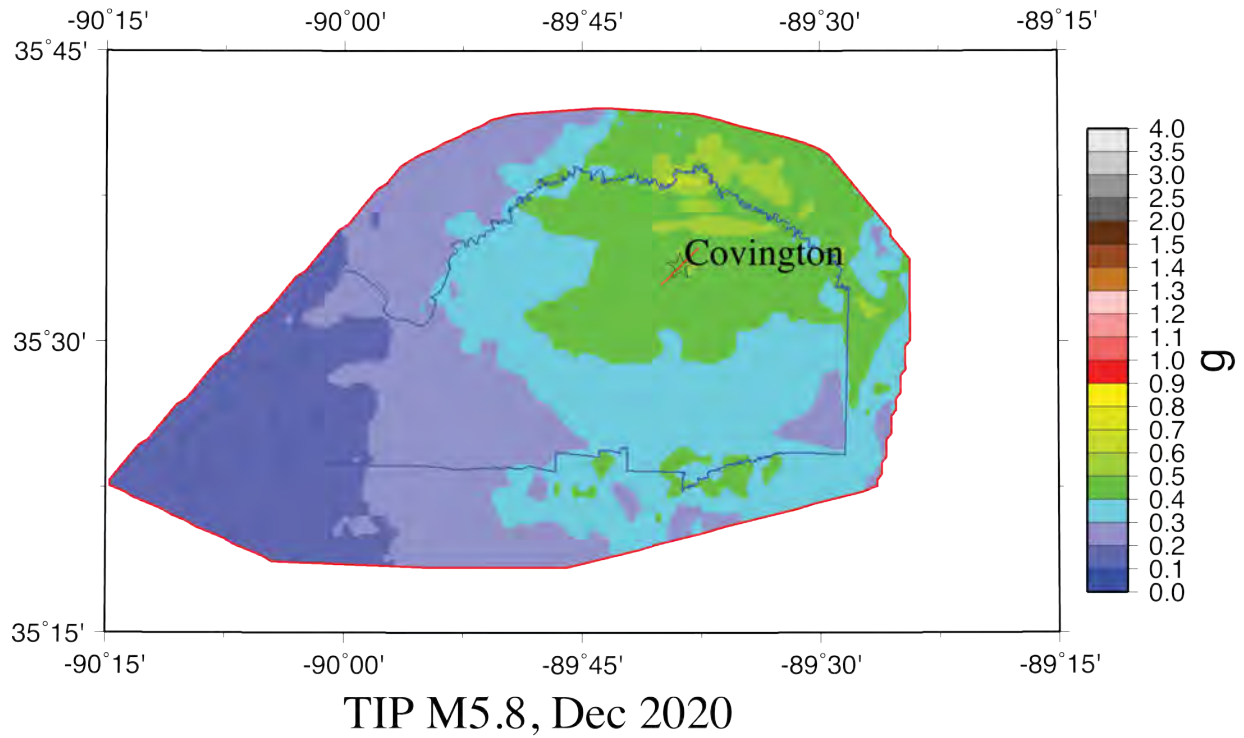


Figure 45B: Scenario 0.2 s hazard map for a M5.8 hypothetical earthquake for Tipton County with the effects of local geology. Red line indicates location of source fault.

# Tipton Co 1.0s Hazard

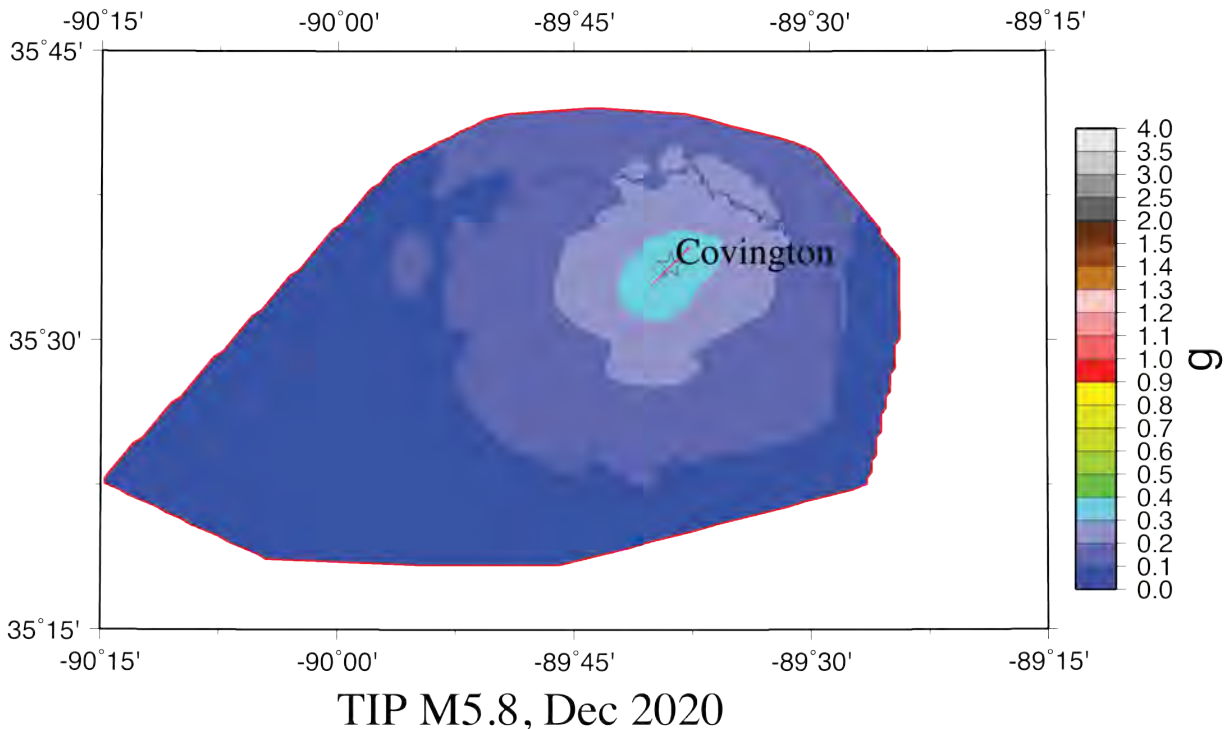


Figure 45C: Scenario 1.0 s hazard map for a M5.8 hypothetical earthquake for Tipton County with the effects of local geology. Red line indicates location of source fault.

## Liquefaction Hazard Maps

To generate the liquefaction hazard maps for Lauderdale County, we used the SPT-based liquefaction probability curves (LPCs) recommended above in Figures 19 and 22 for lowlands and non-lowlands, respectively. The LPCs are for Liquefaction Probability Index (LPI) exceeding 5, which is for the manifestation of liquefaction at the surface (moderate to severe liquefaction). These LPCs were used to maintain compatibility with the liquefaction maps we generated for Lake County (Cramer et al., 2019). Thus, our liquefaction hazard maps are for the probability of moderate to severe liquefaction. If the  $LPI_{ISH}$  moderate to severe liquefaction LPCs for the effects of non-liquefiable crust of Figures 23 and 24 are used, the liquefaction hazard would be reduced.

Figures 46 - 53 show the two probabilistic and six scenario liquefaction hazard maps derived from the equivalent PGA seismic hazard maps shown above. The probabilistic liquefaction hazard maps show 40 – 50% probability of liquefaction in the lowlands and less than 10% in the non-lowlands for 5%-in-50-years, and about 50 – 65% in the lowlands and 10–30% in the non-lowlands for 2%-in-50-years probability of liquefaction in Lauderdale County. The M7.7 scenario on the Reelfoot Thrust liquefaction hazard map shows 30 – 40% probability of

liquefaction in the lowlands and less than 5% in the non-lowlands. For the M7.5 scenario on the SW arm, the liquefaction hazard map shows about 40% in the lowlands and less than 5% in the non-lowlands. The M7.3 scenario on the NE arm shows about 10 – 25% probability of liquefaction in the lowlands and less than 5% probability of liquefaction in the non-lowlands. The largest aftershock alternatives show 15 – 30% probability of liquefaction in the lowlands and less than 5% in the non-lowlands. And the M5.8 hypothetical Lauderdale County earthquake shows 10 – 40% probability of liquefaction in the lowlands and less than 5% probability in the non-lowlands. The 1843 and 1895 M6.2 scenarios do not produce any significant liquefaction hazard and are not shown. The liquefaction hazard is moderate to high in the lowlands for the near M7 and greater earthquake scenarios.

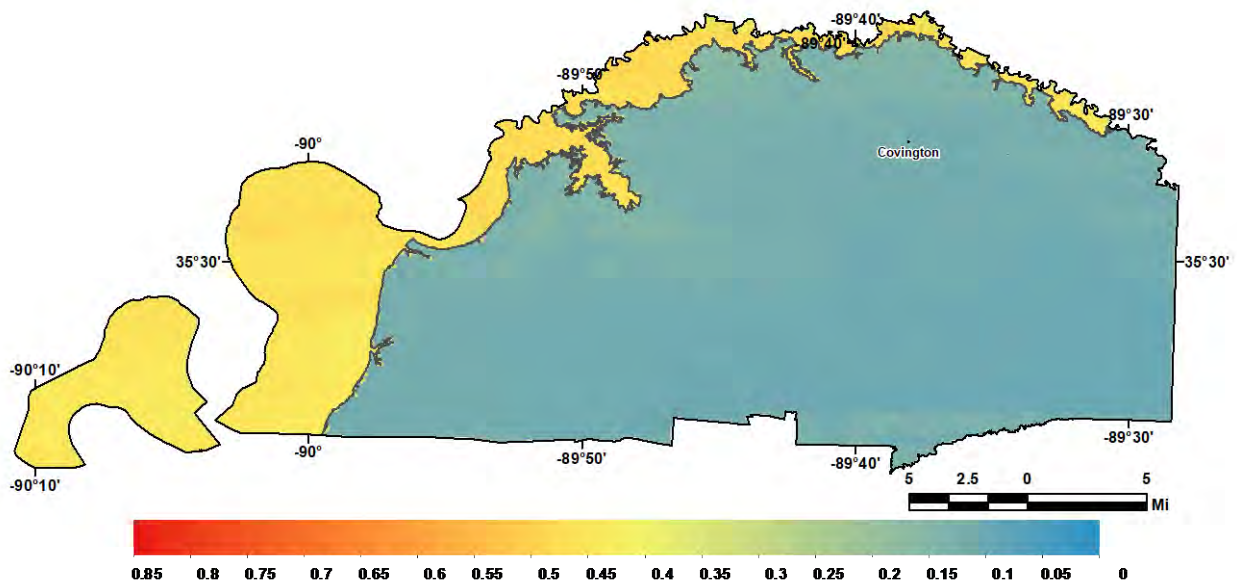


Figure 46: 5%-in-50-year liquefaction hazard map for moderate to severe liquefaction at the surface (LPI > 5) for Tipton County including the effects of local geology.

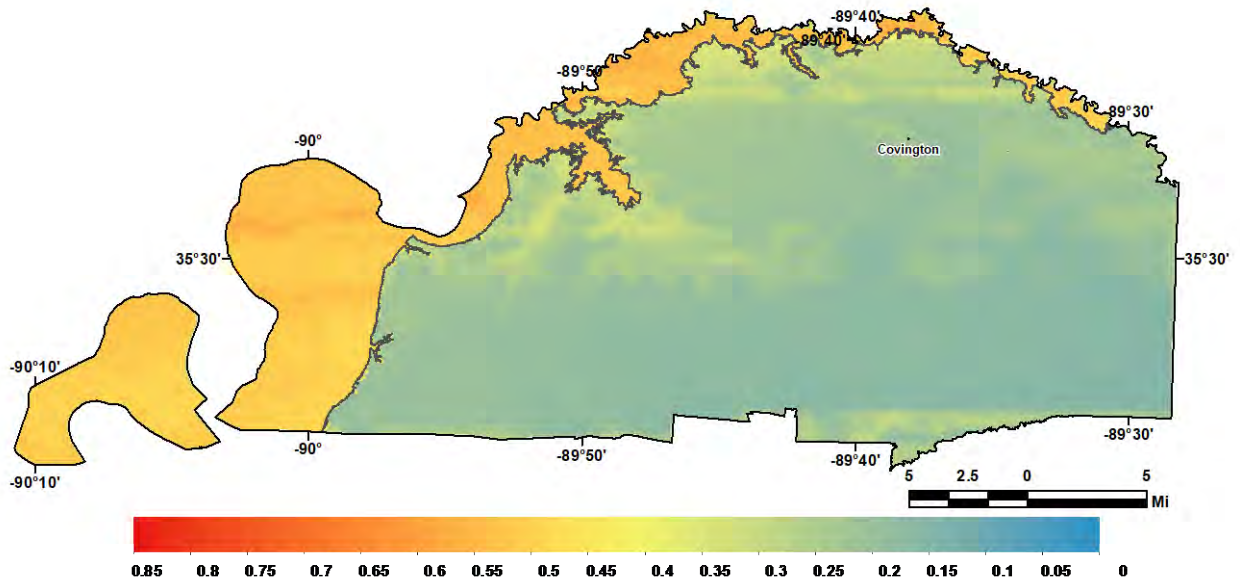


Figure 47: 2%-in-50-year liquefaction hazard map for moderate to severe liquefaction at the surface (LPI > 5) for Tipton County including the effects of local geology.

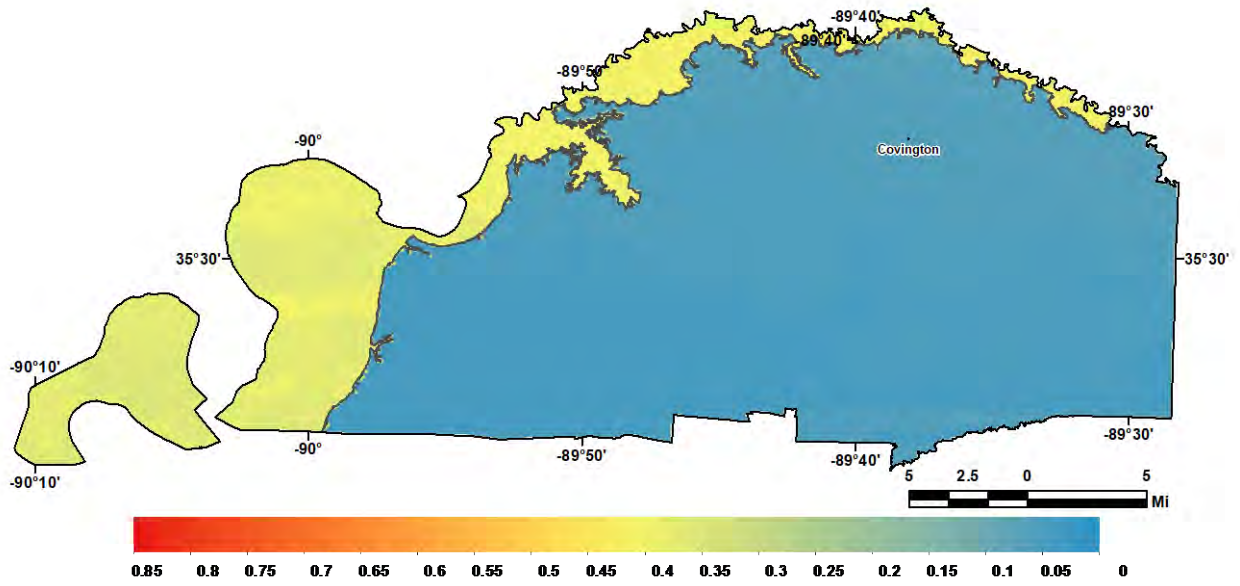


Figure 48: Scenario liquefaction hazard map for moderate to severe liquefaction at the surface (LPI > 5) for a M7.7 earthquake on the Reelfoot Thrust (central segment of NMSZ).

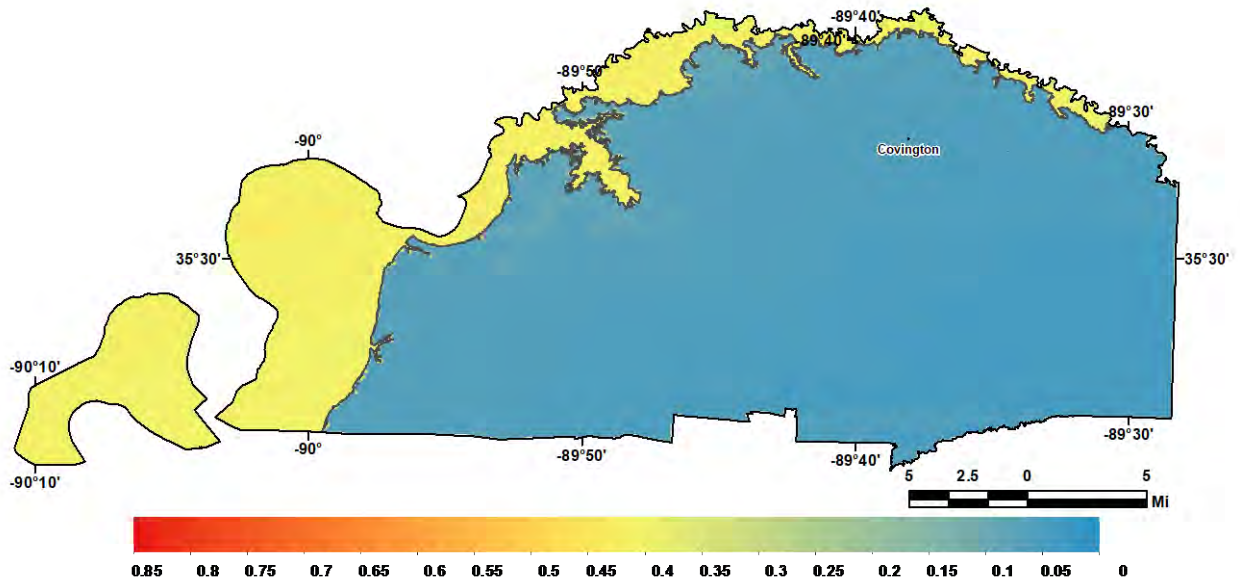


Figure 49: Scenario liquefaction hazard map for moderate to severe liquefaction at the surface (LPI > 5) for a M7.5 earthquake on the Cottonwood Grove Fault (SW segment of NMSZ).

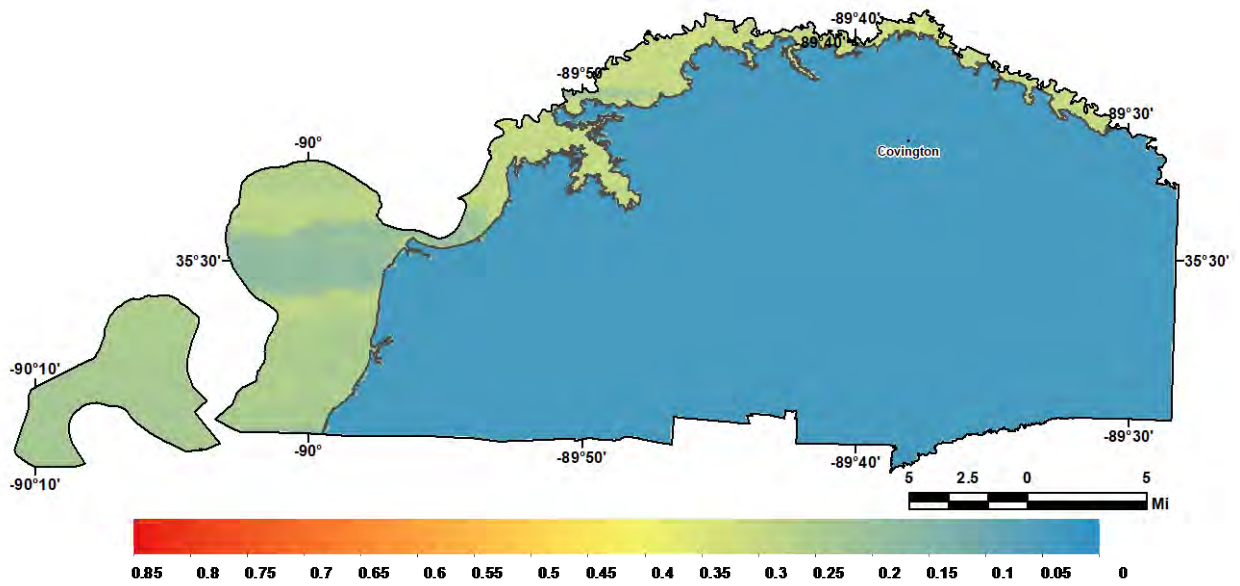


Figure 50: Scenario liquefaction hazard map for moderate to severe liquefaction at the surface (LPI > 5) for a M7.3 earthquake on the New Madrid North Fault (NE segment of NMSZ).

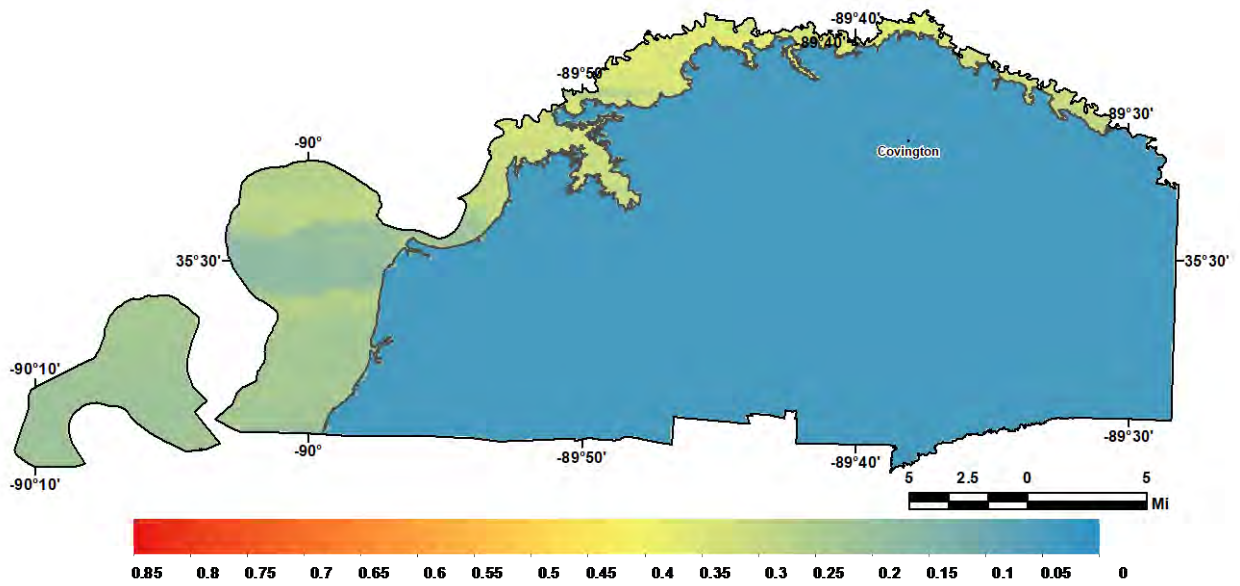


Figure 51: Scenario liquefaction hazard map for moderate to severe liquefaction (LPI > 5) for a M6.9 “Dawn” aftershock (alt. 1) on the Cottonwood Grove Fault (SW segment of NMSZ).

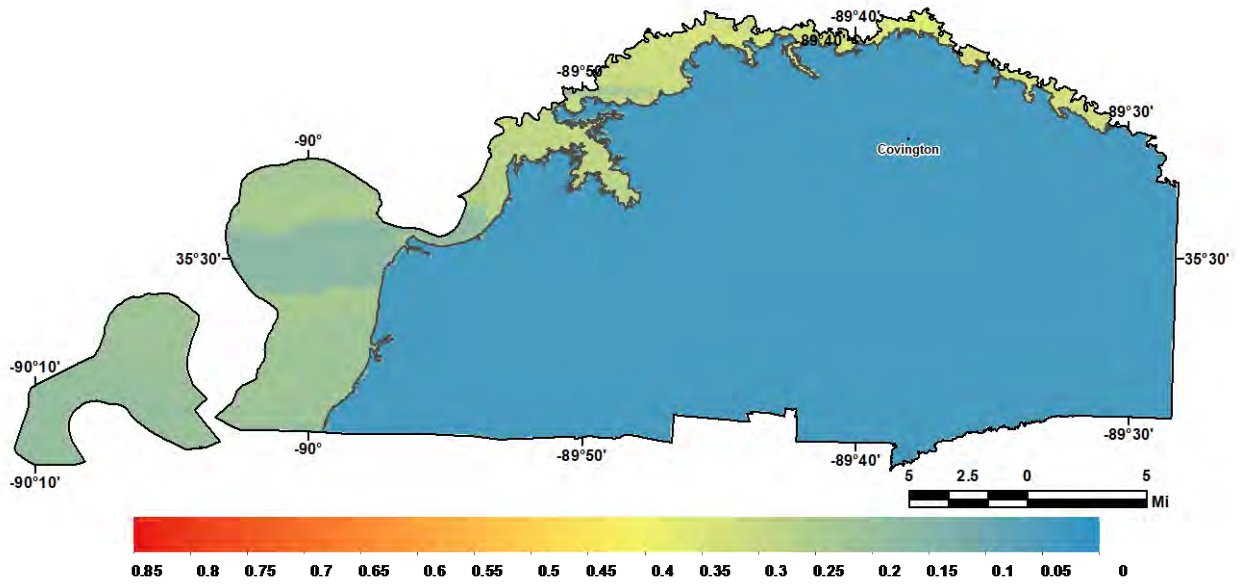


Figure 52: Scenario liquefaction hazard map for moderate to severe liquefaction (LPI > 5) for a M6.9 “Dawn” aftershock (alt. 2) on the Reelfoot Thrust (central segment of NMSZ).

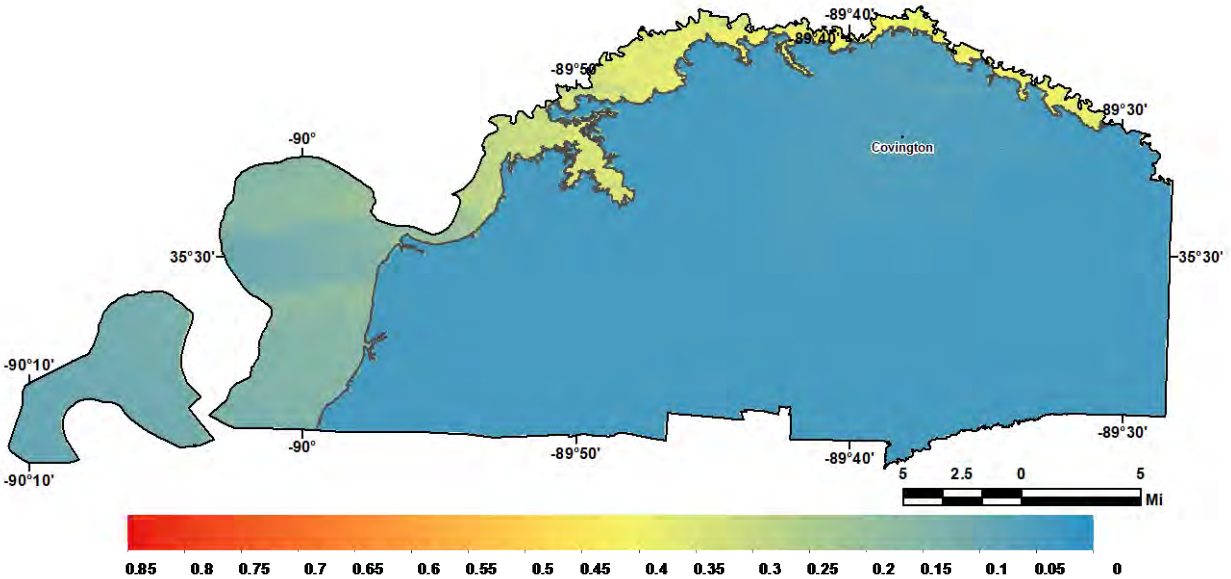


Figure 53: Scenario liquefaction hazard map for moderate to severe liquefaction (LPI > 5) for a M5.8 hypothetical Tipton County earthquake (near Covington).

### Conclusions

We have produced seismic and liquefaction hazard maps that include the effects of local geology for Tipton County. The products from this effort include a 3D geology database and model, a geotechnical database and liquefaction probability curves (LPCs), and probabilistic and scenario hazard maps for Lauderdale County. The geology model is detailed for the Quaternary sediments down to depths of 200 ft (70 m) and more generalized for the Eocene to Paleozoic formations. Paleozoic limestones form the bedrock of the model. The geotechnical database includes information on water table depths, and standard penetration tests (SPT). It was used to generate LPCs based on SPT measurements to add to the published LPCs based on Mississippi embayment CPT measurements. The liquefaction hazard maps for Tipton County were based on our developed LPCs for lowlands and non-lowlands. The Vs measurements from Dyer and Lauderdale Counties were used to generate a typical Quaternary Vs profile for non-lowlands areas. Deeper published information from the region developed for Lake County were used to constrain the Eocene to Paleozoic Vs reference profile used in this study. Seismic and liquefaction hazard maps were generated that include the new geological, geotechnical,

and seismological information gathered. The hazard maps are both probabilistic (5% and 2% probability of being exceeded in 50 years) and for seven earthquake scenarios. Seismic hazard maps show a 10-50% decrease in hazard at short periods and a 10-100% increase at long periods compared with USGS NSHMP maps, which are for a uniform standard geology not found in western Tennessee. Liquefaction hazard maps show moderate to high hazard in Lauderdale County for four of the five M7 New Madrid scenarios, and low hazard for the M7.3 NE arm and M5.8 hypothetical Lauderdale County earthquakes. The 1843 and 1895 M6.2 scenarios do not produce any significant liquefaction hazard due to more distant epicenters and a shorter duration of strong shaking.

## References

- Atkinson, G.M., and I.A. Beresnev, 2002. Ground motions at Memphis and St. Louis from M 7.5–8.0 earthquakes in the New Madrid seismic zone, *Bull. Seism. Soc. Am.* **92**, 1-15-1024.
- Chiu, J. M., Johnston, A. C., and Yang, Y. T., 1992. Imaging the active faults of the central New Madrid seismic zone using PANDA array data. *Seismological Research Letters* **63**, p. 375-93.
- Clark, B. (2011). *Groundwater Availability of the Mississippi Embayment*.
- Clark, B. R., and Hart, R. M. (2009). *The Mississippi Embayment Regional Aquifer Study (MERAS): Documentation of a groundwater-flow model constructed to assess water availability in the Mississippi embayment. The Mississippi Embayment Regional Aquifer Study (MERAS): Documentation of a groundwater-flow model constructed to assess water availability in the Mississippi embayment*, Scientific Investigations Report, USGS Numbered Series, U.S. Geological Survey, Reston, VA.
- Cox, R.T., Van Arsdale, R.B., Harris, J.B., and Larsen, D., 2001, Neotectonics of the southeastern Reelfoot Rift zone margin, central United States, and implications for regional strain accommodation. *Geology* **29**, p. 419-422.
- Cox, R.T., J. Cherryhomes, J. B. Harris, D. Larsen, R. B. Van Arsdale, S. L. Forman, 2006. Paleoseismology of the southeastern Reelfoot rift in western Tennessee and implications for intraplate fault zone evolution. *Tectonics* **25**, p. 1-17.
- Cox, R.T., Van Arsdale, R., Clark, D., Hill, A., and Lumsden, D., 2013, A revised paleo-earthquake chronology on the southeast Reelfoot rift margin near Memphis, Tennessee. *Seismological Research Letters*, v. 84, p. 402-408.
- Cox, R.T., Lumsden, D.N., and Van Arsdale, R.B., 2014. Possible relict meanders of the Pliocene Mississippi River and their implications. *Journal of Geology* **122**, p. 609-622.
- Cramer, C.H., J.S. Gombert, E.S. Schweig, B.A. Waldron, and K. Tucker, 2006. First USGS urban seismic hazard maps predict the effects of soils, *Seism. Res. Lett.* **77**, 23-29.
- Cramer, C.H., 2006. Quantifying the uncertainty in site amplification modeling and its effects on site-specific seismic-hazard estimation in the Mississippi embayment and adjacent areas, *Bull. Seism. Soc. Am.* **96**, 2008-2020.
- Cramer, C.H., G. Rix, and K. Tucker, 2008. Probabilistic liquefaction hazard maps for Memphis, Tennessee, *Seis. Res. Lett.* **79**, 416-423.

Cramer, C.H., and O.S. Boyd, 2014, Why the New Madrid earthquakes are M7–8 and the Charleston earthquake is ~M7, *Bull. Seism. Soc. Am.* **104**, 2884-2903.

Cramer, C.H., R.B. Van Arsdale, M.S. Dhar, D. Pryne, and J. Paul, 2014. Updating of urban seismic-hazard maps for Memphis and Shelby County, Tennessee: geology and Vs observations, *Seis. Res. Lett.* **85**, 986-996.

Cramer, C.H., G. Patterson, and David Arellano, 2015. Final Technical Report, Updating Liquefaction Probability Curves, Seismic Hazard Model, and Urban Seismic Hazard Maps with Public Outreach for Memphis and Shelby County, Tennessee, USGS grant G14AP00099, October 30, 2015, 42 pp (available at <http://earthquake.usgs.gov/research/external/reports/G14AP00099.pdf>).

Cramer, C.H., R.A. Bauer, J. Chung, J.D. Rogers, L. Pierce, V. Voigt, B. Michell, D. Gaunt, R.A. Williams, D. Hoffman, G.L. Hempen, P.J. Steckel, O.S. Boyd, C.M. Watkins, K. Tucker, and N. McCallister, 2017. St. Louis area earthquake hazards mapping projects: seismic and liquefaction hazard maps, *Seis. Res. Lett.* **88**, 206-223.

Cramer, C.H., M.S. Dhar, and D. Arellano, 2018a. Update of the urban seismic and liquefaction hazard maps for Memphis and Shelby County, Tennessee: liquefaction probability curves and 2015 hazard maps, *Seis. Res. Lett.* **89**, 688-701.

Cramer, C., R. Van Arsdale, D. Arellano, S. Pezeshk, S. Horton, T. Weathers, N. Nazemi, J.A. Jimenez, H. Tohidi, and L.P. Ogwen, 2018b, Seismic and liquefaction hazard maps for Lake County, northwestern Tennessee, (2018 SE-GSA abstract). Geological Society of America Abstracts with Programs 50. 10.1130/abs/2018SE-312570.

Cramer, C., R.B. Van Arsdale, V. Harrison, D. Arellano, S. Pezeshk, S.P. Horton, T. Weathers, N. Nazemi, J. Jimenez, H. Tohidi, and L.P. Ogwen, 2019. Lake County seismic and liquefaction hazard maps, CERI Report, 129 pp.

Cramer, C., R.B. Van Arsdale, R. Reichenbacher, D. Arellano, H. Tahidi, S. Pezeshk, S.P. Horton, R. Bhattarai, N. Nazemi, and A. Farhadi, 2020a. Dyer County seismic and liquefaction hazard maps, CERI Report, 90 pp.

Cramer, C. H., Van Arsdale, R. B., Harrison, V., Bouzeid, K., Arellano, D., Tohidi, H., Pezeshk, S., Horton, S. P., Bhattarai, R., Nazemi, N., and Farhadi, A., 2020b, Lauderdale County seismic and liquefaction hazard maps, CERI Report, 85 pp.

Csontos, R., and Van Arsdale, R., 2008. New Madrid seismic zone fault geometry. *Geosphere* **4**, p. 802-813.

Csontos, R., Van Arsdale, R., Cox, R., and Waldron, B., 2008. The Reelfoot Rift and its impact on Quaternary deformation in the central Mississippi River Valley. *Geosphere* **4**, n. 1, p. 145-158, doi: 10.1130/GES00107.1.

Cupples, W., and Van Arsdale, R., 2014, The Preglacial “Pliocene” Mississippi River. *Journal of Geology* **122**, 1-15.

Dhar, M.S., and C.H. Cramer, 2018. Probabilistic seismic and liquefaction hazard analysis of the Mississippi embayment incorporating nonlinear effects, *Seis. Res. Lett.* **89**, 253-267, published online 13 December 2017.

Hardeman, W.D., 1966, Geologic Map of Tennessee: West Sheet. Scale 1:250,000.

Howe, J.R., 1985, Tectonics, Sedimentation, and Hydrocarbon Potential of the Reelfoot Aulacogen [M.S. thesis]: Norman, Oklahoma, University of Oklahoma, 109 p.

Iwasaki, T., Tatsuoka, F., Tokida, K. and Yasuda, S., 1978. A practical method for assessing soil liquefaction potential based on case studies at various sites in Japan, Second International Conference on Microzonation for Safer Construction Research and Application 1978.

Iwasaki, T., Tokida, K., Tatsuoka, F., Watanabe, S., Yasuda, S., and Sato, H., 1982. Microzonation for soil liquefaction potential using simplified methods. Proceedings 3rd International Conference on Microzonation, Seattle, USA. 1319-1330.

Lumsden, D.N., Cox, R.T., Van Arsdale, R.B., and Cupples, W.B., 2016, Petrology of Pliocene Mississippi River alluvium: provenance implications. *The Journal of Geology* **124**, 501-517.

Markewich, H. H., Wysocki, D. A., Pavich, M. J., Rutledge, E. M., Millard, H. T., Rich, F. J., et al. (1998). Paleopedology plus TL, 10Be, and 14C dating as tools in stratigraphic and paleoclimatic investigations, Mississippi River valley, U.S.A. *Quaternary International* **51**, 143–167. doi: 10.1016/s1040-6182(97)00041-4.

Martin, R.V., and Van Arsdale R.B., 2017, Stratigraphy and structure of the Eocene Memphis Sand above the eastern margin of the Reelfoot rift in Tennessee, Mississippi, and Arkansas, USA. *Geological Society of America Bulletin* **129**, 970-996.

Maurer, B. W., Green, R. A., and Taylor, O.-D. S., 2015. Moving towards an improved index for assessing liquefaction hazard: Lessons from historical data, *Soils and Foundations* **55**, 778–787.

Odum, W., Hofmann, F., Van Arsdale, R., and Granger, D., 2020, New <sup>26</sup>Al/<sup>10</sup>Be and (U-Th)/He constraints on the age of the Upland Complex, central Mississippi River Valley, *Geomorphology* **371**, 1-9, 107448.

Parrish, S., and Van Arsdale, R., 2004, Faulting along the southeastern margin of the Reelfoot rift in northwestern Tennessee revealed in deep seismic reflection profiles. *Seismological Research Letters*, v. 75, p. 782-791.

Petersen, M. D., M. Moschetti, P. Powers, C. Mueller, K. Haller, A. Frankel, Y. Zeng, S. Rezaeian, S. Harmsen, O. Boyed, N. Field, R. Chen, K. Rukstales, N. Luco, R. Wheeler, R. Williams, and A. Olsen, 2014, *The 2014 update of the United States national seismic hazard models*, U.S. Geological Survey, OFR 2014-X1091, 255 p.

Rittenour, T.M., Blum, M.D., Goble, R.J., 2007, Fluvial evolution of the lower Mississippi River valley during the last 100 k.y. glacial cycle: response to glaciation and sea-level change. *Geological Society of America Bulletin* **119**, 586-608.

Rodbell, D. T., 1996, Subdivision, subsurface stratigraphy, and estimated age of fluvial-terrace deposits in northwestern Tennessee. U.S. Geologic Survey Bulletin, v. 2128, 24 pp.

Romero, S., and G.J. Rix (2001). Regional variations in near surface shear wave velocity in the Greater Memphis area, *Eng. Geol.* **62**, 137-158.

Saucier, R.T., 1987, Geomorphological interpretations of late Quaternary terraces in western Tennessee and their regional tectonic implication. U.S. Geologic Survey Professional Paper 1336-A, 19 pp.

Saucier, R.T., 1994, Geomorphology and Quaternary Geologic History of the Lower Mississippi Valley: Vicksburg, Mississippi. U.S. Army Engineer Waterways Experiment Station, v. 1, 364 p., and v. 2, map plates.

Schrader, T.P., 2008. Potentiometric surface in the Sparta-Memphis aquifer of the Mississippi embayment, Spring 2007, U.S. Geological Survey Scientific Investigations Map 3014.

Seed, H. B., and Idriss, I. M., 1971. "Simplified procedure for evaluating soil liquefaction potential." *J. Geotech. Eng. Div., ASCE*, 97(9), 1249–1273.

Toprak, S., and Holzer, T. L., 2003. "Liquefaction potential index: Field assessment." *Journal of Geotechnical and Geoenvironmental Engineering, ASCE*, 129(4), 315-322.

Tuttle, M. P., Schweig, E. S., Sims, J. D., Lafferty, R. H., Wolf, L. W., and Haynes, M. L., 2002. The earthquake potential of the New Madrid seismic zone, *Bulletin Seismological Society of America* **92**, 2080–2089, doi: 10.1785/01200 10227.

Van Arsdale, R.B., Bresnahan, R.P., McCallister, N.S., and Waldron, B., 2007. The Upland Complex of the central Mississippi River Valley: Its origin, denudation, and possible role in reactivation of the New Madrid seismic zone, in Stein, S., and Mazzotti, S., eds., *Continental*

Intraplate Earthquakes: Science, Hazard, and Policy Issues. Geological Society of America Special Paper 425, p. 177-192.

Van Arsdale, R.B., Arellano, D., Stevens, K.C., Hill, A.A., Lester, J.D., Parks, A.G., Csontos, R.M., Rapino, M.A., Deen, T.S., Woolery, E.W., Harris, J.B., 2012. Geology, Geotechnical Engineering, and Natural Hazards of Memphis, Tennessee, USA. *Environmental & Engineering Geoscience* **18**, 113-158, doi:10.2113/gseegeosci.18.2.113.

Van Arsdale, R., and Cupples, W., 2013, Late Pliocene and Quaternary deformation of the Reelfoot rift Geosphere, v. 9, n. 6, p. 1819–1831. doi:10.1130/GES00906.1

Vanderlip, C., Larsen, D., Cox, R., and Mitchell, J., 2020, Geologic Map of the Drummonds 7.5' Quadrangle, Tipton and Shelby Counties, Tennessee. 1:24,000.

Weathers, T., and Van Arsdale, R. 2019, Lake County Tennessee: in the Heart of the New Madrid seismic zone. *Frontiers in Earth Science* **7**, 1-20.

Woolery, E.W., Z. Wang, N.S. Carpenter, R. Street, and C. Brengman, 2016. The Central United States Seismic Observatory: site characterization, instrumentation, and recordings, *Seis. Res. Lett.* **87**, 215-228.

Appendix (separate file)

Please see accompanying file Appendix-Tipton\_3d\_model.avi.